Low-energy dynamics of condensed matter from the high-energy point of view

Studies in the effective field theory of matter

Rafael Krichevsky

Submitted in partial fulfillment of the
requirements for the degree of
Doctor of Philosophy
in the Graduate School of Arts and Sciences

COLUMBIA UNIVERSITY

2020

Abstract

Low-energy dynamics of condensed matter from the high-energy point of view: Studies in the effective field theory of matter

Rafael Krichevsky

In this work, we develop effective field theory (EFT) methods for the study of a wide variety of condensed matter systems, including superfluids, ordinary fluids, solids, and supersolids. As a first application, we focus on the dynamics of vortex lines in trapped superfluid condensates, studying their precessional motion and working out the frequency of precession from EFT principles. We consider the effects of trapping in two and three dimensions, as well as implications of trapping for the dispersion relation of Kelvin waves along superfluid vortex lines. We also apply our formalism to study the effects of gravitational fields on sound waves in several different media, discovering that localized sound waves propagate with an associated (negative) net mass, which in turn generates a tiny gravitational field. We confirm that this effect is a robust result that can be found from purely classical, non-relativistic methods. We then present three Lorentz invariant, renormalizable, weakly coupled theories that implement the symmetry-breaking pattern of a perturbative homogeneous and isotropic solid, as potential UV-completions of the low-energy effective theory that we studied. We demonstrate that a particular class of homogeneous, isotropic solids at long distances corresponds to states that are also homogeneous at short distances, unlike typical solids found in nature. We find that each case leads to the same rather unorthodox effective theory of a solid with luminal transverse excitations. Finally, we discuss applications of the methods we have developed and the potential for interesting new directions of this research.

Contents

List of Figures

Acknowledgements

There are many people without whom this work would have been impossible. First, an immense thank you to Alberto Nicolis, who guided this research and taught me most of what I know. I am also extremely grateful to Angelo Esposito, who struggled through many of these calculations with me and never lacked creative ideas or insight. Many others at Columbia helped me in countless ways—so I must thank Lam Hui, Rachel Rosen, Frederik Denef, Austin Joyce, and the rest of the Theory group, as well as Szabolcs Marka, Jeremy Dodd, Bill Zajc, Robert Mawhinney, Brian Cole, Sebastian Will, and other members of the physics faculty with whom I have had the pleasure of working and interacting. The guidance I have received from colleagues and collaborators, including Riccardo Penco and Sebastian Garcia-Saenz, has been truly valuable as well.

Most of all, though, I must acknowledge my gratitude to my family—my parents Mark and Rachel, my grandmother Pnina—and my wife Sidi. Thank you so much for always showing me support, encouraging me to continue, and keeping me sane!

Preface

Relativistic quantum field theory is the shared *lingua franca* of high-energy physicists. It is phenomenal at describing what happens at short distance scales in collider experiments, but of what use is it to someone who wants to understand underwater acoustics? Seismic wave propagation? Vortices in superfluid helium? Dilute Bose–Einstein gases? Thermal conductivity of neutron star matter? Plasma oscillations? Quartz crystals? A chunk of rubber? Any of the ordinary long-wavelength phenomena or condensed matter systems that we encounter on a daily basis? What on earth does the high-energy theorist have to say about such ordinary low-energy things that move at non-relativistic speeds?

If you are tempted to retort "Not much," then this thesis is designed to change your mind. What follows is an exploration (and a celebration) of the power of effective field theory (EFT) techniques to describe low-energy phenomena and condensed matter systems that can be studied in simple laboratory settings. EFT is a highly flexible framework that forms a bridge between the physics of quarks and the physics of black hole echoes, the physics of relativistic strings and the physics of elastic waves. The impressive and almost universal applicability of effective field theory is mitigated, though, by two important limitations: (1.) Breakdown and lack of predictiveness beyond an in-built cutoff scale, and (2.) Methodological agnosticism about theoretical parameters, which are meant to be fixed by experimental measurements. Still, if we humble our intellectual ambitions, turn away (at least temporarily) from grand dreams of all-encompassing, all-predicting theories, and content ourselves with effective descriptions that steadily improve our understanding of observable phenomena, there is a great deal that EFT techniques can teach us.

In this work, we will use the language of quantum field theory to study collective excitations in a variety of condensed matter systems, including superfluids, ordinary fluids, solids, and supersolids. After constructing effective actions for each of these media from symmetry-breaking considerations, we will focus our attention on two case studies. In the first, we will apply field theoretic methods to understand the dynamics of vortex lines in trapped dilute

superfluid condensates; next, we will use similar techniques to study the coupling of sound waves in various media to gravitational fields. Finally, we will attempt to bypass some of the limitations of EFT and formulate a UV completion of a homogeneous, isotropic, weakly coupled solid, in order to shed light on the effective theories we considered in the beginning; in the process, we will see that certain weakly coupled solids that appear homogeneous at long distances need not be inhomogeneous at short distances.

A note on the content and structure of this thesis:

1. Section 1 is a general discussion of the EFT formalism and its application to condensed matter based on an overview of existing literature.

2. Section 2 consists of a review of the literature on the EFTs of superfluids, superfluid vortices, fluids, and solids, as well as a novel extension of this formalism to supersolids—see Section 2.4.

3. Section 3 includes a study of the precessional motion of vortex lines in trapped superfluids based on the EFT formalism developed in Section 2. Part of this work has been published previously by the author and collaborators in [1]. The non-trivial extension of the primary result to three-dimensional trapping configurations and the study of vortex line bending—see Section 3.5—as well as the consideration of Kelvin wave dispersion relations in Section 3.4 are original to this thesis and have not been published before.

4. Section 4 is a second case study in which the EFTs of superfluids, fluids, and solids are used to calculate a "gravitational mass" associated with sound wave packets in various media. This relativistic field theory-based calculation has been published by the author and collaborators in [2]. What has not been published previously is the derivation of the main result in non-relativistic fluids with Galilei symmetry (Section 4.5); neither have supporting calculations which demonstrate that the same result could be obtained from classical fluid dynamics (Section 4.6) or elasticity theory (Section 4.7).

5. Section 5 is an attempt to go beyond EFT and find a UV complete theory of a homogeneous state that corresponds to a homogeneous, isotropic solid in the IR. This work has not appeared in the literature before and is entirely original work by the author, Alberto Nicolis, and Angelo Esposito. It will be republished subsequently to its appearance in this thesis.

6. Section 6 is a summary of the thesis with remarks about possible extensions and further directions for research.

Note on Conventions

Throughout this thesis, we will work in metric signature $(-,+,+,+)$. We will always set $\hbar = 1$, but we will sometimes keep factors of c explicit in order to facilitate taking the non-relativistic limit. It will be clear from context when we are doing so. We will use boldface symbols $\mathbf{x}, \mathbf{y}, \ldots$ for vectors, but not for their components. Greek indices $\mu, \nu, \ldots$ represent space-time indices of vectors and tensors; $i, j, \ldots$ represent purely spatial indices; and $I, J, \ldots$ are the internal indices of quantum fields that form multiplets under various internal symmetry groups. Summation over repeated indices is usually implied, unless stated otherwise.

1 Introduction: An Overview of Effective Field Theory and Applications to the Study of Condensed Matter

1.1 The Power of Effective Field Theory

At a first glance, it may seem counter-intuitive to make use of the techniques of high-energy particle physics to study condensed matter phenomena at low energies, but as we will see in the subsequent sections, this proves to be a highly productive approach. Many condensed matter systems are easily characterized by their underlying symmetries and symmetry-breaking patterns, lending themselves to the formalism of effective field theory (EFT) in a straightforward manner. Instead of modeling systems with a large number of degrees of freedom using phenomenological models that must be justified *post hoc*, computationally intensive simulations, or complicated microscopic descriptions, we appeal to the simplicity and universality of the EFT approach in studying the dynamics of condensed matter systems at low energies. The fundamental underlying idea is the independence of dynamics at low energies (or long distance scales) and high energies (or short distance scales). A physical process that takes place at energy E, much less than some characteristic cutoff energy scale Λ at which more degrees of freedom become relevant, can typically be described in terms of an expansion in powers of E/Λ to some desired level of accuracy [3]. In essence, the methodology allows us to quantify our ignorance of high-energy dynamics when describing experimentally accessible physical systems and make generic predictions about dynamics parametrically below the limiting scale [4]. Symmetry considerations lead one to construct an effective Lagrangian by including all interaction operators consistent with the symmetries governing the theory, and coupling constants are fixed after the fact, in principle by conducting experimental measurements. Parameters of the full theory that are relevant

at high energy do not affect the dynamics of the resulting theory at low energy, except in perturbative corrections; the high-energy dynamics only impose symmetry constraints on the low-energy effective theory [5]. The assumptions that must be made on the microscopic properties of the system are minimal in this approach, and symmetry considerations alone can be used to extract the details of the dynamics at low energy.

As an example to illustrate the relevant principles outside of the context of condensed matter physics, let us consider the effective field theory approach to general relativity. The theory can be constructed as the theory of a massless spin-two graviton field, with local invariance under coordinate transformations, or diffeomorphisms. The gauge symmetry constrains the type of interaction terms that may be present. A generic, diffeomorphism-invariant effective action can be written as

$$S = -\int d^4x\,\sqrt{-g}\left[c_0 + \frac{1}{16\pi G}R + c_1R^2 + c_2R_{\mu\nu}R^{\mu\nu} + \cdots\right], \tag{1}$$

where R is the Ricci scalar and $R_{\mu\nu}$ is the Ricci curvature tensor. We know that the coefficient c_0 matches the cosmological constant, but in the effective field theory philosophy, it is left undetermined, to be fixed by experiment, along with all the other coefficients of the higher-order interaction terms in the action. Note that the additional term $R_{\mu\nu\rho\sigma}R^{\mu\nu\rho\sigma}$ is not independent of the two higher-derivative terms above, R^2 and $R_{\mu\nu}R^{\mu\nu}$, by the Gauss–Bonnet relation. Although the theory is non-renormalizable, this is not a problem when considering physical processes at low energy compared to the cutoff scale of the theory, the Planck mass, which is related to the coefficient $1/16\pi G$. When organized as a derivative expansion, it is clear that the higher-order, higher-derivative terms do not affect the low-energy physics; indeed, current experimental constraints on such higher-derivative interaction terms are very weak [6–8], and the non-renormalizability of the theory guarantees that a tower of such terms is generated from lower-order interactions. If we are interested only in low-energy dynamics, however, the effective field theory approach provides a simple, methodical way

to generate all interactions to some desired order in the derivative expansion; equations of motion determining the dynamics, including quantum corrections, are then obtained by varying the action in the standard way with respect to the spin-two field.

The above example is typical of the "bottom-up" or continuum approach to effective field theory, which may be contrasted with the Wilsonian approach, characterized by integrating out higher-momentum modes in some more complete theory in order to obtain an effective theory usable at low energies [9]. The latter methodology is relevant, for example, when extracting low-energy effective field theories from supergravity or effective string theories. Beginning from a complicated high-energy description that is not conducive to concrete calculations, it is convenient to work one's way down to a lower-energy effective description by integrating out all degrees of freedom but those relevant to the dynamics at the energy scale that one is interested in, resulting in a tailor-made effective theory for a chosen level of analysis. The reverse process is not nearly as straightforward a task; inferring a higher-energy ultraviolet theory from a low-energy effective description is not something that can be done in a unique manner, much like reversing the effects of coarse-graining in renormalization group theory. It is often illuminating to study which properties of an ultraviolet theory persist as higher-momentum degrees of freedom are integrated out. While both approaches are useful in their respective contexts, and we will use both to study condensed matter systems in this work, we will focus at first on the "bottom-up" approach, since the condensed matter systems we wish to consider do not come with readily applicable UV theories or models—and if they did, there would be no need to build simplifying low-energy models to discover their dynamics. The framework lends itself particularly well to the study of condensed matter phenomena because every medium must break some of the fundamental Poincaré symmetries of nature, resulting in the appearance of low-energy excitations, depending on the symmetry-breaking pattern, which describe the fluctuations of the medium about its ground state. We will study this in more detail in subsequent sections.

There are three key theorems that underlie the EFT framework and make it a powerful

conceptual approach in the study of condensed matter. The first is a by-now obvious general theorem that validates the "bottom-up" approach to EFT: perturbation theory using the most general Lagrangian containing invariant operators under a set of assumed symmetries will produce all possible S-matrix elements that are consistent with unitarity, cluster decomposition, and the same set of symmetries [10]. The second, which makes the "top-down" approach possible [11], is the decoupling theorem due to Appelquist and Carrazone [12]; it shows that when there is a large separation of scales between masses of different degrees of freedom in a quantum field theory, at low energies the observable effects of the higher-mass mode are either suppressed by inverse powers of the mass or can be absorbed into renormalized couplings, masses, and fields obtained by integrating it out. The third result, relevant to media that spontaneously break continuous symmetries, is the Goldstone theorem [13–15], which guarantees the appearance of gapless scalar modes in the spectrum of excitations when such symmetries are spontaneously broken. When the broken symmetry generators are those of space-time symmetries, however, the correspondence between broken symmetries and Goldstone modes is no longer one-to-one because some of the Goldstone modes can be removed by the imposition of "inverse Higgs constraints" [16–18]. When the broken generators do not commute with the generators of unbroken space-time translations, some of the Goldstone modes may become gapped [19, 20], in which case they become irrelevant for the dynamics at low energies. Moreover, some Goldstone particles may even become kinematically unstable, as has been shown in superfluid helium, in which a single phonon is allowed to decay into two phonons [20, 21]. In some cases, the inverse Higgs constraints can be interpreted as removing redundancies in the parametrization of the Goldstone excitations. Nonetheless, media that spontaneously break space-time and internal symmetries have low-energy dynamics that are well described by a set of interacting gapless Goldstone modes. Any general Lagrangian compatible with the symmetries of a given medium can be fluctuated and expanded around the ground state to yield a low-energy effective action for the Goldstone modes.

Since Kadanoff, Wilson, and Fisher first introduced effective actions and associated techniques to the study of critical phenomena [22–25], the general methodology of EFT has been adopted throughout high- and low-energy physics with a remarkable track record of success and flexibility, finding applications in the study of such diverse areas as: cosmological large-scale structure [26]; dark energy [27]; general relativity and gravitational radiation [6, 28]; the dynamics of dwarf stars and neutron stars [29, 30]; the fractional quantum Hall effect [31]; hydrodynamics [4, 21, 32–34]; inflationary physics [35, 36]; modified theories of gravity [37, 38]; plasma physics [39, 40]; quark-gluon plasmas and heavy-ion collisions [9, 41]; solids and supersolids [17]; Standard Model particle physics [42, 43] and beyond-Standard Model physics [44]; superfluidity [32, 45, 46]; string phenomenology [47]; and even the simple Schrödinger equation of quantum mechanics [48]. For the rest of this thesis, we will focus on the application of such methods to the study of the dynamics of less exotic media, particularly plain old superfluids, ordinary fluids, and solids.

1.2 Condensed Matter from the Effective Field Theory Point of View

1.2.1 General Discussion

It naturally seems strange to use relativistic field theoretic language and relativistic symmetries to characterize the properties of condensed matter, since in practice, all states of matter that we encounter are highly non-relativistic. The velocities of common types of collective excitations (phonons, rotons, magnons, etc.) found in the types of condensed matter systems encountered in experiments are usually highly non-relativistic, although there are some exceptions. Also, the enthalpy density is typically much lower than the mass density in condensed matter, and the ground state of any such system is obviously not invariant under boosts. That is why theories of condensed matter are typically formulated without reference to relativistic concepts like Lorentz invariance.

Still, it is important to remember that the symmetries of the Poincaré group—space-time translations, spatial rotations, and Lorentz boosts—are, as far as we can tell, symmetries of all the fundamental laws of physics. Since all condensed matter systems break Poincaré symmetry, consistency with the fundamental laws requires that the symmetries are broken *spontaneously*. In particular, every state of matter is a Lorentz-violating state, despite adhering to Lorentz-invariant physical laws, that picks out a single inertial reference frame, the frame in which the system is at rest. Certain types of matter may break other symmetries of the Poincaré group as well, in addition to various internal symmetries that they might possess. In fact, the spontaneous breaking of Poincaré symmetries can be understood as the defining feature of any condensed matter state [16], and many collective excitations of matter can be seen as consequences of Goldstone's theorem. Spontaneously broken symmetry under boosts has highly constraining implications for the dynamics of the Goldstone modes, and consequently the transport properties and other phenomena observed in condensed matter system. The program of studying condensed matter using relativistic field

theory techniques has turned out to be a much more productive endeavor than one might have initially expected[1].

To be sure, EFTs tend to have serious in-built limitations, mostly connected to renormalizability issues and the breakdown of perturbation theory at strong coupling, but applying EFT techniques to the low-energy physics of condensed matter presents a number of significant practical advantages. The first and most obvious is agnosticism about short-distance physics, which is often not well understood or practically intractable for calculations in many-body systems. Secondly, the theories of Goldstone modes in matter are often simple to state; they are typically local actions of bosonic scalar fields with interactions highly constrained by symmetry, or they are dual to simple scalar field theories. Finally, Lorentz invariance is trivial to impose at the level of the action, and the full theoretical arsenal of high-energy physics can be deployed at will to calculate scattering amplitudes from perturbation theory. One might think that non-perturbative phenomena are out of reach of EFT techniques, but that is not entirely true. As we will see, certain macroscopic, non-perturbative phenomena such as vortex lines in superfluids can be treated in EFT formalism as well [49], as long as the vortices themselves move sufficiently slowly. Simplifying assumptions must be made to model the vortices as infinitely thin strings, but interactions between the strings and the long-wavelength superfluid bulk modes can be arrived at by the standard EFT methodology—including all operators that are invariant under the relevant symmetries and organizing the theory as a derivative expansion at low energy.

[1]While we will consider effective theories of solids, fluids, superfluids, etc. that are fully relativistic, it is important to note that one may also use Galilei invariance instead of Lorentz invariance to build such theories. In that case, the theories will be non-relativistic from the outset. We generally see no advantage in using an approximate symmetry of nature to formulate theories of matter, when the exact symmetry will do just as well. It would not even buy us any additional simplicity in calculations.

1.2.2 Classification of Condensed Matter Systems by Spontaneous Symmetry Breaking

Nicolis *et al.* [16] systematically classified all possible condensed matter systems that are homogeneous, static, and isotropic at large distances—whether they are realized in nature or not—on the basis of their space-time symmetry-breaking patterns. We will briefly review their approach to understand how broken symmetries determine dynamics in effective theories of condensed matter. Condensed matter systems can break the generators of Poincaré symmetry in different combinations. From the field theoretic viewpoint, the combination of spontaneously broken boosts and other symmetries can be regarded as a *definition* of condensed matter. The full symmetry group of any system that is homogeneous, static, and isotropic will include the Poincaré generators: P_0 (time translations), P_i (spatial translations), J_i (rotations), and K_i (boosts). There may be additional internal symmetries whose generators commute with the those of the space-time symmetries. The algebra of the Poincaré generators is defined by the commutation relations

$$\begin{aligned} [J_i, J_j] &= i\epsilon_{ijk}J_k\,, \quad [J_i, P_j] = i\epsilon_{ijk}P_k\,, \quad [J_i, K_j] = i\epsilon_{ijk}K_k \\ [K_i, P_0] &= -iP_i\,, \quad [K_i, P_j] = i\delta_{ij}P_0\,, \quad [K_i, K_j] = -i\epsilon_{ijk}J_k\,, \end{aligned} \tag{2}$$

with all other commutators equal to zero. Although boosts are always broken in condensed matter systems, we assume that there remain a set of unbroken generators $\bar{P}_0$, $\bar{P}_i$, and $\bar{J}_i$ that leave the ground state unchanged. These have the same commutation relations with each other as in the Poincaré algebra, but they may be specific linear combinations of the original symmetry generators (including internal symmetries). Their commutation relations with the boost generators may be modified. The unbroken generator $\bar{P}_0$ is the Hamiltonian of collective excitations in the system. As we mentioned previously, whenever the commutators of some unbroken generator of translations $\bar{P}_\mu$ with a set of broken generators Q_i contain another set of broken generators Q'_i, it is possible to impose inverse Higgs constraints. These constraints can be solved to express the Goldstone modes associated with the broken gen-

erators Q_i in terms of derivatives of the Goldstones associated with Q'_i [16]. The result is a non-linear realization of the exact same symmetry-breaking pattern, but with fewer gapped Goldstone modes.

The classification of condensed matter systems distinguishes between systems on the basis of which unbroken generators $\bar{P}_0, \bar{P}_i, \bar{J}_i$ contain combinations of internal symmetries, denoted schematically by Q:

1. $\bar{P}_0 = P_0$, $\bar{P}_i = P_i$, $\bar{J}_i = J_i$ — In the simplest case, none of the unbroken generators include internal symmetries. Nicolis *et al.* call this case the "type-I framid." Since the three boosts are broken, there are three Goldstone bosons, and this symmetry-breaking pattern can be realized in a theory with a four-vector A_μ that takes a VEV of the form $\langle A_\mu \rangle \propto \delta^0_\mu$. This is not a system that occurs in nature, as far as we know, and we will not be concerned with it further.

2. $\bar{P}_0 = P_0 + Q$, $\bar{P}_i = P_i$, $\bar{J}_i = J_i$ — Since P_0 commutes with the other generators, so does Q. In this situation, we have a system that spontaneously breaks an internal $U(1)$ symmetry generated by Q, in addition to the three boosts. This is the symmetry-breaking pattern of the "type-I superfluid," per the terminology of Nicolis *et al.*. Although there are four broken generators in this case, there are not four gapless Goldstones in such a superfluid. From the commutation relation involving K_i and P_j in Eq. (2), we see that $[K_i, \bar{P}_j] = i\delta_{ij}\left(\bar{P}_0 - Q\right)$, so we may impose three inverse Higgs constraints relating the three Goldstones associated with boosts to the Goldstone of the spontaneously broken $U(1)$ [50]. This symmetry-breaking pattern can be realized with a complex scalar field Φ that has a time-dependent VEV $\langle \Phi \rangle \propto e^{it}$ and is symmetric under $U(1)$ phase shifts. Upon decomposing $\Phi = \rho e^{i\phi}$ into a radial mode ρ and a phase ϕ, we see that a $U(1)$-symmetric potential would give ρ a finite gap, so that it can be integrated out at low energies. What remains is a theory of the gapless scalar ϕ that non-linearly realizes the $U(1)$ symmetry, and whose fluctuations about the ground state are the superfluid phonons.

3. $\bar{P}_0 = P_0$, $\bar{P}_i = P_i + Q_i$, $\bar{J}_i = J_i$ — In this case, the commutation relations Eq. (2) imply that $[J_i, Q_j] = i\epsilon_{ijk}Q_k$, so Q_i cannot generate purely internal symmetries. Nicolis *et al.* call this system the "type-I galileid."

4. $\bar{P}_0 = P_0$, $\bar{P}_i = P_i$, $\bar{J}_i = J_i + Q_i$ — The commutation relations Eq. (2) now imply that $[Q_i, Q_j] = i\epsilon_{ijk}Q_k$, so that Q_i generates an internal $SO(3)$ symmetry. As there are now six broken generators and zero available inverse Higgs constraints, there are also six Goldstone modes. This case is known as the "type-II framid" in Nicolis *et al.*.

5. $\bar{P}_0 = P_0 + Q$, $\bar{P}_i = P_i + Q_i$, $\bar{J}_i = J_i$ — The commutation relations Eq. (2) again imply that $[J_i, Q_j] = i\epsilon_{ijk}Q_k$, so Q_i cannot generate an internal symmetry. Accordingly, this system was named the "type-II galileid."

6. $\bar{P}_0 = P_0 + Q$, $\bar{P}_i = P_i$, $\bar{J}_i = J_i + Q_i$ — In this case, the commutation relations show that Q generates an internal $U(1)$ symmetry, while Q_i generates an internal $SO(3)$ symmetry. There are seven broken generators overall, and the boost Goldstones can again be eliminated via the same inverse Higgs constraints as in the type-I superfluid. There remain four gapless Goldstone modes. This scenario is called the "type-II superfluid," and it is realized by the B phase of superfluid helium-3 in the non-relativistic limit [51]. The broken generators Q_i are associated with spin in the limit of negligible spin-orbit coupling. A theory with an $SO(3)$ triplet of complex four-vectors $\mathcal{A}^a_\mu$ realizes this symmetry-breaking pattern if $\langle \mathcal{A}^I_\mu \rangle \propto e^{it}\delta^I_\mu$.

7. $\bar{P}_0 = P_0$, $\bar{P}_i = P_i + Q_i$, $\bar{J}_i = J_i + \tilde{Q}_i$ — It is straightforward to show that both Q_i and $\tilde{Q}_i$ commute with the Poincaré generators, but not with each other. They have the commutation relations $[Q_i, Q_j] = 0$, $[Q_i, \tilde{Q}_j] = -i\epsilon_{ijk}Q_k$, and $[\tilde{Q}_i, \tilde{Q}_j] = i\epsilon_{ijk}\tilde{Q}_k$, which is the algebra of $ISO(3)$. We can identify Q_i as the generator of internal translations and $\tilde{Q}_i$ as the generator of internal rotations. The additional commutation relation $[\bar{P}_0, K_i] = i(Q_i - \bar{P}_i)$ allows for the elimination of three boost Goldstones via three inverse Higgs constraints; since we also have $[\bar{P}_i, \tilde{Q}_j] = i\epsilon_{ijk}Q_k$, we can eliminate

three more Goldstones associated with internal rotations. There remain three gapless Goldstone modes, which can be identified as the acoustic phonons of a solid that is isotropic at large distances. The simplest realization of this symmetry breaking pattern is with an $ISO(3)$ triplet of scalar fields ϕ^I that break boosts and internal rotations with a VEV $\langle \phi^I \rangle \propto x^I$. The scalars ϕ^I can be interpreted as the co-moving coordinates of volume elements in the solid. In principle, one could enlarge the minimal broken symmetry group without increasing the number of Goldstone modes, since they would be removed by additional inverse Higgs constraints. One could even promote $ISO(3)$ to the infinitely large group of volume preserving diffeomorphisms, under which the scalars transform as $\phi^I \to \xi(\phi^I)$, $\det\big(\partial \xi^I / \partial \phi^J\big) = 1$. As we will see, this situation corresponds to a perfect fluid, since volume elements in a perfect fluid may be freely moved around and deformed with no energy cost, as long as they are not compressed in volume. From this point of view, a fluid is just a solid with infinitely enhanced internal symmetry.

8. $\bar{P}_0 = P_0 + Q$, $\bar{P}_i = P_i + Q_i$, $\bar{J}_i = J_i + \tilde{Q}_i$ — The final possibility features internal generators as part of every unbroken combination of generators. It is simple to show that these broken generators obey the commutation relations of the algebra of $ISO(3) \times U(1)$. This situation is a hybrid of a solid and a type-I superfluid, and is accordingly known as a supersolid. There are now 10 broken generators, including boosts, and six inverse Higgs constraints (the same ones we had in the solid), so there are four Goldstone modes remaining. The symmetry-breaking pattern can be realized with an $ISO(3)$ triplet ϕ^I, as in the case of the solid, and an additional light scalar field ψ that transforms as a singlet under $ISO(3)$ and non-linearly realizes $U(1)$ as a phase via shift symmetry, with VEVs $\langle \phi^I \rangle \propto x^I$ and $\langle \psi \rangle \propto t$. This is a theory involving displacements of volume elements in a solid with an added superfluid-like order parameter. Incidentally, promoting the broken internal symmetry group from $ISO(3) \times U(1)$

to Diff′(3) × $U(1)$ [2], by analogy with the solid, makes this the symmetry-breaking pattern of a superfluid at finite temperature.

In each of these cases, the symmetry breaking properties of the system can guide us to build the simplest possible theories that realize them. It is also possible to systematically find the simplest relativistic theories that realize these symmetry patterns from the so-called "coset construction" [50], which implements the inverse Higgs constraints directly and eliminates Goldstone modes through algebraic equations. As an illustration of how this formalism works, let us consider the symmetry-breaking pattern of a supersolid. The procedure is straightforward, as outlined in [50], although it can be computationally rather tedious. The first step is to consider the complete group of symmetries G and the unbroken subgroup H and represent the space of cosets G/H by introducing a Goldstone field for each broken generator. A general element of this space can be parametrized as

$$\mathcal{O}(x) = e^{ix^\mu \bar{P}_\mu} e^{i\eta^i(x) K_i} e^{i\pi^\mu(x) Q_\mu} e^{i\theta^i(x)\tilde{Q}_i} \,, \tag{3}$$

where η^i are the Goldstones of broken boosts, π^0 is the Goldstone of broken internal $U(1)$, π^i are the Goldstones of broken internal translations, and θ^i are the Goldstones of broken internal rotations. An effective action for the theory is constructed by computing the Maurer–Cartan form $\mathcal{O}^{-1}d\mathcal{O}$ for the Lie group under consideration. In the basis of the generators, the Maurer–Cartan form becomes

$$\begin{aligned} \mathcal{O}^{-1}d\mathcal{O} = {} & i e_\alpha{}^\nu dx^\alpha \left(\bar{P}_\nu + \mathcal{D}_\nu \eta^i K_i + \mathcal{D}_\nu \pi^\mu Q_\mu + \mathcal{D}_\nu \theta^i \tilde{Q}_i \right) \\ & + [\text{terms involving unbroken generators}] \,, \end{aligned} \tag{4}$$

where $e_\alpha{}^\nu$ are space-time tetrads and $\mathcal{D}_\nu$ are covariant derivatives. Each term in this expansion transforms covariantly and can be used to construct an invariant effective Lagrangian.

[2] We use Diff′(3) to refer to the group of diffeomorphisms with unit Jacobian, of which $ISO(3)$ is a subgroup.

At the same time, the commutation relations of the Poincaré algebra and $ISO(3) \times U(1)$ can be used to obtain an explicit expression for the Maurer–Cartan form. After some calculation, the result is

$$\begin{aligned} \mathcal{O}^{-1}\partial_\mu \mathcal{O} = & \, i\Lambda_\mu{}^\nu(\boldsymbol{\eta})\bar{P}_\nu + i\left[\delta^0_\mu + \partial_\mu \pi^0 - \Lambda_\mu{}^0(\boldsymbol{\eta})\right] Q_0 \\ & + i\left[\left(\delta^i_\mu + \partial_\mu \pi^i\right) R_i{}^j(\boldsymbol{\theta}) - \Lambda_\mu{}^j(\boldsymbol{\eta})\right] Q_j \\ & + [\text{terms involving } K_i \text{ and } \tilde{Q}_i]\,, \end{aligned} \tag{5}$$

where $\Lambda_\mu{}^\nu$ is a Lorentz transformation and $R_i{}^j$ is an $SO(3)$ rotation. Comparing Eq. (4) and Eq. (5) allows us to find expressions for the covariant derivatives of π^μ. Then, introducing the notation $\phi^\mu = x^\mu + \pi^\mu$ (so that $\langle \phi^i \rangle \propto x^i$ spontaneous breaks rotations, while $\langle \phi^0 \rangle \propto t$ spontaneously breaks $U(1)$ with a time-dependent VEV), the result is

$$\mathcal{D}_\mu \pi^0 = -\delta^0_\mu + \Lambda^\nu{}_\mu \partial_\nu \phi^0\,, \tag{6}$$

$$\mathcal{D}_\mu \pi^i = -\delta^i_\mu + \Lambda^\nu{}_\mu \partial_\nu \phi^j R_j{}^i\,. \tag{7}$$

Now, recall that we have the commutation relations $\left[\bar{P}_0, K_i\right] = i\left(Q_i - \bar{P}_i\right)$ and $[\bar{P}_i, \tilde{Q}_j] = i\epsilon_{ijk}Q_k$ when the symmetry-breaking pattern of a supersolid is realized. This means that the commutators of broken boosts with unbroken time translations contain the broken internal translation generators, and the commutators of broken internal rotations with unbroken spatial translations contain the broken internal translation generators as well. As a result, we have the opportunity to impose six inverse Higgs constraints to express the Goldstones of boosts and internal rotations in terms of the Goldstones of internal translations. This is achieved by imposing six gauge fixing conditions that preserve all the symmetries and eliminate the redundant Goldstone fields. In this case, the appropriate gauge fixing conditions are

$$\mathcal{D}_0 \pi^i = 0\,, \quad \mathcal{D}_i \pi_j - \mathcal{D}_j \pi_i = 0\,. \tag{8}$$

The first condition can be achieved by requiring $\beta^\mu \partial_\mu \phi^i = 0$, where we expressed rapidity $\boldsymbol{\eta}$ in terms of a boost velocity $\beta^\mu = (1, \boldsymbol{\beta})$. This equation can be solved to yield

$$\beta^\mu = \frac{J^\mu}{J^0}\,, \quad J^\mu \propto \epsilon^{\mu\nu\rho\sigma}\epsilon_{ijk}\partial_\nu\phi^i\partial_\rho\phi^j\partial_\sigma\phi^k\,. \tag{9}$$

This eliminates the boost Goldstones η by implicitly expressing them in terms of π^i. We can still use $\mathcal{D}_0\pi^0$ as a building block for the effective Lagrangian, since it is not fixed by either gauge condition. In terms of the solution for β^μ that we found from the first gauge condition, Eq. (6) gives

$$\mathcal{D}_0\pi^0 = -1 + \frac{\beta^\nu\partial_\nu\phi^0}{\sqrt{-\beta_\mu\beta^\mu}} = -1 + \frac{J^\nu\partial_\nu\phi^0}{\sqrt{\det\left(\partial_\mu\phi^i\partial^\mu\phi^j\right)}} \equiv -1 + y\,. \tag{10}$$

We have thus found the first invariant quantity out of which we can build the effective Lagrangian, and we can freely exchange $\mathcal{D}_0\pi^0$ for y.

We have not yet used the second gauge condition $\mathcal{D}_i\pi_j = \mathcal{D}_j\pi_i$. If we define $N_i{}^j \equiv \Lambda^\mu{}_i\partial_\mu\phi^j$, this gauge condition implies that $N_i{}^k R_k{}^j = N_j{}^k R_k{}^i$; in other words, $\mathbf{NR}$ is a symmetric matrix. Therefore, we must have $\mathbf{N^T N} = \mathbf{N^T R^T R N} = (\mathbf{RN})^2$. Since $(\mathbf{N^T N})_{ij} = \partial_\mu\phi^i\partial^\mu\phi^j \equiv B^{ij}$, we find that $\mathbf{NR} = \mathbf{NBN^{-1}}$, which implicitly specifies the angles θ_i—the arguments of the rotation matrix $\mathbf{R}$—in terms of the fields π_i, thus eliminating the Goldstones of the spontaneously broken internal rotations. The only remaining covariant derivatives that we are left with are $\mathcal{D}_{(i}\pi_{j)}$ and $\mathcal{D}_i\pi^0$. The symmetry of $\mathbf{NR}$ also implies that

$$\frac{1}{2}\left(\mathcal{D}_i\pi_j + \mathcal{D}_j\pi_i\right) = -\delta_{ij} + (\mathbf{NR})_{ij} = -\delta_{ij} + \left(\mathbf{NBN^{-1}}\right)_{ij}\,. \tag{11}$$

Therefore we can use the combination B_{ij} instead of the covariant derivative $\mathcal{D}_{(i}\pi_{j)}$ as a building block of invariants to include in the effective Lagrangian of the theory. In addition,

from Eq. (6), notice that we have

$$\mathcal{D}_i\pi^0\mathcal{D}^i\pi^0 = \partial_\mu\phi^0\partial^\mu\phi^0 + y^2 \equiv X + y^2\,. \tag{12}$$

The quantity X is another invariant combination that can be used in the effective Lagrangian. However, there are other index structures in the theory (namely B_{ij}), with which $\mathcal{D}_i\pi^0$ can be contracted. Let us calculate the covariant derivative:

$$\mathcal{D}_i\pi^0 = \left(\mathbf{N^{-1}}\right)^j{}_i\,\partial_\mu\phi^0\partial^\mu\phi_j \equiv \left(\mathbf{N^{-1}}\right)^j{}_i\,A_j\,. \tag{13}$$

We can also exchange this covariant derivative for A_i, in order to build further invariant operators in the effective theory.

The most general low-energy effective Lagrangian compatible with the symmetries of a supersolid must be a function of X, y, A_i, and B_{jk}, which form quantities that are invariant under the unbroken symmetries whenever all the indices are contracted in order to preserve rotational invariance. The symmetry-breaking pattern is realized by the VEVs $\langle\phi^\mu\rangle \propto x^\mu$. The effective action of a superfluid can then be written schematically as

$$S = \int d^4x\, F\left(X, y, A_i, B_{jk}\right)\,. \tag{14}$$

A non-relativistic version of the same action was found by Son [52] to reproduce the Andreev–Lifshitz equations describing the dynamics of a Bose condensate of point defects in a helium-4 crystal, which was conjectured to have supersolid properties [53].

This is an excellent illustration of the power of effective field theory techniques. General symmetry-breaking considerations and Lie group theory allowed us to generate an effective action describing the dynamics of excitations in a highly complex theoretical state of matter, the supersolid. Moreover, the action is automatically Lorentz invariant, making the theory fully relativistic. Each of the invariants can be expanded in small fluctuations around the

VEVs of the ϕ^μ fields to arbitrary order, as long as we remain interested in energies at which perturbation theory is valid, in order to generate an effective action for Goldstone modes. The Goldstones represent the phonons of first sound and second sound. We can then, in principle, calculate all possible S-matrix elements between states of collective excitations in this theory.

We have now reviewed Nicolis *et al.*'s classification of condensed matter systems by symmetry-breaking pattern and seen how symmetry considerations can be used to construct effective actions that realize those patterns. We will not be concerned with exotic phases like framids or galileids, but we will primarily focus instead on well-known phases such as superfluids (type I), solids, and ordinary fluids. Once we know the symmetries of each system and how they are broken by the ground state, it is easy to find invariant field combinations out of which to build effective Lagrangians. Instead of relying on the rather cumbersome formalism of the coset construction, we will use more intuitive symmetry arguments to achieve the same goal of building effective actions for condensed matter systems. Expanding in small fluctuation about VEVs that realize the symmetry-breaking patterns of the systems we are interested in will yield effective theories of phonons in such systems. We are now ready to study such effective theories in more detail.

2 Superfluids, Fluids, Solids, and Vortices in EFT

2.1 Superfluids

In this section, we will review methods that have been developed to formulate an effective field theory of a superfluid. Although there is a rich variety of substances that exhibit superfluid phenomenology in different ways, from our effective field theory point of view, we will not distinguish between types of superfluids based on their microscopic constituents. There is no need to differentiate between Bose liquids, such as superfluid helium-4, and Fermi liquids, such as superfluid helium-3. For the most part, we will not even consider the two-component model of the superfluid; instead we consider superfluids at such low temperatures that the ordinary component can be neglected. What matter for us are the most general properties of a superfluid, such as the spectrum of elementary excitations and the symmetry-breaking processes that create them. As Landau [54] explained, the unique properties of a superfluid—dissipationless flow and absence of shear viscosity—depend on the properties of the excitation spectrum in a superfluid, which satisfies what has become known as the Landau criterion. The general argument is as follows. Consider a $U(1)$ charge-carrying Bose–Einstein condensate flowing at some velocity $\mathbf{v}$ through a straight pipe. Its kinetic energy is reduced if there is friction between the condensate and the wall of the pipe. In the rest frame of the fluid, in which the pipe is moving at $-\mathbf{v}$, energy loss corresponds to the creation of quasiparticle excitations. If a single quasiparticle is produced with momentum $\mathbf{k}$ and energy $\varepsilon(\mathbf{k})$, a Galilean transformation back to the rest frame of the pipe shows that the energy of the fluid is

$$E = E_0 + \mathbf{k} \cdot \mathbf{v} + \varepsilon(\mathbf{k}) \,, \tag{15}$$

where E_0 is the initial ground state energy of the condensate at rest. In order for the fluid to lose energy via the spontaneous creation of collective excitations, $\mathbf{k} \cdot \mathbf{v} + \varepsilon(\mathbf{k})$ must be negative. This can only occur if the velocity is greater than the Landau critical velocity, defined as

$$v_c \equiv \min_{\mathbf{k}} \frac{\varepsilon(\mathbf{k})}{|\mathbf{k}|} \,. \tag{16}$$

For a general dispersion relation $\varepsilon(\mathbf{k})$, this critical velocity may well be zero. However, the distinguishing feature of a superfluid excitation spectrum is a non-zero Landau critical velocity. Take, for example the measured spectrum of helium-II shown in Fig. 1. The spectrum begins approximately linearly at low momenta, before exhibiting a kink and a local minimum around 1.9 Å. Since the energy around the local minimum is non-zero, the Landau critical velocity will also be non-zero. Therefore, the fluid will flow without dissipation below this critical velocity. In the case of superfluid helium-4, the low-momentum, approximately linear region of the spectrum of excitations describes phonons, while the local minimum at higher momentum is the roton part of the spectrum. We will return to this helium excitation spectrum later when considering the effects of gravity on quasiparticle excitations in a superfluid.

We do not need to study the measured excitation spectrum of superfluids, however, to develop an effective field theory of superfluidity. We simply make note of the fact that a superfluid is a condensed matter system at finite density that carries a spontaneously broken $U(1)$ charge. We do not specify what the internal $U(1)$ symmetry is, but for concreteness we may think of $U(1)$ phase symmetry associated with conservation of the number of helium-4 atoms in superfluid helium-4. Bose–Einstein condensation underlies the superfluid properties of helium-4, and below a critical temperature, the ground state of a Bose–Einstein condensate is characterized by a finite, macroscopic occupation number, so that the number density operator acquires a non-zero vacuum expectation value (VEV). In other words, the $U(1)$

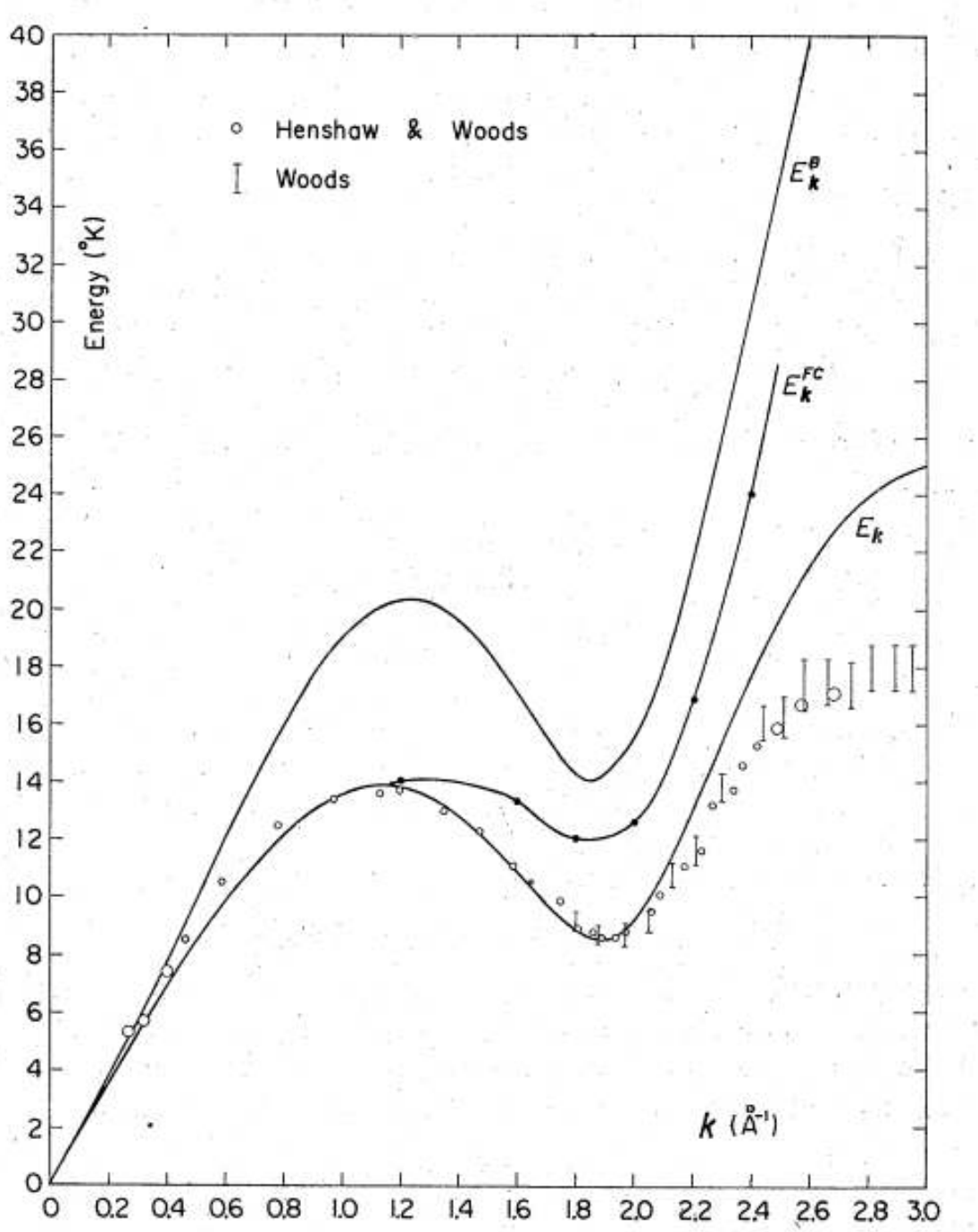

Figure 1: The measured spectrum of excitations in liquid helium II, as reported in [55]. The three curves correspond to phenomenological models considered by the authors of [55].

symmetry associated with the particle number operator is spontaneously broken by the ground state of a Bose–Einstein condensate. Thus, according to our general definition, a condensate has the symmetry-breaking properties of a superfluid.

2.1.1 Superfluidity as a Scalar Field Theory

Although there are different possible descriptions of a quantum field theory with this symmetry-breaking property, we will begin with the simplest implementation involving a single real scalar field ϕ, following Nicolis [45]. We will start from the postulate of spontaneous symmetry breaking, which entails the existence of a gapless excitation mode ϕ, by Goldstone's theorem. This Goldstone boson non-linearly realizes the $U(1)$ symmetry, which acts on the scalar field via constant shifts:

$$\phi \to \phi + a\,, \quad a = \text{const}\,. \tag{17}$$

We furthermore assume that the dynamics of the system at low energy involve only this single degree of freedom. The effective low-energy Lagrangian is constructed as the most general function of $U(1)$-invariant structures involving ϕ, and simultaneously compatible with the Poincaré invariance of space-time, organized as a derivative expansion to focus on the low-energy dynamics. The simplest invariant operator that we must consider, at lowest order in derivatives, is

$$X \equiv -c^2 \partial_\mu \phi \partial^\mu \phi\,, \tag{18}$$

where we included an overall factor of $-c^2$ for our future convenience in studying non-relativistic superfluids. The Lagrangian can therefore be written

$$\mathcal{L} = P(X)\,, \tag{19}$$

and the function $P(X)$ is left unspecified. It is a generic smooth function of the invariant X. We can calculate the Noether current associated with the $U(1)$ symmetry from the

Lagrangian:

$$j_\mu = \frac{\partial P(X)}{\partial(\partial^\mu \phi)} = -2P_X(X)\partial_\mu \phi \,, \tag{20}$$

where P_X represents the first derivative of P with respect to X. The $\mu = 0$ component of the current is, of course, the charge density associated with the $U(1)$ symmetry, so in order for the ground state to be at finite charge density, it must be the case that the VEV of ϕ has a non-zero time derivative. It is sufficient to consider the case where the time derivative of $\langle\phi\rangle$ is constant to achieve non-zero constant charge density. In other words,

$$\langle\phi\rangle = \mu t \,, \tag{21}$$

where the constant of proportionality μ has the interpretation of chemical potential (in a relativistic sense) [46]. It is equal to $\mu = \mu_0 + mc^2$, where μ_0 is the usual non-relativistic chemical potential, which is much less than mc^2. The proper interpretation of m is, of course, the mass of the microscopic constituents of the superfluid. In the ground state, the quantity X is equal to the square of the local relativistic chemical potential μ.

As we will see, the notation $P(X)$ was aptly chosen because the quantity P has can be interpreted thermodynamically as the pressure of the system. In order to see this, we allow the background geometry to fluctuate and vary the action,

$$S = \int d^4x\sqrt{-g}\, P\left(-c^2 g^{\mu\nu}\partial_\mu\phi\partial_\nu\phi\right) \,, \tag{22}$$

with respect to the inverse metric tensor $g^{\mu\nu}$ in order to calculate the (gravitational) energy–momentum tensor on the background flat geometry.

$$\begin{aligned} T_{\mu\nu} &= -\frac{2}{\sqrt{-g}}\,\frac{\delta S}{\delta g^{\mu\nu}}\bigg|_{g^{\mu\nu}=\eta^{\mu\nu}} \\ &= P(X)\eta_{\mu\nu} + 2c^2 P_X(X)\partial_\mu\phi\partial_\nu\phi \,. \end{aligned} \tag{23}$$

Then denoting the background values of X, $P(X)$, and $P_X(X)$ (at $X = \mu^2$) by X, P, and P_X, respectively, we find that the value of the energy–momentum tensor evaluated on the background is given by

$$\langle T_{00} \rangle = -P + 2P_X X \,, \quad \langle T_{0i} \rangle = 0 \,, \quad \langle T_{ij} \rangle = P\delta_{ij} \,. \tag{24}$$

Since the diagonal entries of the spatial part of the energy–momentum tensor of a fluid are equal to the pressure in the fluid's rest frame, we see that $P(X)$ can indeed be given a thermodynamic interpretation as the pressure in the superfluid. The 00 component of the energy–momentum tensor is equal to the energy density ϵ. Therefore, we see that a given equation of state of the superfluid determines the Lagrangian of the theory in our formulation. In addition, if we identify the energy–momentum tensor in Eq. (23) with the standard energy–momentum tensor of a perfect fluid in equilibrium,

$$T_{\mu\nu} = P\eta_{\mu\nu} + (\epsilon + P)\,\frac{u_\mu u_\nu}{c^2} \,, \tag{25}$$

where u_μ is the bulk velocity field, we find that the velocity is equivalent to

$$u_\mu = -c^2 \frac{\partial_\mu \phi}{\sqrt{X}} \,. \tag{26}$$

We used the fact that $\epsilon = -P + 2P_X X$. The negative sign is chosen to match the convention for potential flow. Since the velocity is the gradient of ϕ up to an overall normalization factor, the flow obeys a relativistic generalization of the irrotationality condition, as expected for a superfluid. Incidentally, conformal superfluids, for which $T^\mu{}_\mu = 0$, are of interest in holographic applications [56, 57]. From Eq. (23), we see that conformal superfluids are constrained to have the pressure as a function of chemical potential given by

$$4P(X) - 2XP_X(X) = 0 \implies P(X) \propto X^2 \,. \tag{27}$$

If we are interested in a theory in $d+1$ dimensions, a conformal superfluid will then have $P(X) \propto X^{(d+1)/2}$.

We now introduce small perturbations from the ground state. We perturb the scalar field about the background:

$$\phi = \mu(t + \pi)\,, \tag{28}$$

where $\pi(\mathbf{x}, t)$ is treated as a small perturbation. Then the invariant X becomes

$$X = \mu^2 \left[(1 + \dot{\pi})^2 - c^2(\boldsymbol{\nabla}\pi)^2\right]. \tag{29}$$

It will be useful for us to compute the action expanded to cubic order in small fluctuations, neglecting boundary terms from integration by parts. The resulting cubic action is

$$S_3 = \frac{\mu n c^2}{c_s^2} \int dt\, d^3x \left[\frac{1}{2}\dot{\pi}^2 - \frac{c_s^2}{2}\left(\boldsymbol{\nabla}\pi\right)^2 + \frac{g}{3}\dot{\pi}^3 - \frac{c^2}{2}\left(1 - \frac{c_s^2}{c^2}\right)\dot{\pi}\left(\boldsymbol{\nabla}\pi\right)^2\right] \tag{30}$$

The number density n, speed of sound c_s, and non-linear coupling constant g are given by combinations of derivatives of P, evaluated on the background $\phi = \mu t$. Explicitly, these quantities can be written as

$$n = \frac{dP}{d\sqrt{X}} = \frac{dP}{d\mu}\,, \tag{31}$$

$$c_s^2 = \frac{c^2 P_X}{P_X + 2P_{XX}X} = \frac{c^2 dP/d\mu}{\mu\, d^2P/d\mu^2}\,, \tag{32}$$

$$g = \frac{c^2}{2c_s^2}\left(1 - \frac{c_s^2}{c^2}\right) - \frac{\mu}{c_s}\frac{dc_s}{d\mu}\,. \tag{33}$$

The quantity P_{XX} is the second derivative of P with respect to X, evaluated on the background. It is straightforward to show that the combination $\mu n c_s$ determines the strong coupling cutoff scale of this theory of phonons [21, 58]. In particular, the cutoff momentum scale $k_\star$ of this theory is given by $(\mu n c_s/c^2)^{1/4}$, so that the overall cutoff energy scale Λ of

the theory is

$$\Lambda = c_s \left(\frac{\mu n c_s}{c^2} \right)^{1/4} . \tag{34}$$

In addition, we will later find it useful to expand the energy–momentum tensor component T_{00} to quadratic order in small fluctuations:

$$T_{00} = \frac{\mu n c^2}{c_s^2} \left[\dot{\pi} + \frac{c^2}{2c_s^2} \left(1 - \frac{2\mu c_s}{c^2} \frac{dc_s}{d\mu} \right) \dot{\pi}^2 - \frac{c^2}{2} \left(1 - \frac{2c_s^2}{c^2} \right) (\boldsymbol{\nabla} \pi)^2 \right] . \tag{35}$$

We will use this result in subsequent calculations.

2.1.2 Dual Two-Form Field Description of Superfluidity

In certain contexts, it will be useful to work with a slightly more complicated dual description of a superfluid that exchanges the scalar field for a two-form. This is particularly helpful when considering the interaction between bulk superfluid modes and vortex lines or vortex rings [49,58]. The dual formulation in terms of two-forms has also been used to study a Wess–Zumino-type term in the effective field theory of a two-dimensional superfluid that cannot be described by a local action in the scalar field formulation [59, 60]. Legendre transform techniques allow us to easily switch between dual descriptions. Indeed, it has long been established [61] that any theory of a scalar field with symmetry under constant shifts in $3+1$ dimensions admits just such a dual description in terms of a two-form field $\mathcal{A}_{\mu\nu}$. That two-form is then invariant under corresponding local gauge transformations of the form

$$\mathcal{A}_{\mu\nu} \to \mathcal{A}_{\mu\nu} + \partial_{[\mu}\xi_{\nu]}\,. \tag{36}$$

In $d+1$ dimensions, a scalar field has an analogous dual description in terms of a $d-1$-form field $\mathcal{A}_{\mu_1\cdots\mu_{d-1}}$ [49, 62]. To see this in the $3+1$-dimensional case, let us consider an action for a one-form field U_μ and a two-form field $\mathcal{A}_{\mu\nu}$:

$$\begin{aligned} S &= \int d^4x\, \left[P(X) - F^\mu U_\mu\right]\,, \\ X &\equiv \sqrt{-U_\mu U^\mu}\,, \quad F^\mu \equiv \frac{1}{2}\epsilon^{\mu\nu\rho\sigma}\partial_\nu \mathcal{A}_{\rho\sigma}\,. \end{aligned} \tag{37}$$

The field F^μ is gauge invariant, and it plays a role similar to that of the dual field strength tensor in electrodynamics. Since the two form $\mathcal{A}_{\mu\nu}$ appears only once in this action, it is essentially a Lagrange multiplier. Varying the action with respect to the two-form, we find an equation of motion

$$\partial_\mu U_\nu - \partial_\nu U_\mu = 0\,. \tag{38}$$

A simple solution to this equation of motion is $U_\mu = -c\,\partial_\mu\phi$, where ϕ is a scalar and the constant of proportionality $-c$ was chosen for convenience. Substituting this back into the action, we recover the same action that we found for the superfluid, up to an irrelevant boundary term, upon identifying the function P in this action with the one we used to study the superfluid. This action describes the same dynamics as that of the superfluid.

We may just as well decide to integrate out the one-form U_μ, rather than the two-form. This can be accomplished by varying the action with respect to U_μ and solving its classical equation of motion,

$$\frac{P'(X)}{X}U_\mu + F_\mu = 0\,. \tag{39}$$

Multiplying by F^μ gives

$$P'(X)^2 + F_\mu F^\mu = 0 \implies P'(X) = \sqrt{-F_\mu F^\mu} \equiv \sqrt{Y}\,. \tag{40}$$

Substituting the classical solution of U_μ into the original action, we find

$$S = \int d^4x\,[P(X) - XP'(X)] \equiv \int d^4x\,G(Y)\,. \tag{41}$$

This new form of the action uses the two-form field $\mathcal{A}_{\mu\nu}$ to describe the same dynamics as the action of the superfluid we considered previously. Recalling that we identified $P'(X)$ with the number density n, we see that the invariant Y containing the two-form field has the physical interpretation of n^2. Notice that Eq. (39) provides a completely local relationship between $F_\mu \sim \partial\mathcal{A}_{\mu\nu}$ and $U_\mu \sim \partial\phi$, in other words, between derivatives of the two-form field and derivatives of the scalar field. There is no such local relationship between the fields themselves, however. The precise relation between ϕ and $\mathcal{A}_{\mu\nu}$ is highly non-local, as is typically the case in dual field theoretic descriptions [49].

The superfluid action in dual two-form language still has gauge invariance under trans-

formations of the type in Eq. (36). We may specify the gauge from the action by adding a gauge-fixing term that we choose to write as

$$S_{\rm gf} \propto -\frac{1}{2\xi}\int d^4x\, \left(\partial_i \mathcal{A}^{i\mu}\right)^2 , \tag{42}$$

where ξ is an unspecified positive parameter. Since the gauge symmetry is Abelian, adding such a term fixes the gauge in the path integral and there is no need to introduce ghost fields to compute amplitudes in this theory. Whenever we will deal with the dual superfluid description in the future, a gauge-fixing term in the action will be understood, but there is no need to dwell on this detail further at the moment.

It is important to understand the symmetry-breaking pattern in this dual superfluid language. In the scalar field formulation, we have a Lorentz-violating background configuration with a time-dependent VEV $\langle\phi\rangle = \mu t$. To relate this to the dual description, let us first calculate the energy–momentum tensor in this language. We find $T_{\mu\nu} = p\eta_{\mu\nu} + (\epsilon + p)u_\mu u_\nu/c^2$, where now

$$\epsilon = -G(Y)\,, \quad p = G(Y) - 2YG'(Y)\,, \quad u_\mu = -\frac{cF_\mu}{\sqrt{Y}}\,. \tag{43}$$

Comparing the four-velocity to the one we found in the scalar theory, we can immediately make the identification

$$\frac{F_\mu}{\sqrt{Y}} = \frac{c\partial_\mu\phi}{\sqrt{X}}\,. \tag{44}$$

On the background then, if $\bar{n} = \left\langle \sqrt{Y} \right\rangle$ is the equilibrium number density, we must have

$$\langle F_0 \rangle = \bar{n} = -\frac{1}{2}\epsilon_{ijk}\partial_i \langle \mathcal{A}_{jk} \rangle\ , \tag{45}$$

$$\langle F_i \rangle = 0 = -\frac{1}{2}\epsilon_{ijk}\partial_t \langle \mathcal{A}_{jk} \rangle + \epsilon_{ijk}\partial_j \langle \mathcal{A}_{0k} \rangle\ . \tag{46}$$

We can use gauge freedom to set $\langle \mathcal{A}_{0i} \rangle$ to zero, leaving the solution

$$\langle \mathcal{A}_{ij} \rangle = -\frac{1}{3}\bar{n}\epsilon_{ijk}x^k\,, \quad \langle \mathcal{A}_{0i} \rangle = 0\,. \tag{47}$$

The next step for us will be to introduce fluctuations about the background via two three-vectors, $\mathbf{A}$ and $\mathbf{B}$. We parametrize the fluctuations in such a way that both $\mathbf{A}$ and $\mathbf{B}$ will have regular propagators in the non-relativistic limit:

$$\mathcal{A}_{0i}(x) = \frac{\bar{n}}{c}A_i(x)\,, \quad \mathcal{A}_{ij}(x) = \bar{n}\epsilon_{ijk}\left[-\frac{1}{3}x^k + B_k(x)\right]\,. \tag{48}$$

With this parametrization, the invariant quantity Y becomes

$$Y = \bar{n}^2\left[(1 - \boldsymbol{\nabla}\cdot\mathbf{B})^2 - \frac{1}{c^2}\left(\dot{\mathbf{B}} - \boldsymbol{\nabla}\times\mathbf{A}\right)^2\right]\,. \tag{49}$$

We can use this expression to expand the action (now without the gauge-fixing term) to cubic order in the small fluctuation fields A_i and B_i. We find that the cubic action for these fields can be written as[3]

$$\begin{aligned} S_{\text{bulk}} = \frac{\bar{w}}{2c^2}\int dt\, d^3x \Bigg[& (\boldsymbol{\nabla}\times\mathbf{A})^2 + \dot{\mathbf{B}}^2 - c_s^2\,(\boldsymbol{\nabla}\cdot\mathbf{B})^2 \\ & + \left(1 - \frac{c_s^2}{c^2}\right)(\boldsymbol{\nabla}\cdot\mathbf{B})\left(\dot{\mathbf{B}} - \boldsymbol{\nabla}\times\mathbf{A}\right)^2 - \frac{\bar{g}c_s^2}{3}\,(\boldsymbol{\nabla}\cdot\mathbf{B})^3\Bigg]\,, \end{aligned} \tag{50}$$

which determines the dynamics of bulk modes in the superfluid. We defined the background enthalpy density $\bar{w} = \epsilon + p$, the velocity of sound $c_s = \sqrt{dp/d\rho}$, and the cubic coupling

[3]The bulk action reported in [1] is missing the final cubic term. It is irrelevant for the leading-order behavior of vortices in a trapped superfluid condensate, but it turns out to be crucially important when studying the non-linear interactions of superfluid phonons, as we will do in Section A.

constant $\bar{g}$ of the $(\boldsymbol{\nabla}\cdot\mathbf{B})^3$ term as

$$\begin{aligned} \bar{w} &\equiv -2\bar{n}^2 G'(\bar{n}^2)\,, \quad \frac{c_s^2}{c^2} \equiv 1 + \frac{2\bar{n}^2 G''(\bar{n}^2)}{G'(\bar{n}^2)}\,, \\ \bar{g} &\equiv 1 - \frac{c_s^2}{c^2} - \frac{4\bar{n}^2}{c_s} c_s'(\bar{n}^2)\,. \end{aligned} \tag{51}$$

Notice that we implicitly chose a gauge in which the $\mathbf{A}$ field is purely transverse and the $\mathbf{B}$ field is longitudinal—see Horn *et al.* [49] for a more detailed explanation. Since $\mathbf{B}$ is a field that propagates longitudinally at the velocity of sound c_s, we can identify it with the phonon field in the fluid. The transverse mode $\mathbf{A}$ is non-propagating and constrained by the equations of motion, although it can still mediate long-range interactions in this theory. It plays a role similar to that of the vector potential in electrodynamics, and for this reason, it has been dubbed the "hydrophoton" field [63]. In terms of the phonon and hydrophoton fields, the bulk velocity in the superfluid, $u_i = -cF_i/n$, becomes

$$\mathbf{u} = \frac{\dot{\mathbf{B}} - \boldsymbol{\nabla}\times\mathbf{A}}{1 - \boldsymbol{\nabla}\cdot\mathbf{B}}\,, \tag{52}$$

to leading order. It will also be useful for us to write down their propagators for future reference:

$$G_A^{ij}(\omega,\mathbf{k}) = \frac{ic^2}{\bar{w}}\frac{\delta_{ij} - \hat{k}_i\hat{k}_j}{k^2}\,, \quad G_B^{ij}(\omega,\mathbf{k}) = \frac{ic^2}{\bar{w}}\frac{\hat{k}_i\hat{k}_j}{\omega^2 - c_s^2 k^2}\,. \tag{53}$$

Although not written out in the above expressions, the $i\epsilon$ prescription is implied. Note that the propagators of both fields come with an extra factor of $c^2/\bar{w}$ because the fields in the action Eq. (50) are not canonically normalized. It is straightforward to work out the Feynman rules and calculate scattering amplitudes for processes involving phonons and non-dynamical hydrophoton modes. We will do so later on when considering the interactions of vortex lines with the superfluid bulk modes.

2.2 Fluids

The hydrodynamics of fluids has long been studied and well understood at the level of equations of motion derived from the conservation of energy and momentum, with phenomenological modifications to account for dissipative and viscous effects. What ordinary hydrodynamics fails to do is account for either thermal or quantum fluctuations, which are ubiquitous and highly relevant when considering certain types of critical behavior, long-range correlations around dynamical flows, non-equilibrium states, non-linear interactions of sound, and corrections to classical behavior [33,64,65]. Effective field theory naturally lends itself as a simple framework for incorporating the effects of fluctuations into ordinary hydrodynamics, with the added bonus of accounting for relativistic effects from the outset. The program of reformulating fluid dynamics from a relativistic action principle has a long and fruitful history [66–69]. The modern effective field theory of a perfect, dissipationless fluid, giving rise to the Euler equations in the non-relativistic limit, is now well known. It was developed in Dubovsky *et al.* [4,70] and Endlich *et al.* [21]. Dissipative effects, however cannot arise directly from a local, Lorentz invariant action principle for fluctuation fields in a fluid. A more recent program has seen numerous studies of the quantum origins of viscosity in a modified effective field theory framework, typically involving Schwinger–Keldysh closed-time path formalism to account for non-equilibrium dynamics—see Grozdanov & Polonyi [71], Torrieri [72], and Crossley *et al.* [33]. Alternatively, one can explicitly neglect certain degrees of freedom in the theory of the perfect fluid, essentially carrying out a coarse-graining procedure, in order to introduce dissipative effects [73]. For our purposes, we need not consider dissipation or viscous effects; perfect fluid theory will suffice.

Our primary goal in this section is to review the effective field theory of a perfect fluid, following the notation of Dubovsky *et al.* [70] and development by Endlich *et al.* [21], in order to lay out the theory in sufficient detail for subsequent use in calculations. We consider a fluid with volume elements labeled by co-moving, or Lagrangian, coordinates ϕ^I. The Lagrangian coordinates depend on time t and physical, or Eulerian, position coordinates $\mathbf{x}$, occupied by

the fluid element at that time. We thus have three scalar functions of spatial coordinates and time,

$$\phi^I = \phi^I(\mathbf{x}, t)\,, \quad I = 1, 2, 3\,. \tag{54}$$

Although one could easily invert this and formulate a field theory of hydrodynamics in terms of Eulerian coordinates, this approach turns out to be more useful when implementing Poincaré invariance. We will formulate the theory relativistically, even though Galilei symmetry is more relevant in laboratory settings. However, there is no reason to approximate from the beginning, as it does not lead to any helpful simplifications. We will treat the coordinates ϕ^I as scalar fields under the space-time symmetries of the Poincaré group. We choose to consider a system for which the static and homogeneous "ground state" at some given pressure picks out a definite configuration such that the Lagrangian and Eulerian coordinates are aligned:

$$\left\langle \phi^I \right\rangle \propto x^I\,. \tag{55}$$

The system will have the symmetries of a fluid if we impose a number of internal (rather than Poincaré) symmetries. In particular, the dynamics must be symmetric under constant shifts and internal $SO(3)$ rotations in order for the fluid to be homogeneous and isotropic. The corresponding symmetry transformations are

$$\phi^I \to \phi^I + a^I\,, \tag{56}$$

$$\phi^I \to O^I{}_J\, \phi^J\,, \tag{57}$$

where a^I is constant and $O^I{}_J$ is an $SO(3)$ rotation matrix. There is one additional symmetry we need to implement for this theory to describe a fluid, namely invariance under volume-preserving diffeomorphisms. This symmetry has the effect of making the dynamics invariant

under the rearrangement of fluid elements without compression or expansion of the elements. While the fluid is resistant to compression or expansion, there are no transverse shear stresses as in a solid. The symmetry under volume-preserving diffeomorphisms is implemented as follows:

$$\phi^I \to \xi^I(\phi^J)\,, \quad \det \frac{\partial \xi^I}{\partial \phi^J} = 1\,. \tag{58}$$

Following the standard effective field theory logic, we construct the Lagrangian by building quantities from the scalar fields ϕ^I that are invariant under the symmetry transformations of Eqs. (56) to (58), and we organize it as a long-wavelength derivative expansion with terms with the fewest number of derivatives coming in at lowest order. Symmetry under shifts, Eq. (56), requires that the fields ϕ^I always enter the Lagrangian with at least one derivative ∂_μ. Poincaré symmetry requires that at lowest order, the effective Lagrangian must depend only on the matrix B^{IJ}, defined as

$$B^{IJ} \equiv \partial_\mu \phi^I \partial^\mu \phi^J\,. \tag{59}$$

Furthermore, symmetry under internal rotations, Eq. (57), requires that the Lagrangian depend only on $SO(3)$-invariant terms involving B^{IJ}. We can form three different mutually independent $SO(3)$ invariants—for example, $\mathrm{tr}\, B$, $\mathrm{tr}\, B^2$, and $\mathrm{tr}\, B^3$. We may exchange one of those invariants for the determinant of B^{IJ}, since

$$\det B^{IJ} = \frac{1}{6}\left[(\mathrm{tr}\, B)^3 - 3(\mathrm{tr}\, B)(\mathrm{tr}\, B^2) + 2(\mathrm{tr}\, B^3)\right]\,. \tag{60}$$

After imposing symmetry under volume-preserving diffeomorphisms, Eq. (58), we are left with only functions of the determinant. It will be convenient to work with the quantity $b \equiv \sqrt{\det B^{IJ}}$. We therefore conclude that the Lagrangian describing a perfect fluid can be

written as a generic function of b, so that the action is

$$S = -w_0 \int dt\, d^3x\, f(b)\,. \tag{61}$$

We choose to pull out a constant w_0 that has units of mass density. It will be convenient to choose w_0 to be proportional to $1/c^2$ times the background of the relativistic enthalpy density, $\epsilon + p$, where ϵ is the energy density and p is the pressure. To compute the energy–momentum tensor of the fluid, we will need to rewrite the action as $S = -\int dt\, d^3x\, \sqrt{-g} f\left(\sqrt{\det g^{\mu\nu}\partial_\mu\phi^I\partial_\nu\phi^J}\right)$ and perturb the metric. The resulting (gravitational) energy–momentum tensor has the form

$$T_{\mu\nu} = w_0\left[-f(b)\eta_{\mu\nu} + bf'(b)B^{-1}_{IJ}\partial_\mu\phi^I\partial_\nu\phi^J\right]\,. \tag{62}$$

Comparing to the standard form of the energy–momentum tensor of a perfect fluid, *i.e.* $T_{\mu\nu} = \eta_{\mu\nu}p + (\epsilon + p)u_\mu u_\nu/c^2$, where u_μ is the bulk velocity field, we make the identifications

$$\epsilon = w_0 f(b)\,, \tag{63}$$

$$p = w_0\left[-f(b) + bf'(b)\right]\,, \tag{64}$$

$$u^\mu = \frac{c}{6b}\epsilon^{\mu\nu\rho\sigma}\epsilon_{IJK}\partial_\nu\phi^I\partial_\rho\phi^J\partial_\sigma\phi^K\,. \tag{65}$$

We will choose the normalization in this theory such that w_0 is equal to $1/c^2$ on the background times the ground state enthalpy density, scaled by the background value of $1/b$, so that $df/db = c^2$ on the background. We will use this normalization condition implicitly in subsequent calculations.

Phonons appear in the theory when we consider fluctuations around the ground state, which breaks the overall symmetry group down to an unbroken combination of spatial and

internal transformations. We will choose to write the VEV of the fields ϕ^I as

$$\langle \phi^I \rangle = \sqrt[3]{b_0}\, x^I \,, \tag{66}$$

where b_0 is a dimensionless quantity. Although b_0 is dimensionless, it can be thought of as an overall compression factor that stretches or compresses the fluid uniformly in response to changes in external pressure. The cube root is chosen for the quantity b to correspond to b_0 on the background. Fluctuating about the VEV, we have

$$\phi^I = \sqrt[3]{b_0}\left(x^I + \pi^I\right) \,, \tag{67}$$

where π^I are small perturbing fields. We expand the action to cubic order in perturbations to find

$$\begin{aligned} S_3 = w_0 b_0 \int dt\, d^3x \Bigg[& \frac{1}{2}\dot{\boldsymbol{\pi}}^2 - \frac{c_s^2}{2}\left(\boldsymbol{\nabla}\cdot\boldsymbol{\pi}\right)^2 + \frac{1}{2}\left(1 + \frac{c_s^2}{c^2}\right)\dot{\boldsymbol{\pi}}^2 \boldsymbol{\nabla}\cdot\boldsymbol{\pi} - \dot{\pi}_i \dot{\pi}_j \partial_i \pi_j \\ & - g_3 \left(\boldsymbol{\nabla}\cdot\boldsymbol{\pi}\right)^3 + \frac{c_s^2}{2}\left(\boldsymbol{\nabla}\cdot\boldsymbol{\pi}\right)\partial_i \pi_j \partial_j \pi_i \Bigg] \,. \end{aligned} \tag{68}$$

We defined

$$c_s^2 \equiv b_0 f''(b_0) \,, \tag{69}$$

$$g_3 \equiv \frac{1}{3}\left[c_s^2 + b_0 c_s c_s'(b_0)\right] \,. \tag{70}$$

This will be of use later. Notice that we stopped differentiating between upper-case (internal) indices and lower-case (spatial) indices. That is because the ground state $\langle \phi^I \rangle = \sqrt[3]{b_0} x^I$ breaks the full symmetry under internal and spatial rotations down to a diagonal subgroup, so that any equations of motion derived from the cubic action in Eq. (68) will be invariant under combined rotations that are elements of the unbroken diagonal subgroup. There is no need to distinguish between these two sets of indices any longer. For reference, we also

expand the energy density to quadratic order:

$$T_{00} = w_0 b_0 c^2 \left[\boldsymbol{\nabla} \cdot \boldsymbol{\pi} + \frac{1}{2c^2} \dot{\boldsymbol{\pi}}^2 + \frac{1}{2} \left(1 + \frac{c_s^2}{c^2} \right) (\boldsymbol{\nabla} \cdot \boldsymbol{\pi})^2 - \frac{1}{2} \partial_i \pi_j \partial_j \pi_i \right] . \tag{71}$$

This will be useful when we study the interaction of sound waves in fluids with gravity later on.

Incidentally, now that we know the action of a fluid in the EFT framework, we can return to thinking about superfluids, this time at finite temperature. At non-zero but small temperatures T, liquid helium, for example, has an ordinary fluid helium-I component and a superfluid helium-II component that coexist. The general Lagrangian of a superfluid at finite temperature but low energy is a combined function of the two invariants b and X, as well as one additional invariant that couples the two components and is compatible with the symmetries in question,

$$y = \frac{1}{6b} \epsilon^{\mu\nu\rho\sigma} \epsilon_{ijk} \partial_\mu \psi \partial_\nu \phi^i \partial_\rho \phi^j \partial_\sigma \phi^k \,, \tag{72}$$

where ψ is the superfluid component phase and ϕ^I are the ordinary fluid co-moving coordinates. This is the same invariant quantity we encountered when studying the symmetries of a supersolid in Eq. (10). It represents the direct coupling of the superfluid component to the velocity field of the ordinary fluid. We can therefore write the general action of a finite-temperature superfluid, with both superfluid and ordinary fluid components, as

$$S_{T>0} = \int dt \, d^3x \, F(X, b, y) \,. \tag{73}$$

The fields ψ and ϕ^I can be expanded about their VEVs, $\langle \psi \rangle \propto t$ and $\phi^I \propto x^I$, in order to obtain an effective action for phonons in this medium. In this expansion, one finds that there is generally mixing between the gradient energy of phonons $\delta\phi^I$ and the kinetic energy of the superfluid component $\delta\psi$. Diagonalization is possible for generic equations of state,

leading to two distinct, non-dispersive propagating solutions to the wave equation that are combinations of $\delta\psi$ and the longitudinal component of $\delta\phi^I$, as long as solutions can be found for the secular equation for eigenfrequencies ω_k [45],

$$\det \begin{pmatrix} b_0^2 F_{bb} k^2 - (b_0 F_b - y_0 F_y)\,\omega_k^2 & -y_0\,(F_y - b_0 F_{by} - 2b_0 y_0 F_{bX})\,k\omega_k \\ -y_0\,(F_y - b_0 F_{by} - 2b_0 y_0 F_{Xb})\,k\omega_k & y_0^2\,[(2F_X + F_{yy}) + 4y_0 F_{Xy} + 4y_0^2 F_{XX}]\,\omega_k^2 \\ & +2y_0^2 F_X k^2 \end{pmatrix} = 0\,, \tag{74}$$

where the subscripts X, b, y represent partial derivatives of the Lagrangian with respect to those arguments.

2.3 Solids

The low-energy effective field theory of a solid is a straightforward generalization of the framework developed for a fluid in the previous section. From the effective field theory viewpoint, a fluid is simply a solid with highly enhanced symmetry, as shown in, for example, Nicolis *et al.* [16] and Endlich *et al.* [74]. The notation we will use is largely drawn from the latter reference.

The starting point is, once again, a set of three scalar fields, ϕ^I $(I = 1, 2, 3)$, associated with the co-moving (Lagrangian) coordinates of volume elements in the solid. As before, the ground state picks out a configuration in which Lagrangian and Eulerian coordinates become aligned. We will once again use the normalization $\langle \phi^I \rangle = \sqrt[3]{b_0}\, x^I$ for the VEV of the scalar fields, where, as before, b_0 represents the degree of overall compression or dilation of the solid. The internal symmetry of the scalars is $ISO(3)$ as usual, but the additional requirement of invariance under volume-preserving diffeomorphisms no longer applies in this case. Solids generally do have shear stresses that resist the free rearrangement of volume elements, unlike in a perfect fluid. The scalars must appear with at least one derivative due to symmetry under constant shifts, $\phi^I \to \phi^I + a^I$. Poincaré invariance dictates that invariant quantities must be built out of the combination $B^{IJ} = \partial_\mu \phi^I \partial^\mu \phi^J$, as we are again organizing the effective theory as a low-energy derivative expansion. The determinant of B^{IJ} is not the only invariant quantity under all relevant symmetries in this case. We can now have three linearly independent $SO(3)$-invariant combinations of B^{IJ}, if we are interested in a solid that is isotropic at large distances. We will find it convenient to work with the following invariant quantities:

$$b \equiv \sqrt{\det B}\,, \quad Y \equiv \frac{\operatorname{tr} B^2}{(\operatorname{tr} B)^2}\,, \quad Z \equiv \frac{\operatorname{tr} B^3}{(\operatorname{tr} B)^3}\,. \tag{75}$$

Of these three invariants, only b contains the parameter b_0 and is therefore sensitive to the overall level of compression or dilation of the solid. Also, after introducing small fluctuations

of ϕ^I about the VEV via $\phi^I = \sqrt[3]{b_0}\left(x^I + \pi^I\right)$, expanding the three invariant quantities in small fluctuations shows that only b begins at linear order in the fields π^I; the quantities Y and Z both begin at quadratic order. These are the only invariants we must consider if we are interested in a solid that is isotropic at large distances, but if we want to build a theory of a solid with a discrete symmetry point group, a more careful analysis is needed, since the invariants we use must be unchanged under the discrete symmetry transformations of the point group. We will encounter an example of a theory of a solid with cubic symmetry later in this work.

Our Lagrangian will now be a generic function of b, Y, and Z, which we choose to normalize in the same way as the fluid, pulling out an overall constant w_0 with units of mass density. The general action of the solid is

$$S = -w_0 \int dt\, d^3x\, f(b, Y, Z)\,. \tag{76}$$

We will again choose w_0 to be related to the enthalpy density of the ground state in such a way that the first derivative of f with respect to b, denoted $f' \equiv \partial f/\partial b$, is equal to c^2 on the background. Since the internal symmetry group of a perfect fluid is not just a subgroup of $SO(3)$, but the group of volume-preserving diffeomorphisms, we can obtain the effective action of a fluid by simply restricting to functions f whose derivatives with respect to Y and Z are equal to zero.

Let us calculate the (gravitational) energy–momentum tensor of a solid in the usual way—by varying the metric[4] and using $T_{\mu\nu} = -2(-g)^{-1/2}\delta S/\delta g^{\mu\nu}$. Then from the action in

[4]The action we are varying with respect to the metric is a generalization appropriate for a solid

Eq. (76), we find

$$\begin{aligned} T_{\mu\nu} = w_0 \Bigg[& - f(b,Y,Z) g_{\mu\nu} + b f'(b,Y,Z) B^{-1}_{IJ} \partial_\mu \phi^I \partial_\nu \phi^J \\ & + \frac{4}{(\operatorname{tr} B)^2} f_Y(b,Y,Z) B^{IJ} \partial_\mu \phi^I \partial_\nu \phi^J - \frac{4}{\operatorname{tr} B} Y f_Y(b,Y,Z) \partial_\mu \phi^I \partial_\nu \phi^I \\ & + \frac{6}{(\operatorname{tr} B)^3} f_Z(b,Y,Z) B^{IJ} B^{JK} \partial_\mu \phi^I \partial_\nu \phi^K - \frac{6}{\operatorname{tr} B} Z f_Z(b,Y,Z) \partial_\mu \phi^I \partial_\nu \phi^I \Bigg] , \end{aligned} \tag{77}$$

where $f_Y \equiv \partial f / \partial Y$ and $f_Z \equiv \partial f / \partial Z$. As in the case of the fluid, we have the thermodynamic interpretation $\epsilon = w_0 f(b,Y,Z)$, but the presence of shear stresses makes this energy–momentum tensor not directly comparable to that of a fluid.

As before, we introduce small fluctuations π^I, corresponding to longitudinal and transverse phonons, about the ground state via $\phi^I = \sqrt[3]{b_0}(x^I + \pi^I)$. For future reference, it will be useful for us to expand the action of Eq. (76) to cubic order in small fluctuations. The resulting action becomes

$$\begin{aligned} S_3 = w_0 b_0 \int dt\, d^3x \Bigg[& \frac{1}{2} \dot{\boldsymbol{\pi}}^2 - \frac{c_L^2}{2} (\boldsymbol{\nabla} \cdot \boldsymbol{\pi})^2 - \frac{c_T^2}{2} (\boldsymbol{\nabla} \times \boldsymbol{\pi})^2 - g_1 \dot{\boldsymbol{\pi}} \boldsymbol{\nabla} \cdot \boldsymbol{\pi} - g_2 \dot{\pi}_i \dot{\pi}_j \partial_i \pi_j \\ & - g_3 (\boldsymbol{\nabla} \cdot \boldsymbol{\pi})^3 - g_4 (\partial_i \pi_j)^2 \boldsymbol{\nabla} \cdot \boldsymbol{\pi} - g_5 (\boldsymbol{\nabla} \times \boldsymbol{\pi})^2 \boldsymbol{\nabla} \cdot \boldsymbol{\pi} - g_6 \partial_i \pi_j \partial_k \pi_i \partial_k \pi_j \\ & - g_7 \partial_i \pi_j \partial_k \pi_i \partial_j \pi_k \Bigg] . \end{aligned} \tag{78}$$

The longitudinal and transverse sound speeds (c_L and c_T, respectively) and the seven nonlinear (cubic) coupling constants are combinations of derivatives of the function f with

---

in a curved background. Explicitly,

$$\begin{aligned} S &\to -w_0 \int dt\, d^3x \sqrt{-g} f(b,Y,Z) , \\ b &= \sqrt{\det g^{\mu\nu} \partial_\mu \phi^I \partial_\nu \phi^J} , \\ Y &= \frac{g^{\mu\nu} g^{\rho\sigma} \partial_\mu \phi^I \partial_\nu \phi^J \partial_\rho \phi^J \partial_\sigma \phi^I}{(g^{\mu\nu} \partial_\mu \phi^I \partial_\nu \phi^I)^2} , \\ Z &= \frac{g^{\mu\nu} g^{\rho\sigma} g^{\lambda\tau} \partial_\mu \phi^I \partial_\nu \phi^J \partial_\rho \phi^J \partial_\sigma \phi^K \partial_\lambda \phi^K \partial_\tau \phi^I}{(g^{\mu\nu} \partial_\mu \phi^I \partial_\nu \phi^I)^3} . \end{aligned}$$

respect to the invariants b, Y, Z, evaluated on the background. These are defined as

$$c_L^2 = b_0 f'' + \frac{16}{27}\frac{f_Y + f_Z}{b_0}\,, \tag{79}$$

$$c_T^2 = \frac{4}{9}\frac{f_Y + f_Z}{b_0}\,, \tag{80}$$

$$g_1 = -\frac{1}{2} - \frac{c_L^2}{2c^2} + \frac{c_T^2}{c^2}\,, \tag{81}$$

$$g_2 = 1 - \frac{c_T^2}{c^2}\,, \tag{82}$$

$$g_3 = \frac{c_L^2 - c_T^2}{3} + \frac{1}{3}b_0 c_L c_L' - \frac{10}{9}b_0 c_T c_T' + \frac{16}{243}\frac{f_Z}{b_0}\,, \tag{83}$$

$$g_4 = -\frac{c_L^2}{2} + 2b_0 c_T c_T' - \frac{8}{27}\frac{f_Z}{b_0}\,, \tag{84}$$

$$g_5 = \frac{c_L^2 - c_T^2}{2} - b_0 c_T c_T' + \frac{4}{27}\frac{f_Z}{b_0}\,, \tag{85}$$

$$g_6 = c_T^2 + \frac{2}{9}\frac{f_Z}{b_0}\,, \tag{86}$$

$$g_7 = \frac{2}{27}\frac{f_Z}{b_0}\,. \tag{87}$$

In the above equations, the prime ($'$) symbol denotes differentiation with respect to b, and all the derivatives are evaluated on the background. We also implicitly used the normalization condition $f' = c^2$ on the background in the above calculation. Note that the longitudinal and transverse sound speeds are generally different. For ordinary solids (that have $f'' > 0$), we will generally have

$$c_L^2 > \frac{4}{3}c_T^2\,, \tag{88}$$

which is consistent with results in, *e.g.*, Landau *et al.* [75].

It will also be useful for us to calculate the component T_{00} of the energy–momentum tensor and expand to quadratic order in small fluctuations. From the expression in Eq. (77),

we find

$$T_{00} = w_0 b_0 \Bigg[c^2 \boldsymbol{\nabla} \cdot \boldsymbol{\pi} + \frac{1}{2}\dot{\boldsymbol{\pi}}^2 + \frac{c^2}{2} \left(\boldsymbol{\nabla} \cdot \boldsymbol{\pi} \right)^2 - \frac{c^2}{2} \partial_i \pi_j \partial_j \pi_i \\ + \frac{1}{2} \left(b_0 f'' - \frac{4}{27} \frac{f_Y + f_Z}{b_0} \right) \left(\boldsymbol{\nabla} \cdot \boldsymbol{\pi} \right)^2 + \frac{2}{9} \frac{f_Y + f_Z}{b_0} \left((\partial_i \pi_j)^2 + \partial_i \pi_j \partial_j \pi_i \right) \Bigg] . \tag{89}$$

It is straightforward to show that the action in Eq. (78) and the stress–energy tensor component in Eq. (89) reduce to Eq. (68) and Eq. (71), respectively, when we set f_Y and f_Z to zero, recovering the results we found from the effective field theory of a perfect fluid.

2.4 Supersolids

The supersolid state of matter has been both puzzling to theorists and elusive to experimentalists. It is a somewhat paradoxical condensed matter system that exhibits both crystalline order, like ordinary solids, and the dissipationless flow of material elements observed in superfluids. While experiments with ultrapure helium-4 at temperatures far below the lambda point have failed to demonstrate a supersolid transition [76], a series of recent experiments involving dipolar Bose–Einstein condensates indicate that supersolid properties can be supported, at least in transient states characterized by the coexistence of stripe-like spatial modulation and phase coherence [77–79]. Still, the rather contentious question of whether long-lived supersolid states are realized as a fundamental phase of matter is irrelevant from the effective field theory point of view. EFT supersolids are trivial to create, and one need not use dipolar quantum gases; simply submerge a permeable lattice structure in superfluid helium and zoom out to distances much greater than the lattice spacing, and you have effectively created an approximate supersolid.

Let us review the relativistic action for supersolids we found in Eq. (14). There are four scalar fields, the $U(1)$ phase ψ (the superfluid component) and the $ISO(3)$ multiplet ϕ^I (the co-moving coordinates of material elements). In the ground state, these break the global symmetries by taking VEVs

$$\langle \psi \rangle = y_0 t \,, \quad \langle \phi^I \rangle = \sqrt[3]{b_0} x^I \,. \tag{90}$$

The Lagrangian is built out of invariant combinations of

$$X = -\partial_\mu \psi \partial^\mu \psi \,, \tag{91}$$

$$y = \frac{1}{6b} \epsilon^{\mu\nu\rho\sigma} \epsilon_{ijk} \partial_\mu \psi \partial_\nu \phi^i \partial_\rho \phi^j \partial_\sigma \phi^k \,, \tag{92}$$

$$A_i = \partial_\mu \psi \partial^\mu \phi_i \,, \tag{93}$$

$$B_{ij} = \partial_\mu \phi_i \partial^\mu \phi_j \,. \tag{94}$$

As we will not be interested in studying supersolids in the non-relativistic limit, we are setting all factors of c to 1 in this subsection. The quantity y is already manifestly rotationally invariant, since all the spatial indices are contracted. Out of B_{ij}, we can build the usual three independent $SO(3)$ invariants of the solid, $b = \det B$, $Y = (\mathrm{tr}\, B^2)/(\mathrm{tr}\, B)^2$, and $Z = (\mathrm{tr}\, B^3)/(\mathrm{tr}\, B)^3$. Using A_i, we can also form the invariant quantities

$$T \equiv \frac{A_i A^i}{y^2\, \mathrm{tr}\, B}\,, \tag{95}$$

$$U \equiv \frac{A^i A^j B_{ij}}{y^4 (\mathrm{tr}\, B)^2}\,, \tag{96}$$

$$V \equiv \frac{A^i A^j B_{ik} B_{jk}}{y^4 (\mathrm{tr}\, B)^3}\,, \tag{97}$$

$$W \equiv \frac{A^i A^j B_{ik} B_{kl} B_{lj}}{y^4 (\mathrm{tr}\, B)^4}\,. \tag{98}$$

It is simple to show that T is not independent of X, b, Y, Z, and y, so we need not include it in the effective action. To leading order in the derivative expansion, there are no additional invariant terms to consider. We write the action as

$$S_{\text{eff}} = \int d^4x\, F\left(X, b, Y, Z, y, U, V, W\right)\,. \tag{99}$$

A similar action was found by Celoria *et al.* [80], although they used a different parametrization. Naturally, this is a generalization of all the other media we have been studying. Setting to zero all the derivatives of F with respect to Y, Z, U, V, W gives a finite-temperature superfluid; setting to zero derivatives of F with respect to X, y, U, V, W gives a solid; and so on.

Now let us fluctuate the fields about their VEVs by introducing Goldstone fields σ and π_i:

$$\psi = y_0\left(t + \sigma\right)\,, \quad \phi_i = b_0^{1/3}\left(x_i + \pi_i\right)\,. \tag{100}$$

We will only be interested in the effective action at quadratic order. After Taylor expanding the action, we find an expression of the form

$$\begin{aligned} S_{\text{eff}} \simeq \int d^4x \Big\{ & \frac{1}{2}\left[K_N \dot{\boldsymbol{\pi}}^2 - G_L \left(\boldsymbol{\nabla}\cdot\boldsymbol{\pi}\right)^2 - G_T \left(\boldsymbol{\nabla}\times\boldsymbol{\pi}\right)^2\right] \\ & + \frac{1}{2}\left[K_S \dot{\sigma}^2 - G_S \left(\boldsymbol{\nabla}\sigma\right)^2\right] + M\dot{\sigma}\left(\boldsymbol{\nabla}\cdot\boldsymbol{\pi}\right) \Big\}, \end{aligned} \tag{101}$$

where the coefficients are equal to

$$\begin{aligned} K_N &= y_0 F_y - b_0 F_b + \frac{2}{81}\left(9F_U + 3F_V + F_W\right) , \\ G_L &= -b_0^2 F_{bb} - \frac{16}{27}\left(F_Y + F_Z\right) , \\ G_T &= -\frac{4}{9}\left(F_Y + F_Z\right) , \\ K_S &= 2y_0^2 F_X + 4y_0^4 F_{XX} + y_0^2 F_{yy} + 4y_0^3 F_{Xy} , \\ G_S &= 2y_0^2 F_X - \frac{2}{81}\left(9F_U + 3F_V + F_W\right) , \\ M &= -y_0 F_y + 2y_0^2 b_0 F_{Xb} + y_0 b_0 F_{by} - \frac{2}{81}\left(9F_U + 3F_V + F_W\right) . \end{aligned} \tag{102}$$

Following [45], in our terminology K, G, M, N, L, T, and S respectively stand for "kinetic energy," "gradient energy," "mixing," "normal component," "longitudinal polarization," "transverse polarization," and "superfluid component." This may seem like a very complicated expression, but the qualitative nature of the dynamics is clear from the structure of the action. There is a propagating transverse excitation mode of ordinary matter in the supersolid, whose sound speed is $c_T^2 = G_T/K_N$. This component is completely decoupled from the superfluid component at the level of the quadratic action, although there will be interactions between both components at higher order. The longitudinal phonon mode gets mixed with the superfluid component, however. As in the case of the finite-temperature superfluid, barring extraordinary cancellations due to a special equation of state, we expect to be able to diagonalize the longitudinal phonon–superfluid phonon system. In that case, there will again be two propagating non-dispersive modes whose eigenfrequencies ω_k satisfy

the following secular equation:

$$\det \begin{pmatrix} K_N \omega_k^2 - G_L k^2 & M k \omega_k \\ M k \omega_k & K_S \omega_k^2 - G_S k^2 \end{pmatrix} = 0 \,. \tag{103}$$

Like in a finite temperature superfluid, there is both first sound and second sound, corresponding to the eigenfrequencies found by this procedure, but there is also an additional transverse mode in the supersolid that is not present in the superfluid. In principle, we could continue the expansion to higher order and find the leading-order interactions, and we could also compute components of the stress–energy tensor of a supersolid, but the expressions will quickly balloon to extraordinary size due to the number of invariants involved. We will set aside the supersolid at the moment and leave detailed study for the future.

2.5 "Effective String Theory" of Vortex Lines in a Superfluid

When liquid helium-4 is cooled below below the lambda point (roughly 2.17 K) and carries a net angular momentum, vortex lines form spontaneously [81]. In finite-temperature superfluids, these vortices form complicated mesh structures, tracking the background flows; see Fig. 2 for a visualization of this phenomenon created by Bewley *et al.* [82]. The vortex cores are usually around a couple ångströms in thickness in superfluid helium, and the vortices carry circulation that is quantized in units of $\Gamma = \oint \mathbf{v} \cdot d\mathbf{s} = 2\pi\hbar/m$, as first suggested by Onsager [82, 83]. Feynman calculated that when superfluid helium-4 is rotated around an axis with an angular velocity of Ω radians per second, the areal density of vortex lines in the plane parallel to the rotation axis should be close to 2000Ω cm^{-2}, a result now known as "Feynman's rule" [81, 84]. In zero-temperature superfluids, however, the quantized vortices are less complicated structures, typically simple long string-like configurations, sometimes bent or kinked, but not arranged in messy networks. Since Kelvin's theorem [85] states that the convective derivative of the circulation in a perfect fluid must vanish, a vortex line cannot escape from any co-moving contour initially drawn to fully encircle it, no matter how small the contour is [86]. Naïvely, this might imply that vortices remain stationary at all times with respect to the background fluid flow. However, vortices have been observed to precess around the centers of trapped Bose–Einstein condensates. Nilsen *et al.* [87] showed that this naïve argument is erroneous, and the motion of vortex lines with respect to the background flow is compatible with Kelvin's theorem in the case of harmonically trapped, rotating condensates, since small circular contours can become highly deformed over time in the stationary frame of the lab. We will return to the study of vortex precession later. First we must develop a framework for incorporating vortex lines—energetic, highly non-perturbative phenomena—into the low-energy effective theory of superfluids, so that we can study their dynamics.

We will now see how to study the motion of superfluid vortex lines within the effective

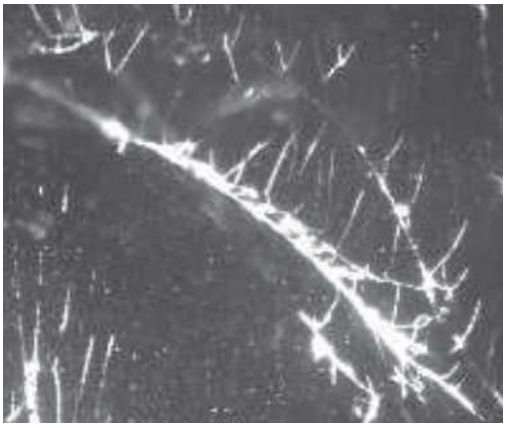

Figure 2: Visualization of quantized vortex cores in superfluid helium-II, as reported in [82].

field theory language we developed in Section 2.1.2. We will use the dual two-form description, since it lends itself more readily to describing interactions with vortex lines. A vortex line can be approximated as an infinitely thin, long string at length scales much larger than the core radius. We can take inspiration from string theory and parametrize its space-time position as $X^\mu(\tau, \sigma)$, where τ and σ are two arbitrary world-sheet coordinates. The dynamics of the vortex line will be invariant under reparametrizations of the world-sheet coordinates. Following the philosophy of effective field theory, we add to the action arbitrary combinations of vortex coordinates X^μ and two-form fields $\mathcal{A}_{\mu\nu}$, localized on the world-sheet of the vortex line, that are invariant under the relevant symmetries of the theory—namely, Poincaré symmetry, local gauge symmetry for the two-form field, and reparametrization invariance of the world-sheet coordinates. Using the two-form language allows us to write Lorentz invariant combinations directly at the level of the potential. We also organize the terms as a derivative expansion and keep only those terms with the fewest number of derivatives acting on the vortex line position, which is assumed to move slowly at low energy.

Following the formalism introduced by Horn *et al.* [49], we can immediately write down a contribution to the action that is the analogue of the action of a relativistic string coupled

to a Kalb–Ramond field. This term takes the form

$$S_{\mathrm{KR}} = \lambda \int d\tau\, d\sigma\, A_{\mu\nu} \partial_\tau X^\mu \partial_\sigma X^\nu \,, \tag{104}$$

where λ is an associated coupling constant. Endlich and Nicolis [63] showed that this coupling constant is related to the vortex circulation $\Gamma = \oint \partial_t \mathbf{X} \cdot d\mathbf{s}$ by $\Gamma = \bar{w}\lambda/\bar{n}c^2$. The Kalb–Ramond-like combination is the only invariant term that is linear in the two-form field and without derivatives acting on it, at lowest order in the derivative expansion. We can also include Nambu–Goto-type terms in the action,

$$S_{\mathrm{NG}} = \int d\tau\, d\sigma \sqrt{-\det G_{\mu\nu}[\mathbf{X}] \partial_\alpha X^\mu \partial_\beta X^\nu} \,, \tag{105}$$

where the indices α, β range over τ, σ. Unlike in the Nambu–Goto action of string theory, we can form any number of tensor structures $G_{\mu\nu}$ out of the bulk fields here, not just $\eta_{\mu\nu}$, since the superfluid spontaneously breaks Poincaré symmetry. In particularly, we can also form a metric proportional to $u_\mu u_\nu$ from $u_\mu = -F_\mu/\sqrt{Y}$, the bulk 4-velocity. Defining two tensors

$$g_{\alpha\beta} = \eta_{\mu\nu} \partial_\alpha X^\mu \partial_\beta X^\nu \,, \quad h_{\alpha\beta} = u_\mu u_\nu \partial_\alpha X^\mu \partial_\beta X^\nu \,, \tag{106}$$

we can borrow the formalism of bimetric gravity [88] to write the most general Lagrangian with diffeomorphism invariance, to lowest order in derivative expansion, as a generic function of $g^{\alpha\beta} h_{\alpha\beta}$ times the determinant of $g_{\alpha\beta}$. Since we wish to include all possible interactions with bulk modes, the function can also take the scalar Y as a direct argument. The resulting contribution to the action, which we will call the modified Nambu–Goto term, can be expressed as

$$S_{\mathrm{NG}'} = -\int d\tau\, d\sigma\, \sqrt{-g}\, \mathcal{T}\left(g^{\alpha\beta} h_{\alpha\beta}, Y\right) \,. \tag{107}$$

That is all. There are no other invariant terms that we can add to the action at lowest order in the derivative expansion. To summarize, we now have all the ingredients to study the dynamics of vortex lines in a superfluid. The full action including bulk modes and vortex coordinates reads

$$\begin{aligned} S &= S_{\text{bulk}} + S_{\text{KR}} + S_{\text{NG}'} + S_{\text{gf}} \\ &= \int dt\, d^3x\, G(Y) + \lambda \int d\tau\, d\sigma\, A_{\mu\nu} \partial_\tau X^\mu \partial_\sigma X^\nu \\ &\quad - \int d\tau\, d\sigma\, \sqrt{-g}\, \mathcal{T}\left(g^{\alpha\beta} h_{\alpha\beta}, Y\right) - \frac{1}{2\xi} \int dt\, d^3x\, \left(\partial_i \mathcal{A}^{i\mu}\right)^2 . \end{aligned} \tag{108}$$

It will also be helpful to work in a physical gauge $X^0 = \tau = t$ and expand the action in powers of the string velocity $\mathbf{v} = \partial_t \mathbf{X}$, which we expect to be small compared to the sound velocity c_s in the superfluid. We can simultaneously expand in the bulk fluctuation fields $\mathbf{A}$ and $\mathbf{B}$. Then the Kalb–Ramond-like term becomes [49]

$$S_{\text{KR}} \to \bar{n}\lambda \int dt\, d\sigma\, \left[\epsilon_{ijk} \left(-\frac{1}{3} X^k + B^k\right) \partial_t X^i \partial_\sigma X^j + A_i \partial_\sigma X^i\right] . \tag{109}$$

Defining the string tensions as

$$T_{mn} \equiv a^m b^n (\partial_a)^m (\partial_b)^n \mathcal{T}(a, b)\,, \tag{110}$$

the expansion of the Nambu–Goto-like term action is given by

$$S_{\text{NG}'} \to \int dt\, d\sigma\, |\partial_\sigma \mathbf{X}| \left[-T_{(00)} + 2T_{(01)} \boldsymbol{\nabla} \cdot \mathbf{B} + 2T_{(10)} \left(\dot{\mathbf{B}} - \boldsymbol{\nabla} \times \mathbf{A}\right)_\perp \cdot \frac{\mathbf{v}_\perp}{c^2}\right] . \tag{111}$$

The subscript $\perp$ denotes coordinates that are locally perpendicular to the vortex line. Like other coupling parameters in this theory, the tensions $T_{(mn)}$ are completely undetermined and run with the energy scale. They are fixed by taking measurements at some reference energy. The running of the couplings is easy to calculate by considering diagrams of the

sort we will study in the next section (such as the second diagram of Fig. 7). As a result of renormalization by divergent one-loop diagrams, one finds that the couplings $T_{(00)}$, $T_{(01)}$, and $T_{(10)}$ scale logarithmically with energy: $T(\mu) \propto \bar{w}\Gamma^2 \log(\mu/\mu_0)$ [49].

As a quick illustration of what this theory is capable of, let us choose a gauge where $\sigma = z$ and consider a vortex configuration parametrized in a straight line, $\mathbf{X} = (0, 0, \sigma)$. Then add a small transverse perturbing field $\boldsymbol{\phi}(t, z)$ along the vortex line around the static configuration by writing

$$\mathbf{X}(t, z) = [\phi^x(t, z), \phi^y(t, z), z] \ . \tag{112}$$

This perturbing field represents transverse string excitations, and we assume that its wavelength is much longer than the thickness of the vortex core. The relevant terms in the action for describing the gradient energy and kinetic energy of these excitations are $-T_{(00)} |\partial_z \mathbf{X}|$ from the modified Nambu–Goto action and $-\frac{1}{3}\bar{n}\lambda\epsilon_{ijk}X^k\partial_t X^i \partial_z X^j$ from the Kalb–Ramond part, respectively. Together, these give an effective action for string excitations,

$$S_{\text{eff}} = \int dt\, dz \, \left[-T_{(00)}\sqrt{1 + (\partial_z \boldsymbol{\phi})^2} - \frac{\bar{n}\lambda}{2}\epsilon_{ab}\phi^a \dot{\phi}^b \right] , \tag{113}$$

where the indices a, b range over the transverse coordinates x, y only.

The dispersion relations obeyed by these excitation modes are straightforward to find by varying the effective action with respect to ϕ^a and considering the resulting equations of motion to linear order. Using the fact that $\lambda \simeq \Gamma/m$ in non-relativistic superfluids, we can write the equations of motion as

$$0 = T_{(00)}\partial_z^2 \phi^a - \frac{\bar{n}\Gamma}{m}\epsilon_{ab}\dot{\phi}^b \, . \tag{114}$$

Looking for plane wave solutions of the form $\phi^a = \phi_0^a e^{i(kz-wt)}$ immediately results in

$$\omega(k) \propto \frac{T_{(00)}}{\Gamma} k^2 \,, \tag{115}$$

$$\begin{pmatrix} \phi_0^x \\ \phi_0^y \end{pmatrix} \propto \begin{pmatrix} 1 \\ -i \end{pmatrix} . \tag{116}$$

From the first condition, recalling the running of the coupling $T_{(00)}$ with momentum, we find the dispersion relation

$$\omega(k) \propto \Gamma k^2 \log(k\ell) \,, \tag{117}$$

where ℓ^{-1} is a UV cutoff momentum scale comparable to the inverse healing length if the vortex is moving in a Bose–Einstein condensate. This is the classic result for the dispersion relation of Kelvin waves propagating along a vortex line [85]. The second condition tells us that $\boldsymbol{\phi}$ is circularly polarized. In other words, this is a corkscrew-like helical wave, and its two components $\phi_\pm \sim \phi^x \pm i\phi^y$ carry opposite charges under the global $U(1)$ symmetry $\phi_\pm \to \phi_\pm e^{\pm i\alpha}$, $\alpha = \text{const}$, that becomes evident when rewriting the effective action in Eq. (113) in terms of the complex fields ϕ_+ and ϕ_-:

$$S_{\text{eff}} = \int dt\, dz \, \left[-T_{(00)} \sqrt{1 + \partial_z \phi_+ \partial_z \phi_-} + i\bar{n}\lambda \dot{\phi}_+ \phi_- \right] . \tag{118}$$

3 Case Study 1: Motion of Vortex Lines in Trapped Superfluids

3.1 Overview of Vortex Precession

As a first detailed case study, we will consider the phenomenon of vortex precession in a trapped superfluid. As explained in Section 2.5, a vortex line is type of linear topological defect observed in superfluids and superconductors, around which circulation is quantized. Although the velocity field is irrotational far from the vortex core, it nonetheless does carry circulation. In a typical liquid helium superfluid, quantum vortices are a few ångströms in radius [83], while in a trapped, dilute Bose gas the core radius is of the same order of as the healing length, $\xi = 1/\sqrt{8\pi n_0 a}$, where n_0 is the peak condensate density and a is the scattering length. This length scale could be as large as thousands of ångströms in a dilute Bose gas. Rokhsar [89] first predicted that trapped, dilute Bose gases at relatively strong coupling could support off-center vortices, which would be unstable to perturbations and spiral around the center of the trap. However, Rokhsar's prediction that vortices would quickly spiral out of the trap was not borne out in subsequent theoretical and experimental studies. It turned out that under the appropriate conditions, persistent quantum vortices can be sustained in a trapped, dilute Bose gas, and they can be observed to precess around the center of the cloud in elliptical orbits. This is shown schematically in Fig. 3.

Standard theoretical studies of the motion of vortices in Bose–Einstein condensates rely heavily on Gross–Pitaevskii theory, which treats the wave function of a zero-temperature Bose gas in the Hartree, or mean field, formalism, meaning that it is assumed to be the symmetrized product of single-particle wave functions. The typical interparticle separation is assumed to be much greater than the scattering length a in the many-body system. An effective pseudopotential Hamiltonian with pairwise interactions is introduced, an energy functional is constructed, and variational analysis minimizing the energy $E - \mu N$ leads to

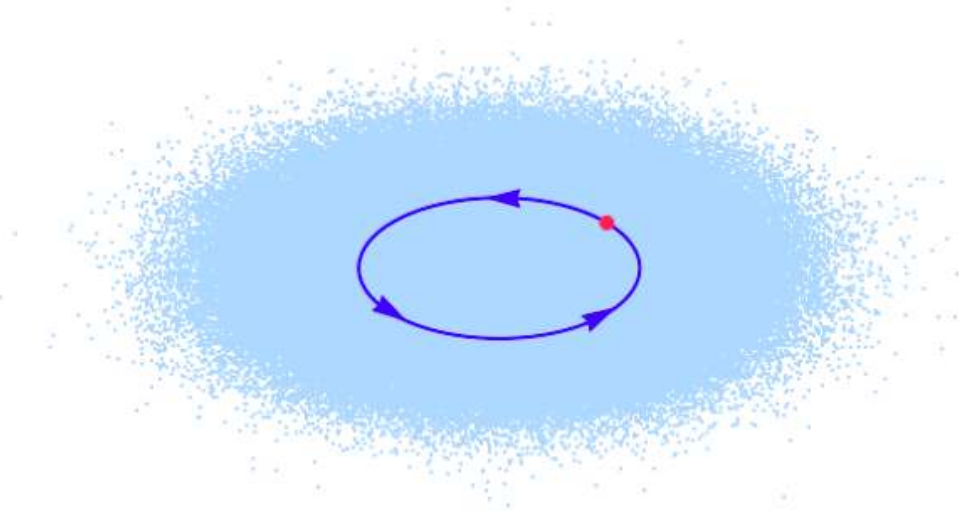

Figure 3: Schematic diagram of precessional motion of a vortex line (red dot) in a trapped elliptical atomic cloud; taken from Esposito *et al.* [1].

the well-known Gross–Pitaevskii equation [83, 90–92],

$$-\frac{\hbar^2}{2m}\nabla^2\psi\left(\mathbf{x}\right)+\left[V\left(\mathbf{x}\right)-\mu\right]\psi\left(\mathbf{x}\right)+g\left|\psi\left(\mathbf{x}\right)\right|^2\psi\left(\mathbf{x}\right)=0\,, \tag{119}$$

where m is the mass of the atoms in the condensate, $\psi\left(\mathbf{x}\right)$ is the order parameter, or macroscopic wave function of the condensate, normalized so that the square of its norm is equal to the number density, $V\left(\mathbf{x}\right)$ is the external potential, μ is the chemical potential, and $g=4\pi\hbar^2a/m$ is the effective coupling of pairwise interactions of the form $g\,\delta\left(\mathbf{x}_i-\mathbf{x}_j\right)$, which accounts for the effects of high-momentum degrees of freedom that have been integrated out. It is the non-linear third term that takes into account the mean field produced by other bosons in the system. Effects of a rotating trap in the co-rotating frame are typically accounted for by adding an interaction term proportional to $\mathbf{x}\times\boldsymbol{\nabla}\psi\left(\mathbf{x}\right)$ to the energy functional and using variational methods to obtain a modified Gross–Pitaevskii equation [93]. The effects of trapping can be studied more easily in the Thomas–Fermi limit, when gradients in the external trapping potential are small compared to the Fermi momentum. The dynamics of a vortex line in this formalism are typically studied by introducing an Ansatz trial wave

function characteristic of circular flow around a vortex. For example, Fetter and Kim [93] used a trial wavefunction whose phase included a piece proportional to $\arctan\left(\frac{y-y_0}{x-x_0}\right)$, where (x_0, y_0) are the coordinates of the vortex line in the xy-plane.

Jackson *et al.* [94] attempted to calculate the precession frequency of a vortex line about the center of a trapped condensate using Gross–Pitaevskii theory and an argument based on the Magnus effect, in which a spinning body moving through a fluid is deflected due to a pressure gradient perpendicular to the direction of the background flow. They calculated the precession frequency of a persistent, singly quantized vortex line aligned with the z-axis in a trapped condensate with a trapping potential given by

$$V(\mathbf{r}) = \frac{1}{2}m\left(\omega_x x^2 + \omega_y y^2 + \omega_z z^2\right) . \tag{120}$$

In the Thomas–Fermi limit, they found that near the center of the cloud, the precession frequency ω_p is given by

$$\omega_p = \frac{\hbar}{\mu}\omega_x\omega_y\left(\log\frac{R_\perp}{\xi} - \frac{5}{4}\right) , \tag{121}$$

where μ is the chemical potential, ξ is the healing length, $R_\perp = \frac{2\mu}{m\sqrt{\omega_x^2+\omega_y^2}}$ is the length scale of the size of the cloud in the plane perpendicular to the vortex line, and m is the mass of the microscopic constituents of the atomic cloud. The logarithmic factor is particularly important to note, since it appears in many formulas characterizing the dynamics of vortex lines.

The result of Jackson *et al.* can be compared to the calculation of Svidzinsky and Fetter [95], who used asymptotic expansions and a time-dependent variational analysis in the Gross–Pitaevskii formalism to study vortex line precession in a non-axisymmetric trapped Bose–Einstein condensate in the Thomas–Fermi approximation. Their result for the preces-

sion frequency of a vortex line aligned with the z-axis and moving in the xy-plane was

$$\omega_p = \frac{3\hbar}{4\mu}\omega_x\omega_y \log\frac{R_\perp}{\xi}\,, \tag{122}$$

again valid at positions near the center of the elliptical cloud.

Fetter and Kim [93] returned to the problem using time-dependent Lagrangian variational analysis, but without resorting to asymptotic expansions, finding a similar result for the precession of the vortex line near the center of an elliptical trap in the case when the angular velocity of the external rotation is small compared to $\omega_\perp = \sqrt{\omega_x^2 + \omega_y^2}$. Then the precession frequency is similar, but the numerical pre-factor is different:

$$\omega_p = \frac{\hbar}{\mu}\omega_x\omega_y \log\frac{R_\perp}{\xi}\,. \tag{123}$$

The above results are all quite similar, up to an overall order-one factor, as long as there is a large separation of scales between the size of the atomic cloud and the condensate healing length. Fetter and Kim's result agrees with the calculations of Lundh and Ao [96] and McGee and Holland [97] in the appropriate limits, except the logarithmic factor is shifted by a position-dependent value of order one in the results of the latter two studies.

Experimentally, Matthews *et al.* [98] created and observed the first persistent vortices in a trapped, two-component rubidium-87 Bose–Einstein condensate; they mapped the phase of the condensate in order to confirm that the vortices possessed angular momentum. Anderson *et al.* [99] were the first to observe the precessional behavior of vortex lines in a trapped rubidium-87 Bose–Einstein condensate about the condensate axis. They prepared the system from a two-component condensate with two quantum states, one forming the vortex, and the other filling the core, which was steadily removed using resonant light pressure until the vortex had minimal thickness. The filling material was allowed to expand until the vortex could be imaged, and a successive time series of images of the atoms in the non-core state was taken. Anderson *et al.* captured a beautiful series of images demonstrating vortex precession

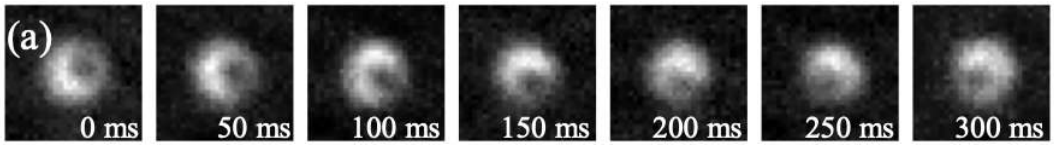

Figure 4: Times series of images demonstrating vortex precession in a trapped rubidium-87 Bose–Einstein condensate; taken from Anderson *et al.* [99].

(see Fig. 4). The precession frequency was observed to vary slightly with core radius, with larger-core vortices precessing at a somewhat lower rate.

While the experiment of Anderson *et al.* seemed to confirm the observation of vortex line precession, the two-dimensional, cross-sectional view of the images left open the possibility of alternate interpretations of the observed motion of the defects, which were not necessarily linear in the third dimension. Ku *et al.* [100] performed another experiment in which a solitonic vortex was formed in a strongly interacting superfluid Fermi gas of lithium-6 atoms near a Feshbach resonance using phase imprinting. The motion of vortices was then observed over a range of chemical potentials including the BEC–BCS crossover regime. In the limit of tight molecular binding, the atomic gas can be understood as a Bose–Einstein condensate, as most atoms participate in pairing, while in the BCS regime, the long-range Cooper pairs overlap and fewer atoms near the Fermi surface are paired [101]. Tomographic imaging revealed that the defect was in fact a solitonic vortex line and its precessional motion was observed over time. An illustrative figure from Ku *et al.* clearly demonstrating the linear nature of the solitary wave is shown in Fig. 5. Careful analysis of the position of the vortex core in the transverse plane demonstrated that the vortex lines followed roughly elliptical orbits about the center of the atomic cloud, with dimensions determined by the shape of the trapping potential.

Ku *et al.* found that the period of precession as a function of normalized chemical potential agreed fairly well with predictions from Gross–Pitaevskii theory for a molecular Bose–Einstein condensate [93, 96]. The precision of the measurement, however, was not sufficient to resolve the tensions between previous theoretical predictions—see Eqs. (121)

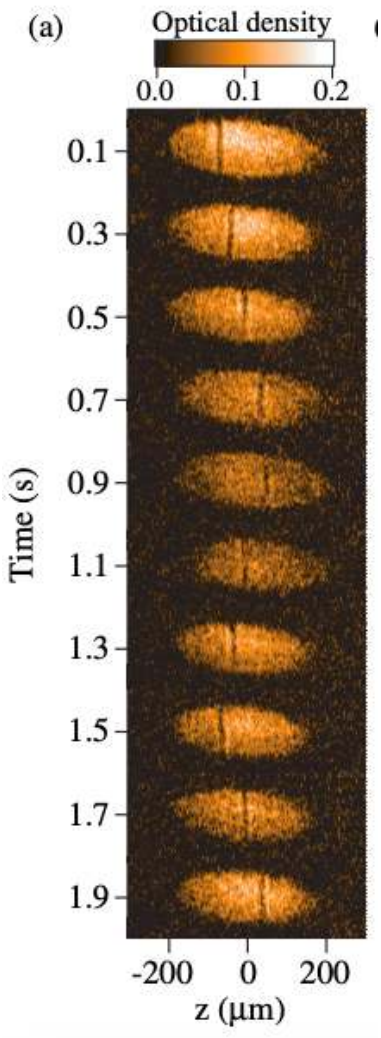

Figure 5: Vortex precession in a fermionic superfluid observed via tomographic imaging in horizontal slices of a cigar-shaped cloud of Li-6 atoms; taken from Ku *et al.* [100].

to (123).

The purpose of this theoretical study, part of which has been published in Esposito *et al.* [1], is to take an approach orthogonal to those of Jackson *et al.* [94], Svidzinsky and Fetter [95], Lundh and Ao [96], Fetter and Kim [93], McGee and Holland [97], and others who have studied this problem using the formalism of the Gross–Pitaevskii equation in the Thomas–Fermi limit. Instead, we will examine the effective field theory of vortex lines in trapped superfluids and derive the precessional motion of vortices in a more universal manner, with minimal assumptions about the microscopic physics of the superfluid, the precise form

of the energy functional, or the shape of the trapping potential. We will see that our result is consistent with the theoretical calculations based on Gross–Pitaevskii theory, as well as the data presented by Ku *et al.* [100]. In addition to deriving the result more efficiently and from more general considerations and resolving the tension between previous calculations, we will see that our treatment of trapping in this formalism has immediate implications for the phenomenon of Kelvin wave propagation along vortex lines, which is affected by the trapping potential. Overall, our analysis will demonstrate the power of the effective field theory methodology to treat very concrete phenomenological problems in condensed matter physics. Our approach relies on an action built from general symmetry considerations and a low-energy derivative expansion, taking advantage of the weak coupling of low-energy/long-distance superfluid degrees of freedom. An additional benefit of our framework is that the analysis can be performed in fully relativistic language—it is, in fact, easier to perform relativistically—and as a result, relativistic corrections in powers of $1/c$ are easily obtainable. While they might not be relevant to regular cold Bose gas experiments, they may prove to be of theoretical relevance to the study of superfluid vortices in more exotic relativistic or astrophysical settings.

3.2 The Trapping of Superfluid Condensates

Numerous experimental techniques have been developed to trap and manipulate ultracold dilute atomic gases and realize Bose–Einstein condensation, facilitated by advances in laser technology. The general approach involves slowing a beam of alkali atoms using a Zeeman slower, to the point that they can be confined using some combination of optical and magnetic atomic trapping techniques, after which evaporative cooling removes the most energetic atoms, leaving behind a condensate with a macroscopically occupied ground state [83]. The first experimental realization of Bose–Einstein condensation was achieved by Anderson *et al.* [102] using a dilute vapor of rubidium-87 atoms in a time orbiting potential (TOP) trap. The trapping configuration in their experiment consisted of a large spherical quadrupole field with a superimposed uniform transverse magnetic field, rotating at a high frequency in the 7.5 kHz range, resulting in an effectively harmonic trapping potential. The cold rubidium atoms were optically trapped, cooled, and loaded into the trap, after which a modulating radiofrequency magnetic field was used to force higher-energy atoms into an untrapped spin state. Numerous refinements have since been made in trapping and cooling techniques to observe Bose–Einstein condensates and their behavior—see [103] for a historical overview. What matters for us are not the details of the experimental techniques, but the geometry of the possible traps that can be formed and the symmetry breaking properties of the trapping techniques. Typical traps are harmonic and oblate, although steeper effective trapping potentials can also be formed [83]. The Ioffe cylindrical trapping configuration usually produces a roughly symmetric harmonic radial potential and a tightly confining trapping potential in the transverse direction, resulting in a cigar-shaped cloud. Both optical and magnetic trapping techniques can be used, which have slightly different implications for the symmetries of the system from the field theoretic point of view, affecting which possible bulk mode–trapping potential interactions we must consider in our field theoretic formalism.

For the purposes of this calculation, we will begin by assuming that the trapping occurs in two dimensions, x and y, while the trapping in the z direction is sufficiently weak to

be neglected over the distance scales that we are considering. The shape of the trap we are interested in is elliptical and roughly planar. We make this assumption in order to work with straight-line vortices, which are more conducive to simple analytic calculations. We will see that this simplifying assumption is mild enough to allow us to observe the precessional dynamics we are interested in studying; we will modify this assumption later and assess the implications of adding weak trapping along the third dimension.

Let us now recall the effective field theory of superfluids in the dual two-form language (see Section 2.1.2) and incorporate an external trapping potential into the formalism. The full effective action for superfluid excitations and vortices is given by Eq. (108). To this we add a trapping term that couples the invariant operator $\sqrt{Y}$ (the density) to the superfluid velocity field $\mathbf{u}$ and the Eulerian (spatial) position coordinate $\mathbf{x}$ in the most general manner consistent with the symmetries of the system. In terms of the superfluid excitations, $\mathbf{A}$ (hydrophoton field) and $\mathbf{B}$ (phonon field), the density $\sqrt{Y}$ and velocity $\mathbf{u}$ are given by

$$Y = \bar{n}^2 \left[(1 - \boldsymbol{\nabla} \cdot \mathbf{B}) - \frac{1}{c^2} \left(\dot{\mathbf{B}} - \boldsymbol{\nabla} \times \mathbf{A} \right)^2 \right] , \tag{124}$$

$$\mathbf{u} = \frac{1}{1 - \boldsymbol{\nabla} \cdot \mathbf{B}} \left(\dot{\mathbf{B}} - \boldsymbol{\nabla} \times \mathbf{A} \right) . \tag{125}$$

The additional trapping term to be added to the action is simply the space-time integral of a generic (sufficiently smooth) energy density functional $\mathcal{E}$ with the appropriate arguments to lowest order in the derivative expansion:

$$S_{\text{tr}} = - \int dt \, d^3x \, \mathcal{E} \left(\sqrt{Y}, \mathbf{u}, \mathbf{x} \right) . \tag{126}$$

This action can now be expanded perturbatively in small fluctuations of the density and the velocity field. Let us define the following partial derivatives of the energy functional $\mathcal{E}$,

which we will use in the expansion of the trapping term in the action:

$$V(\mathbf{x}) \equiv \frac{\partial \mathcal{E}}{\partial \sqrt{Y}}, \quad \rho_{ij}(\mathbf{x}) \equiv \frac{\partial^2 \mathcal{E}}{\partial u^i \partial u^j}, \tag{127}$$

where both partial derivatives are evaluated on the background—*i.e.* $\sqrt{Y} = \bar{n}$ and $\mathbf{u} = 0$. Notice that $\mathcal{E}$ has dimensions of energy density and $\sqrt{Y}$ has dimensions of number density, so the function V has dimensions of energy; we will see that it will have the interpretation of the external trapping potential. The tensor ρ_{ij} has dimensions of mass density, since u^i has dimensions of velocity. We will not be concerned with odd-power derivatives of the functional $\mathcal{E}$ with respect to the velocity, since we will assume that the trapping mechanism does not break time reversal symmetry, thus allowing us to set terms in the expansion with an odd power of the velocity to zero. Notice that this assumption does not hold in the case of magnetic trapping of charged ions, for example, in which case the term in the expansion of $\mathcal{E}$ that is first-order in the velocity will become relevant. Assuming this assumption holds, however, we find several new interaction terms in the action due to the trapping action. To lowest order in superfluid excitations and derivatives, these interaction terms due to trapping are given by:

$$\begin{aligned} S_{\mathrm{tr}} \to \int dt\, d^3x \Bigg\{ \bar{n} V(\mathbf{x}) \left[\boldsymbol{\nabla} \cdot \mathbf{B} + \frac{1}{2c^2} \left(\dot{\mathbf{B}} - \boldsymbol{\nabla} \times \mathbf{A} \right)^2 \right] \\ - \frac{1}{2} \rho_{ij}(\mathbf{x}) \left(\dot{\mathbf{B}} - \boldsymbol{\nabla} \times \mathbf{A} \right)^i \left(\dot{\mathbf{B}} - \boldsymbol{\nabla} \times \mathbf{A} \right)^j \Bigg\}. \end{aligned} \tag{128}$$

This truncation of the expanded trapping functional is sufficient to compute lowest-order results in perturbation theory for vortex precession.

To make contact with the usual Gross–Pitaevskii approach to the phenomenon of trapped vortex precession, in which an explicit external trapping potential $V_{\mathrm{tr}}(\mathbf{x})$ is introduced, notice that the standard approach involves only coupling between the trapping potential and the density. Coupling to the velocity field is generally not considered. In our framework, this would amount to considering the particular energy density functional

$\mathcal{E}\left(\sqrt{Y}, \mathbf{u}, \mathbf{x}\right) = V_{\rm tr}\left(\mathbf{x}\right)\sqrt{Y}$, which is less general than our starting point. Nonetheless, notice that the two approaches do coincide to lowest order in perturbation theory if we neglect the velocity dependence of the energy density functional $\mathcal{E}$, since the second line of Eq. (128) would be absent.

Now, note that to leading order in V and ρ_{ij}, which we assume to be small for now, the terms in Eq. (128) provide a simple linear external source for the phonon field $\mathbf{B}$. There is no similar linear source for the hydrophoton field $\mathbf{A}$. The source term is given by

$$\mathbf{J}_B(x) = -\bar{n}\boldsymbol{\nabla} V\left(\mathbf{x}\right) . \tag{129}$$

From standard Green's function theory, we know that the vacuum expectation value for the $\mathbf{B}$ field in the presence of an external source $\mathbf{J}_B$ is found from

$$\left\langle B^i\left(\mathbf{x}\right)\right\rangle = i\int \frac{d^3k\, d\omega}{(2\pi)^4} G_B^{ij}(k) J_B^j(k) e^{ik\cdot x} , \tag{130}$$

where $G_B^{ij}(k)$ is the momentum-space phonon propagator we saw in Eq. (53) and $J_B^i(k)$ is the momentum-space source term—in our case, the four-dimensional Fourier transform of Eq. (129). Substituting into Eq. (130), we find that the expectation value of the divergence of the $\mathbf{B}$ field is directly proportional to the trapping energy V:

$$\left\langle \boldsymbol{\nabla}\cdot\mathbf{B}\left(\mathbf{x}\right)\right\rangle = \frac{\bar{n}c^2}{\bar{w}c_s^2} V\left(\mathbf{x}\right) . \tag{131}$$

The divergence of the phonon field acquires an expectation value proportional to the strength of the trapping potential at every position in the cloud. Since there are no linear sources for the field $\mathbf{A}$, we find that the equilibrium value of the density in the presence of trapping must be

$$n(x) = \sqrt{Y} = \bar{n}\left[1 - \frac{\bar{n}c^2}{\bar{w}c_s^2} V\left(\mathbf{x}\right)\right] , \tag{132}$$

as long as the external trapping potential is weak, or inside the bulk of the atomic cloud, where gradients of the trapping potential are small. In the non-relativistic limit, the background enthalpy density $\bar{w}$ is approximately equal to $m\bar{n}c^2$, so the density becomes

$$n(x) \to \bar{n}\left[1 - \frac{1}{mc_s^2}V(\mathbf{x})\right] \tag{133}$$

when $c_s \ll c$. Note that at this order in perturbation theory, the geometry of the density field matches that of the external trapping potential, in the sense that they have identical constant-value contour surfaces. This is because the divergence term entering into the leading-order expansion of the density $\sqrt{Y}$ and the gradient operator in the source term $\mathbf{J}_B$ effectively compensate for the non-local nature of the phonon propagator G_B^{ij}, thus turning the trapping interaction into a simple contact term.

It is illuminating to compare the result in Eq. (133) to the density in the presence of trapping calculated from Gross–Pitaevskii theory in the Thomas–Fermi approximation. Consider Eq. (119) in the limit of negligible kinetic energy:

$$\left[V(\mathbf{x}) - \mu\right]\psi(\mathbf{x}) + g\left|\psi(\mathbf{x})\right|^2\psi(\mathbf{x}) = 0\,. \tag{134}$$

Recalling that $\left|\psi(\mathbf{x})\right|^2 = n(\mathbf{x})$, this has the immediate solution

$$n(\mathbf{x}) = \frac{\mu}{g}\left[1 - \frac{1}{\mu}V(\mathbf{x})\right]\,, \tag{135}$$

as long as the order parameter is non-zero, and it is equal to zero at the boundary of the cloud, which is determined by $V(\mathbf{x}) = \mu$. Eq. (135) expression matches the result in Eq. (133) exactly. To lowest order in perturbation theory and in the non-relativistic limit, the correspondence between our notation and the parameters of Gross–Pitaevskii theory is

given by

$$\bar{n} = \mu/g\,, \quad c_s^2 = \mu/m\,. \tag{136}$$

The equations for the density Eqs. (132) and (133) are only valid in regions where the strength of the trapping potential is weak and V can be treated in a perturbative manner. This will not be a valid assumption everywhere in the atomic cloud, certainly not near the edge. However, since the position in the cloud that we are considering is arbitrary, we can treat the expansion procedure as an expansion in small *variations* of the trapping potential, or small gradients of V, rather than an expansion in V itself. We can therefore rewrite Eqs. (132) and (133) as non-linear differential equations valid to all orders in V and corresponding to a formal resummation of tree-level diagrams of the form shown in Fig. 6. In the non-relativistic case, Eq. (133) can be rewritten in the differential form

$$c_s^2(n)\frac{dn}{n} = -\frac{dV}{m}\,. \tag{137}$$

This equation can be integrated to obtain the relation between the density $n(\mathbf{x})$ and the trapping potential $V(\mathbf{x})$ valid to all orders, provided that one assumes a definite equation of state of the superfluid, $c_s^2(n)$. For example, in Gross–Pitaevskii theory we have $c_s^2 \propto n$, so we recover the linearized solution Eq. (133). In the case of a more general power-law equation of state of the form $c_s^2(n) \propto n^\gamma$, we will have $n(x) \propto [1 - V(\mathbf{x})/\mu]^{1/\gamma}$ if $V = \mu$ at the edge of the atomic cloud, which still exhibits the same level surfaces as the trapping potential. If we consider a truncated virial-type equation of state, say $c_s^2(n) = Bn + Cn^2$, then the relationship has the form $n(x) \propto \sqrt{1 + \frac{2C\mu}{B^2 m}\left[1 - V(\mathbf{x})/\mu\right]} - 1$. More complicated equations of state can lead to rather large non-linear, but still local, corrections to the relationship between the density and the trapping potential in the bulk of the cloud.

Our setup is general enough to accommodate any trapping potential that is smooth and has small gradients in the interior of the atomic cloud, regardless of the precise geometry

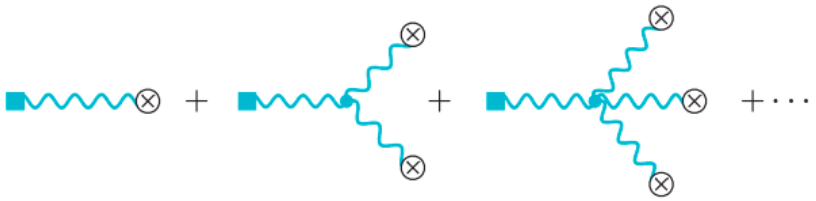

Figure 6: Resummation of non-linear corrections to Eqs. (132) and (133) from tree-level diagrams. In these diagrams, wavy blue lines represent phonon propagators and crossed circles represent the trapping potential $V(\mathbf{x})$, which sources the phonon field. Blue dots at vertices represent phonon self-interactions and blue squares represent the density $n(\mathbf{x})$.

of the trapping potential, and we need not assume anything *a priori* about the equation of state. Typical trapping potentials are harmonic (*i.e.* quadratic in radial distance from the center of the trap), although it is certainly possible to have trapping configurations that are flatter near the center. For the time being, we will keep $V(\mathbf{x})$ arbitrary until the end of the calculation, when we will consider specific types of trapping. For convenience, let us restate the relevant parts of the action for superfluid excitations and vortices, now including the effects of trapping:

$$\begin{aligned} S = \frac{\bar{w}}{c^2}\int dt\, d^3x \Bigg\{ & \frac{1}{2}\left(\boldsymbol{\nabla}\times\mathbf{A}\right)^2 + \frac{1}{2}\left[\dot{\mathbf{B}}^2 - c_s^2\left(\boldsymbol{\nabla}\cdot\mathbf{B}\right)^2\right] - \frac{\bar{g}c_s^2}{6}\left(\boldsymbol{\nabla}\cdot\mathbf{B}\right)^3 \\ & + \frac{1}{2}\left(1-\frac{c_s^2}{c^2}\right)\boldsymbol{\nabla}\cdot\mathbf{B}\left(\dot{\mathbf{B}}-\boldsymbol{\nabla}\times\mathbf{A}\right)^2 + \bar{n}V(\mathbf{x})\left[\boldsymbol{\nabla}\cdot\mathbf{B} + \frac{1}{2c^2}\left(\dot{\mathbf{B}}-\boldsymbol{\nabla}\times\mathbf{A}\right)^2\right] \\ & - \frac{1}{2}\rho_{ij}(\mathbf{x})\left(\dot{\mathbf{B}}-\boldsymbol{\nabla}\times\mathbf{A}\right)^i\left(\dot{\mathbf{B}}-\boldsymbol{\nabla}\times\mathbf{A}\right)^j\Bigg\} \\ & + \int dt\, d\sigma \Bigg\{ -\frac{1}{3}\bar{n}\lambda\epsilon_{ijk}X^k\partial_t X^i\partial_\sigma X^j - T_{(00)}\left|\partial_\sigma\mathbf{X}\right| + \bar{n}\lambda A_i\partial_\sigma X^i \\ & + \bar{n}\lambda\epsilon_{ijk}B^k\partial_t X^i\partial_\sigma X^j + \left|\partial_\sigma\mathbf{X}\right|\left[2T_{(01)}\boldsymbol{\nabla}\cdot\mathbf{B} + 2T_{(10)}\left(\dot{\mathbf{B}}-\boldsymbol{\nabla}\times\mathbf{A}\right)\cdot\frac{\mathbf{v}_\perp}{c}\right]\Bigg\}. \end{aligned} \tag{138}$$

We will use this action for reference in subsequent sections of the calculation, when we consider vortex precession in two dimensions. As mentioned previously, this action would have to be slightly modified if the trap breaks time reversal symmetry, or if direct coupling to the superfluid velocity field becomes important.

3.3 Precession in Two Dimensions

3.3.1 Effective Potential for Vortex Lines

We will now study the precessional motion of a single vortex line in a superfluid with strong two-dimensional trapping. For simplicity, we will consider the cylindrical case only, in which trapping occurs along the $(x, y) \equiv \mathbf{x}_\perp$ directions. We will assume that trapping in the z direction is sufficiently weak to treat the vortices as essentially straight lines perpendicular to the xy-plane, with little or no variation along the z-direction. This is a purely simplifying assumption that could be relaxed, but it is sufficient for the purposes of this calculation. We choose to write the parametrization of the vortex line's coordinates as $\mathbf{X}(t, z) = (X(t), Y(t), z)$, and we will assume that the distance of the vortex from the center of the cloud, $\sqrt{X(t)^2 + Y(t)^2}$, remains small compared to the typical transverse size of the cloud, $R_\perp$, throughout its motion. Near the center of the cloud, the trapping potential is assumed to be sufficiently flat that higher-order gradients of the potential can be neglected. Moreover, we will begin by working in the non-relativistic limit, which is relevant for most experimental settings. Later, we will explain how to extend the analysis for the computation of relativistic corrections using our formalism. We will assume that the third line in Eq. (138), which includes $\rho_{ij}(\mathbf{x})$, can be treated as a relativistic correction, meaning that it is secretly suppressed by powers of c, since it characterizes the direct coupling of the superfluid velocity to the trapping potential. Such interactions typically may arise from Doppler-like mechanisms [104], which would be suppressed by inverse powers of c, as we assumed. In other words, we are assuming that

$$\rho_{ij}(\mathbf{x}) = \frac{1}{c^2}\bar{n}V_{ij}(\mathbf{x}) \ , \quad V_{ij} \sim V \ . \tag{139}$$

Note again that this assumption must be lifted in the case of magnetic trapping mechanisms, which would also entail that the third line of Eq. (138) must be replaced by a linear coupling between the trap and the velocity field $\mathbf{u}$. Taking the non-relativistic limit of the action in

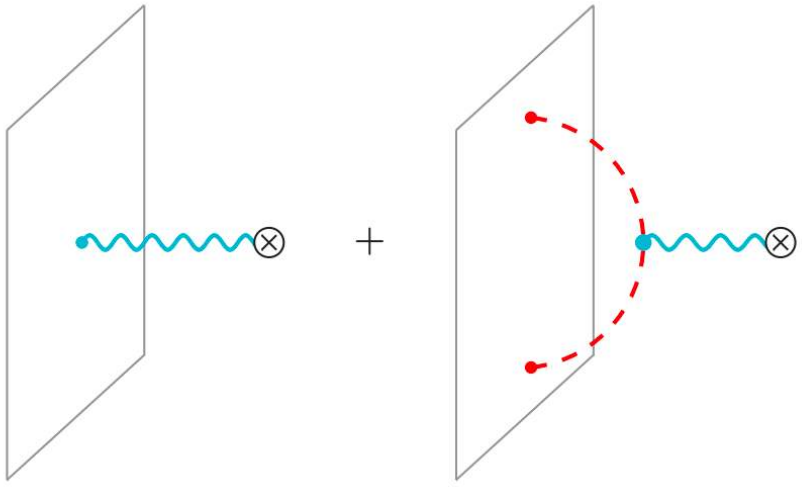

Figure 7: Feynman diagrams representing the leading-order contributions to the non-relativistic interactions between the world-sheet of a vortex line (flat plane) and the trapping potential (crossed circle). The interactions are mediated by both phonons (blue wavy line) and hydrophotons (red dashed line).

Eq. (138), we find that only the cubic interaction term $\frac{1}{2}\boldsymbol{\nabla}\cdot\mathbf{B}\,(\boldsymbol{\nabla}\times\mathbf{A})^2$ survives, as well as source terms for the $\mathbf{A}$ and $\mathbf{B}$ fields arising from the trapping potential and the motion of the vortex, which are given by

$$\mathbf{J}_A(x) = \bar{n}\lambda\,\delta^2\left(\mathbf{x}_\perp - \mathbf{X}(t)\right)\hat{\mathbf{z}}\,, \tag{140}$$

$$\mathbf{J}_B(x) = \left[\left(\bar{n}\lambda\epsilon_{ab}\dot{X}^b - 2T_{(01)}\partial_a\right)\delta^2\left(\mathbf{x}_\perp - \mathbf{X}(t)\right) - \bar{n}\partial_a V\left(\mathbf{x}_\perp\right)\right]\hat{\mathbf{x}}^a_\perp\,, \tag{141}$$

where we are now allowing the indices a, b to run over the tranverse directions x, y only, with summation over repeated indices implied.

In order to study the motion of the vortices without accounting in detail for the low-energy excitations of the superfluid, the effective field theory methodology dictates that we must integrate out the modes $\mathbf{A}$ and $\mathbf{B}$ from the action in Eq. (138), leaving only an effective action for $\mathbf{x}$, the coordinates of the vortex line. Following the methods of Horn *et al.* [49], we proceed by replacing the fields $\mathbf{A}$ and $\mathbf{B}$ with the solutions to their classical equations of

motion, resulting in contributions to the effective action for $\mathbf{X}$ from each of the form

$$S_{\text{eff}}^{(A)}[\mathbf{X}] = \frac{i}{2}\int \frac{d^3k\,d\omega}{(2\pi)^4} J_A^i(-k) G_A^{ij}(k) J_A^j(k)\,, \tag{142}$$

$$S_{\text{eff}}^{(B)}[\mathbf{X}] = \frac{i}{2}\int \frac{d^3k\,d\omega}{(2\pi)^4} J_B^i(-k) G_B^{ij}(k) J_B^j(k)\,. \tag{143}$$

Both contributions will include terms coupling the vortex position to the trapping potential, arising from diagrams of the type shown in Fig. 7. We will neglect the term with the time derivative in the source for the phonon field, Eq. (143), since there is already a single-time-derivative kinetic term for the vortex line in the fourth line of Eq. (138), and any additional corrections of order $\mathcal{O}(V)$ can be neglected as a first approximation. Notice, however, that there are no terms in the free string action—the first two terms of the fourth line of Eq. (143)—that break translation invariance, so there are no position-dependent terms in the potential for the vortex arising from the free action. Any $\mathcal{O}(V)$ non-derivative terms with position dependence that we find will, in fact, be the leading source of "forces" experienced by the vortex line.

Now, let us drop the irrelevant parts of the source terms in Eqs. (140) and (141) and Fourier transform them to momentum space:

$$\mathbf{J}_A(k) = (2\pi)\bar{n}\lambda\delta\left(k_z\right)\hat{\mathbf{z}}\int dt\, e^{i\omega t - i\mathbf{k}_\perp\cdot\mathbf{X}(t)}\,, \tag{144}$$

$$\mathbf{J}_B(k) = -2\pi i\delta\left(k_z\right)\mathbf{k}_\perp\left[2T_{(01)}\int dt\, e^{i\omega t - i\mathbf{k}_\perp\cdot\mathbf{X}(t)} + 2\pi\bar{n}\delta(\omega)V\left(\mathbf{k}_\perp\right)\right]\,, \tag{145}$$

where $\mathbf{k}_\perp \equiv (k_x, k_y)$ and $V\left(\mathbf{k}_\perp\right) = \int d^2x_\perp e^{-i\mathbf{k}_\perp\cdot\mathbf{x}_\perp} V\left(\mathbf{x}_\perp\right)$. Substituting Eq. (145) and the expression for the phonon propagator in Eq. (53) into the effective action Eq. (143), we find that the effective action includes the following contribution in the low momentum limit:

$$\begin{aligned} S_{\text{eff}}^{(B)}[\mathbf{x}] &\supset \frac{2\bar{n}c^2T_{(01)}}{\bar{w}c_s^2}\int dt\,dz\,V\left(\mathbf{X}\right) \\ &\simeq \frac{2T_{(01)}}{mc_s^2}\int dt\,dz\,V\left(\mathbf{X}\right)\,. \end{aligned} \tag{146}$$

In the second equality, we used the fact that $\bar{w} \simeq \bar{n}mc^2$ in a non-relativistic superfluid, as noted previously. Once again, we see that the derivatives associated with the interaction between the trapping potential and the phonon field and the interaction between the vortex world-sheet and the phonon field precisely counteract the non-locality of the propagator, leaving a purely local interaction between the trap and the vortex line. We would not generally expect this to happen, since integrating out gapless modes typically leads to long-range interactions in the resulting effective theory. The contribution that we calculated in Eq. (146) corresponds to a simple Feynman diagram of the type displayed on the left side of Fig. 7.

An additional contribution arises when accounting for the effects of cubic interaction $(\boldsymbol{\nabla} \cdot \mathbf{B}) (\boldsymbol{\nabla} \times \mathbf{A})^2$ in the second line of Eq. (138). In the presence of a trapping potential, that interaction can be thought of as a modification to the hydrophoton propagator, as shown in the diagram on the right side of Fig. 7. The zz component of the propagator gets a contribution of the form $\delta G_A^{33}(k) \propto \int d^4x\, d^4p\, d^4q\, e^{-i(p+q)x} V(\mathbf{x}_\perp) \frac{\mathbf{q}_\perp \cdot \mathbf{p}_\perp}{(k-p)^2(k+q)^2}$ from such an interaction. The resulting contribution to the vortex line effective action is found from Eq. (142) and the expression for the hydrophoton source term, Eq. (144). After some calculation, we find that

$$S_{\text{eff}}^{(A)}[\mathbf{x}] \supset \frac{\bar{n}^3 \lambda^2 c^4}{8\pi^2 \bar{w}^2 c_s^2} \left(1 - \frac{c_s^2}{c^2}\right) \int dt\, dz\, d^2x_\perp \frac{V(\mathbf{x}_\perp + \mathbf{X}(t))}{x_\perp^2} \,. \tag{147}$$

Finally, omitting terms that do not depend on the position of the vortex line, we are ready to write the full non-relativistic vortex line effective action to leading order in perturbation theory. From the action in Eq. (138) and the contributions calculated in Eqs. (146) and (147), and once again using the fact that $\bar{w} \simeq \bar{n}mc^2$ in the non-relativistic limit, the

result is

$$S_{\text{eff}}^{(\text{NR})}[\mathbf{X}] = \int dt\, dz \left[\frac{\bar{n}\lambda}{3} \epsilon_{ab} X^a \dot{X}^b + \frac{2T_{(01)}}{mc_s^2} V(\mathbf{X}) + \frac{\bar{n}\lambda^2}{8\pi^2 m^2 c_s^2} \int d^2x_\perp \frac{V(\mathbf{x}_\perp + \mathbf{X})}{x_\perp^2} \right]. \tag{148}$$

The second line of Eq. (148) involves a non-local term, in the sense that it depends on positions in the atomic cloud far from the position of the vortex line itself. It thus represents a long-range interaction between the vortex line and the trapping potential. Nonetheless, the problem of determining the motion of the vortex has been reduced to one of point-particle mechanics in two dimensions, given the action in Eq. (148), and the equations of motions can be obtained directly through standard variational analysis.

Let us now vary the effective vortex line action with respect to vortex position X^a. The resulting equations of motion can be written as

$$\frac{2\bar{n}\lambda}{3} \epsilon_{ab} \dot{X}^b - \partial_a V_{\text{eff}}(\mathbf{X}) = 0\,, \tag{149}$$

where we have defined an effective potential

$$V_{\text{eff}}(\mathbf{X}) \equiv -\frac{2T_{(01)}}{mc_s^2} V(\mathbf{X}) - \frac{\bar{n}\lambda^2}{8\pi^2 m^2 c_s^2} \int d^2x_\perp \frac{V(\mathbf{x}_\perp + \mathbf{X})}{x_\perp^2}\,. \tag{150}$$

The meaning of this expression becomes more clear when we restrict to vortex line positions near the center of the atomic cloud—*i.e.* small values of (X, Y). We can expand $V(\mathbf{X})$ and $V(\mathbf{x}_\perp + \mathbf{X})$ in Eq. (150) to quadratic order in X^a, in which case we find

$$V_{\text{eff}}(\mathbf{X}) \simeq -\frac{1}{2} X^a X^b \left[\frac{2T_{(01)}}{mc_s^2} \partial_a \partial_b V(\mathbf{x} = 0) + \frac{\bar{n}\lambda^2}{8\pi^2 m^2 c_s^2} \int d^2x_\perp \frac{\partial_a \partial_b V(\mathbf{x}_\perp)}{x_\perp^2} \right]. \tag{151}$$

We assume here that linear terms do not contribute. We may take the vanishing of linear terms in the effective potential to define what we mean precisely by the "center" of the

atomic cloud. We must now consider two qualitatively different possibilities to determine the motion of the vortex line: (a.) when $\partial_a \partial_b V(\mathbf{x}=0) \neq 0$ (harmonic trapping) and (b.) when $\partial_a \partial_b V(\mathbf{x}=0) = 0$ (non-harmonic trapping).

3.3.2 Harmonic Trapping

Consider the case of approximately harmonic trapping, when $V(\mathbf{x}_\perp)$ is quadratic near the center of the atomic cloud, so that $\partial_a \partial_b V(\mathbf{x}=0)$ is non-vanishing. In this case, the first term in the effective potential for vortex lines, Eq. (151), is non-zero. Also, the integral in the second term of the effective potential has a logarithmic divergence arising from the position $\mathbf{x}_\perp = 0$. Taking a to be an arbitrary ultraviolet cutoff length scale, we find that the value of the divergent integral can be written as

$$\int d^2x_\perp \frac{\partial_a \partial_b V(\mathbf{x}_\perp)}{x_\perp^2} = -2\pi \partial_a \partial_b V(\mathbf{x}=0) \log a + \cdots , \tag{152}$$

where the dots represent additional terms that are finite in the limit $a \to 0$. This statement is not physically meaningful, however, since a is a quantity with dimensions of length. As is typically the case when dealing with ultraviolet logarithmic divergences, the UV length scale must appear in a ratio with a corresponding infrared cutoff length scale. In our case, the only such length scale in the problem is $R_\perp$, the typical tranverse size of the atomic cloud. Beyond this large length scale, our perturbative analysis certainly becomes pathological, so it would not be reasonable to extrapolate integrals such as the one above to radial positions larger than $R_\perp$. Therefore, we find that the integral can be written as

$$\int d^2x_\perp \frac{\partial_a \partial_b V(\mathbf{x}_\perp)}{x_\perp^2} = 2\pi \partial_a \partial_b V(\mathbf{x}=0) \log \frac{R_\perp}{a} , \tag{153}$$

and the second term in Eq. (151) can thus be considered a renormalization of the first term.

According to the standard logic of renormalization group theory, we can take the coupling constant $T_{(01)}$ to run with momentum scale q and reparametrize the effective potential in terms of the running coupling evaluated at some typical momentum q of order $1/R_\perp$. By

this logic, we rewrite Eq. (151) as

$$V_{\text{eff}}\left(\mathbf{X}\right) \simeq -\frac{1}{mc_s^2} T_{(01)}\left(1/R_\perp\right) \partial_a \partial_b V\left(\mathbf{x}=0\right) X^a X^b \,, \tag{154}$$

where we now have

$$T_{(01)}(q) = -\frac{\bar{n}\lambda^2}{8\pi m} \log(q\ell) \,. \tag{155}$$

The quantity ℓ is understood to be a microscopic physical length scale. We would expect its value to be of the order of the healing length in the case of a Bose condensate, but the precise value is left to be fixed from experiment, according to the standard renormalization group reasoning. It is interesting to note that the running of the tension that must be introduced to renormalize the first term in our effective potential is identical to the running found using other methods by Horn *et al.* [49] in the non-relativistic limit (see Eq. (6.23) in the reference).

We will expand the potential near the center of the atomic cloud as a harmonic function of position, similar to the potential considered in Eq. (120), up to quadratic order:

$$V\left(\mathbf{x}_\perp\right) = \frac{1}{2} m \left(\omega_x^2 x^2 + \omega_y^2 y^2\right) + \mathcal{O}\left(x_\perp^4\right) \,. \tag{156}$$

In this approximation, the equations of motion, Eq. (149), become

$$\dot{X}(t) - \frac{\omega_y}{\omega_x}\omega_p Y(t) = 0 \,, \quad \dot{Y}(t) + \frac{\omega_x}{\omega_y}\omega_p X(t) = 0 \,, \tag{157}$$

where we defined

$$\omega_p \equiv \frac{3\Gamma}{8\pi c_s^2}\omega_x\omega_y \log\frac{R_\perp}{\ell} \,. \tag{158}$$

Here, we used the fact that the circulation Γ is approximately equal to λ/m in the non-

relativistic limit. The solutions to these equations of motion are simple elliptical orbits with angular frequency ω_p:

$$\begin{aligned} X(t) &= X_0 \cos(\omega_p t) + \frac{\omega_y}{\omega_x} Y_0 \sin(\omega_p t) \,, \\ Y(t) &= Y_0 \cos(\omega_p t) - \frac{\omega_x}{\omega_y} X_0 \sin(\omega_p t) \,. \end{aligned} \tag{159}$$

The orbits have the same aspect ratio and orientation as the harmonic trapping potential. Since the quantum of circulation is also equal to $2\pi\hbar/m$, our result for a singly quantized vortex is formally equivalent to that of Svidzinsky and Fetter [95] (see Eq. (122)), up to ambiguity in the definition of the large logarithmic factor. We emphasize that we never relied on any sort of Hartree or mean field approximation, unlike the analysis of vortex precession in the formalism Gross–Pitaevskii theory.

We must be careful about the somewhat ambiguous meaning of the large logarithmic factor in Eq. (158), however, since it includes an undetermined short length scale, which is to be fixed by experiment. The result can be made more predictive, though, by considering the combination of frequencies

$$\chi \equiv \frac{\omega_p}{\omega_x \omega_y} \,. \tag{160}$$

We can eliminate the free parameter ℓ by considering differences between this quantity χ in setups with different trapping potentials, and therefore different cloud sizes $R_\perp$. We would expect the difference between values of χ for different trapping potentials to be equal to

$$\chi_1 - \chi_2 = \frac{3\Gamma}{8\pi c_s^2} \log \frac{R_{\perp,1}}{R_{\perp,2}} \,. \tag{161}$$

Notice that this result *is*, in fact, completely predictive and all free parameters have been eliminated. This equation can be used to make direct contact with experimental measurements without any ambiguity.

3.3.3 Flatter Trapping Potentials

Let us now return to the second possibility for the trapping potential, that of non-harmonic trapping. In this case, we have the vanishing of second derivatives of the trapping potential near the center, so that $\partial_a \partial_b V(\mathbf{x} = 0) = 0$. Then the first term in the effective potential for vortex lines, Eq. (151), is equal to zero. The second term involving the integral is now completely convergent, and is therefore easier to treat than in the case of harmonic trapping. Let us parametrize the trapping potential in a more general manner:

$$V(\mathbf{x}_\perp) = mc_s^2 f(\mathbf{x}_\perp / R_\perp) \,, \tag{162}$$

where f is a generic dimensionless function with vanishing second derivatives near the origin and order-one coefficients. We choose the overall pre-factor mc_s^2 to match the factor found in Eq. (133). In this case, the integral in Eq. (151) becomes

$$\int d^2x_\perp \frac{\partial_a \partial_b V(\mathbf{x}_\perp)}{x_\perp^2} = \frac{mc_s^2}{R_\perp^2} f_{ab} \,, \tag{163}$$

where the tensor f_{ab} is constant and symmetric with generically order-one entries. We may choose to align our x and y axes with the eigenvectors of the tensor f_{ab}, in which case we find that the equations of motion in Eq. (149) become

$$\dot{X}(t) - \sqrt{\frac{f_{yy}}{f_{xx}}} \omega_p Y(t) = 0 \,, \quad \dot{Y}(t) + \sqrt{\frac{f_{xx}}{f_{yy}}} \omega_p X(t) = 0 \,. \tag{164}$$

The solutions are once again elliptical trajectories of the form

$$\begin{aligned} X(t) &= X_0 \cos(\omega_p t) + \sqrt{\frac{f_{yy}}{f_{xx}}} Y_0 \sin(\omega_p t) \,, \\ Y(t) &= Y_0 \cos(\omega_p t) - \sqrt{\frac{f_{xx}}{f_{yy}}} \sin(\omega_p t) \,. \end{aligned} \tag{165}$$

The aspect ratio of the elliptical orbits is now equal to $\sqrt{f_{yy}/f_{xx}}$ and the angular frequency is given by

$$\omega_p = \frac{3\Gamma}{16\pi^2 R_\perp^2}\sqrt{f_{xx}f_{yy}}\,. \tag{166}$$

The logarithmic correction does not survive, as in the case of harmonic trapping. Our results indicate that if $\omega_x \sim \omega_y \sim \omega$, the precession frequency scales as $\frac{\Gamma\omega^2}{c_s^2}\log\omega$ when the trapping is harmonic, since $R_\perp \sim c_s/\omega$, but when the trapping is anharmonic, the precession frequency scales only as $\Gamma\omega^2/c_s^2$, because the tensor f_{ab} has order-one numerical entries in general. This is consistent with the theoretical results found by Kevrekidis *et al.* [105] from standard Gross–Pitaevskii theory in the case of a non-parabolic external potential. Their analysis of general trapping potentials of the form $V(r) \propto r^p$ when $p > 2$ indicates that the precession frequency exhibits the same $\omega_p \propto 1/R_\perp^2$ scaling without any logarithmic factors of the sort seen in harmonic trapping, when $p = 2$, and they corroborated this observation with numerical analysis.

It is important to note that the precise value of the precession frequency in Eq. (166) depends on both the specific functional form of $f\,(\mathbf{x}_\perp)$ that defines the shape of the trapping potential and on how we decide to cut off the integral in Eq. (163), which determines the entries in the tensor f_{ab}. For a radially symmetric cloud, we would certainly expect the tensor f_{ab} to be proportional to δ_{ab}, but in more general scenarios the implementation of the cutoff can lead to different tensor structures. Since our perturbative analysis becomes invalid when gradients of the trapping potential become large near the edge of the atomic cloud, we cannot definitively say which cutoff procedure for computing the integral in Eq. (163) would be the most physical in all situations. At the moment, we leave the tensor f_{ab} undetermined for general, non-radially symmetric, non-harmonic trapping potentials. We hope to return to this detail in the future, perhaps appealing to the type of renormalization group ideas that led to Eq. (137) in order to determine a precise physical scheme for implementing a

cutoff and making the integral in Eq. (163) finite in the infrared.

3.3.4 Addendum: Note on Relativistic Corrections

It is not difficult to calculate further relativistic corrections to the above result by reinstating relevant terms that we neglected from the full action in Eq. (138). Of these, the leading-order contribution (assuming the motion of the vortex is still slow) will come from the interaction

$$S \supset \frac{\bar{n}}{2c^2} \int dt\, d^3x\, U_{ij}\left(\mathbf{x}_\perp\right) \left(\boldsymbol{\nabla} \times \mathbf{A}\right)^i \left(\boldsymbol{\nabla} \times \mathbf{A}\right)^j \ , \tag{167}$$

where we defined the combination

$$U_{ij}\left(\mathbf{x}_\perp\right) \equiv V\left(\mathbf{x}_\perp\right) \delta_{ij} - V_{ij}\left(\mathbf{x}_\perp\right) \ . \tag{168}$$

This has the effect of modifying the original source term for $\mathbf{A}$, Eq. (144), leading to a hydrophoton-mediated interaction between the vortex world-sheet and the trapping potential of the form shown in Fig. 8 below.

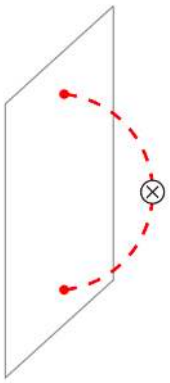

Figure 8: Feynman diagram representing the leading-order relativistic interaction between the trapping potential and the vortex line. The crossed circle represents the trapping potential, now given by the modified expression Eq. (168). The red dashed lines are hydrophoton propagators.

This additional interaction term modifies our expression for the vortex line effective action, Eq. (148). When we account for relativistic corrections and integrate out the bulk

modes, we are left with the following effective action for vortex lines:

$$\begin{aligned} S_{\text{eff}}^{(\text{R})} &\supset -\frac{\bar{n}^3\lambda^2 c^2}{2\bar{w}^2}\int dt\, d^3x\, \epsilon^{ab}\epsilon^{cd}U_{ac}\left(\mathbf{x}_\perp+\mathbf{X}\right)\int\frac{d^2p_\perp d^2q_\perp}{(2pi)^4}e^{-i(\mathbf{p}_\perp+\mathbf{q}_\perp)\cdot\mathbf{x}_\perp}\frac{p_\perp^b q_\perp^d}{p_\perp^2 q_\perp^2} \\ &= \frac{\bar{n}^3\lambda^2 c^2}{8\pi^2\bar{w}^2}\int dt\, dz\int d^2x_\perp\,\epsilon^{ab}\epsilon^{cd}U_{ac}\left(\mathbf{x}_\perp+\mathbf{X}\right)\frac{x_\perp^b x_\perp^d}{x_\perp^4}\,. \end{aligned} \tag{169}$$

Now, including the phonon-mediated interaction of the vortex line with the trapping potential, as well as the contribution arising from the Kalb–Ramond vortex line action, we find that the full relativistic effective action for vortex lines is given by

$$\begin{aligned} S_{\text{eff}}^{(\text{R})}\left[\mathbf{X}\right] = \int dt\, dz\Bigg[&\frac{\bar{n}\lambda}{3}\epsilon_{ab}X^a\dot{X}^b+\frac{2T_{(01)}\bar{n}c^2}{\bar{w}c_s^2}V\left(\mathbf{X}\right)+\frac{\bar{n}^3\lambda^2c^4}{8\pi^2\bar{w}c_s^2}\int d^2x_\perp\frac{V\left(\mathbf{x}_\perp+\mathbf{X}\right)}{x_\perp^2} \\ &-\frac{\bar{n}^3\lambda^2c^2}{8\pi^2\bar{w}^2}\int d^2x_\perp\,\epsilon^{ab}\epsilon^{cd}V_{ac}\left(\mathbf{x}_\perp+\mathbf{X}\right)\frac{x_\perp^b x_\perp^d}{x_\perp^4}\Bigg]\,. \end{aligned} \tag{170}$$

In principle, given any trapping configuration, equations of motion for vortex lines with relativistic corrections can be calculated by varying this effective action with respect to $\mathbf{X}$. Notice that when there is no coupling between the trapping potential and the bulk velocity of the superfluid—that is, when $V_{ab}=0$—the relativistic and non-relativistic results are completely equivalent. This is because the leading-order relativistic correction we calculated in Eq. (147) exactly cancels the new piece from the diagram in Fig. 8.

3.4 An Aside on Kelvin Waves

In Section 2.5, we briefly encountered the phenomenon of Kelvin waves, excitations of vortex lines in superfluids that take the form of helical traveling waves and have a distinctive dispersion relation in the long wavelength limit characterized by

$$\frac{\partial\left(\omega/k^2\right)}{\partial\left(\log k\right)} = -\frac{\Gamma}{4\pi}\,, \tag{171}$$

where Γ is the quantized circulation around the vortex line [92]. See, for example, [49, 63] for more detail on the treatment of Kelvin waves in effective field theory. The question of what happens to the Kelvin wave dispersion relation in the case of trapped, rotating Bose–Einstein condensates has been studied theoretically and numerically using the Gross–Pitaevskii equation and Bogolyubov–de Gennes mean field theory, with most methods relying on matched asymptotic expansions [106–108]. It has not been treated before using effective field theory, to the best of our knowledge. We will briefly consider this question here, since all the necessary ingredients are already in place.

All that we must do to study the propagation of Kelvin waves in the presence of trapping is add the effective vortex potential in Eq. (150) to the kinetic terms for vortex lines in the original vortex effective action. Using the approximate expression Eq. (151), valid near the center of the cloud, we find

$$S_{\text{eff}}[\mathbf{X}] = \int dt\, dz\, \left[-T_{(00)}\left|\partial_z \mathbf{X}\right| - \frac{\bar{n}\lambda}{3}\epsilon_{ijk}X^k\partial_t X^i \partial_z X^j + \frac{1}{2}\mathcal{M}_{ab}X^a X^b\right]\,, \tag{172}$$

where we defined the symmetric matrix

$$\mathcal{M}_{ab} \equiv \begin{cases} \frac{2T_{(01)}}{mc_s^2}\partial_a\partial_b V\left(\mathbf{x}=0\right) & \text{(harmonic trapping)} \\ \frac{\bar{n}\lambda^2}{8\pi^2 m^2 c_s^2}\int d^2x_\perp \frac{\partial_a\partial_b V(\mathbf{x}_\perp)}{x_\perp^2} & \text{(non-harmonic trapping)} \end{cases}\,. \tag{173}$$

To lowest order near the center of the cloud, the trapping potential produces an extra

quadratic term in the effective action, which takes the form above in the case of trapping that is predominantly along two dimensions.

For reference, let us first note the expressions for the renormalized tensions $T_{(00)}$ and $T_{(01)}$, including the running with momentum scale k, which are derived in [49]:

$$T_{(00)}(k) = -\frac{\bar{n}\lambda^2}{4\pi m}\log(k\ell)\ , \tag{174}$$

$$T_{(01)}(k) = -\frac{\bar{n}\lambda^2}{8\pi m}\left(1-\frac{c_s^2}{c^2}\right)\log(k\ell)\ , \tag{175}$$

where ℓ is again a UV cutoff length scale, expected to be of the order of the healing length in the condensate. In the simplest case, we can consider a straight-line vortex located right in the center of the atomic cloud, $\mathbf{X} = (0, 0, z)$ and introduce a tranverse perturbing kelvon field $\boldsymbol{\phi}(t, z) = (\phi^x, \phi^y, 0)$. Following the same procedure as in Section 2.5, our effective action for vortex line excitations becomes

$$S_{\text{eff}} \to \int dt\, dz\, \left[-T_{(00)}\sqrt{1+(\partial_z\boldsymbol{\phi})^2} - \frac{\bar{n}\lambda}{2}\epsilon_{ab}\phi^a\dot{\phi}^b + \frac{1}{2}\mathcal{M}_{ab}\phi^a\phi^b\right]\ . \tag{176}$$

Expanding the action to quadratic order, this leads to equations of motion that are a straightforward generalization of Eq. (114). Looking for plane wave solutions $\boldsymbol{\phi} = \boldsymbol{\phi}_0 e^{i(kz-\omega t)}$ is tantamount to solving the eigenvalue problem

$$\begin{pmatrix} -i\mathcal{M}_{xy} & T_{(00)}k^2 - \mathcal{M}_{yy} \\ T_{(00)}k^2 - \mathcal{M}_{xx} & i\mathcal{M}_{xy} \end{pmatrix}\begin{pmatrix} \phi_0^x \\ i\phi_0^y \end{pmatrix} = \bar{n}\lambda\omega\begin{pmatrix} \phi_0^x \\ i\phi_0^y \end{pmatrix}\ , \tag{177}$$

which in general has eigenfrequencies

$$\omega^2 = \frac{1}{\bar{n}^2\lambda^2}\left[T_{(00)}^2k^4 - (\mathcal{M}_{xx}+\mathcal{M}_{yy})\,T_{(00)}k^2 + \mathcal{M}_{xx}\mathcal{M}_{yy} - \mathcal{M}_{xy}^2\right]\ . \tag{178}$$

When this quantity is real, we will again have two circularly polarized helical traveling waves propagating along the vortex line, but the dispersion relation will in general be rather

different from the usual one in Eq. (171).

Let us first consider the case of harmonic trapping, with a trapping potential of the form $V(\mathbf{x}) = \frac{1}{2}m\left(\omega_x^2 x^2 + \omega_y^2 y^2\right)$. When the momentum k is much greater than the inverse transverse length scale of the cloud, $R_\perp^{-1}$, the appropriate IR momentum scale at which to evaluate the tension $T_{(01)}$ is k, since we can safely assume that the long-wavelength kelvon modes do not probe regions of the atomic cloud beyond k^{-1}; otherwise, the IR cutoff scale is again $R_\perp^{-1}$. So putting everything together now, from Eqs. (173) to (175) and (178) and the relation $m\Gamma \simeq \lambda$, we find the following modified dispersion relation in the non-relativistic limit:

$$\omega(k) \simeq \pm\frac{\Gamma}{4\pi}\sqrt{\left(k^2 - \frac{\omega_x^2}{c_s^2}\right)\left(k^2 - \frac{\omega_y^2}{c_s^2}\right)}\begin{cases}\log(k\ell)\,, & k \gg R_\perp^{-1}\\ \log\left(R_\perp/\ell\right)\,, & \text{otherwise}\end{cases}. \tag{179}$$

Of course, the standard result is recovered when $\omega_x = \omega_y = 0$ (in which case we also have $R_\perp^{-1} \to 0$). Notice, however, that the low-momentum region of this dispersion relation has completely qualitatively different behavior when weak harmonic trapping occurs and $R_\perp^{-1}$ is very small, since $\omega \sim \frac{\Gamma\omega_x\omega_y}{c_s^2}\log(k\ell)$ for low momenta. In such a scenario, it takes arbitrarily high energy to sustain a kelvon mode with arbitrarily low momentum k. There is also an instability at momenta between ω_x/c_s and ω_y/c_s, since the modes begin to probe regions of stronger potential and the solutions we found blow up exponentially. In a general harmonic trapping configuration, for momenta below $R_\perp^{-1}$, the energy of kelvon modes approaches a constant non-zero value of $\frac{\Gamma\omega_x\omega_y}{4\pi c_s^2}\log\left(R_\perp/\ell\right)$ at vanishing momentum $k \to 0$, which does not occur in the absence of trapping.

Next let us think about what happens in flatter trapping potentials, in particular where $\partial_a\partial_b V\left(\mathbf{x}=0\right) = 0$. In that case, we must again assess the integral in Eq. (163), but now at the IR cutoff scale k^{-1} when the momentum is much greater than the inverse transverse

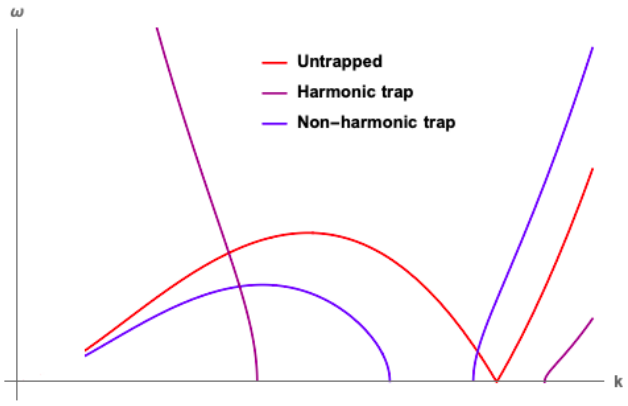

Figure 9: Qualitative features of the dispersion relations of Kelvin wave modes with and without two-dimensional trapping.

length scale of the atomic cloud. The resulting dispersion relation is now

$$\omega(k) \simeq \pm\frac{\Gamma}{4\pi}k^2 \begin{cases} \sqrt{[\log(k\ell)]^2 + \frac{f_{xx}+f_{yy}}{2\pi}\log(k\ell) + \frac{f_{xx}f_{yy}-f_{xy}^2}{4\pi^2}}\,, & k \gg R_\perp^{-1} \\ \sqrt{[\log(R_\perp/\ell)]^2 - \frac{f_{xx}+f_{yy}}{2\pi R_\perp^2 k^2}\log(R_\perp/\ell) + \frac{f_{xx}f_{yy}-f_{xy}^2}{4\pi^2 R_\perp^4 k^4}}\,, & \text{otherwise} \end{cases} . \qquad (180)$$

In the case of weak non-harmonic trapping with very small $R_\perp^{-1}$, the energy of the kelvon modes now becomes arbitrarily small for small momenta k, which does not occur when there is weak harmonic trapping. There is again an instability, this time when $\log(k\ell)$ is between $f_{xx}/2\pi$ and $f_{yy}/2\pi$ in the diagonal case. If the entries of f_{ab} are of order one, this situation corresponds to high momenta at which the effective theory breaks down. In a general non-harmonic trapping configuration, the energy of kelvon modes again approaches a constant value of $\frac{\Gamma}{8\pi^2 R_\perp^2}\sqrt{f_{xx}f_{yy}-f_{xy}^2}$ for vanishing momentum $k \to \infty$. This is generically non-zero, unless the trapping is axisymmetric and the matrix f_{ab} has no non-zero off-diagonal entries. For non-axisymmetric non-harmonic traps, the low-momentum limit of the dispersion relation differs from the untrapped case.

As we have seen, when there is two-dimensional trapping, there are important modifications to the dispersion relation of Kelvin waves propagating along vortex lines near the center of a condensate. A sketch of the qualitative features of each case is shown in Fig. 9. It is worth mentioning that when the vortex line begins off-center and precesses around the

center of the atomic cloud, the exact same Kelvin modes can be sustained, with the same dispersion relations, but superimposed on the precessing solutions we found in Section 3.3. Solitonic solutions do not arise from this linearized analysis, but we could also look for non-linear solutions to equations of motion at higher order in ϕ.

Let us now use the action Eq. (176) to study the equations of motion at non-linear order. In order to do so, it will be helpful to perform a field redefinition

$$\phi_\pm = \frac{1}{\sqrt{2}} \left(\phi^x \pm i\phi^y\right) , \tag{181}$$

assuming that ϕ^x and ϕ^y are real scalar fields. Then the action becomes

$$S_{\text{eff}} = \int dt\, dz \, \left[-T_{(00)} \sqrt{1 + \partial_z \phi_+ \partial_z \phi_-} + i\bar{n}\lambda \dot{\phi}_+ \phi_- + \frac{1}{2} \mathcal{M}_{rs} \phi_r \phi_s \right] , \tag{182}$$

where now r, s range over the signs $+, -$. In this parametrization, we have

$$\mathcal{M}_{++} = \mathcal{M}_{--} = \frac{1}{2} \left(\mathcal{M}_{xx} - \mathcal{M}_{yy} - 2i\mathcal{M}_{xy} \right) , \tag{183}$$

$$\mathcal{M}_{+-} = \mathcal{M}_{-+} = \frac{1}{2} \left(\mathcal{M}_{xx} + \mathcal{M}_{yy} \right) . \tag{184}$$

This leads to two non-linear equations of motion

$$0 = T_{(00)} \partial_z \left[\frac{\partial_z \phi_\pm}{\sqrt{1 + 2\partial_z \phi_+ \partial_z \phi_-}} \right] \pm i\bar{n}\lambda \dot{\phi}_\pm + \mathcal{M}_{\mp r} \phi_r \, . \tag{185}$$

We will be interested in solutions that can be parametrized as traveling helical waves of the form $\phi_\pm = \frac{1}{\sqrt{2}} \rho e^{\pm i(kz - \omega t)}$. The parameter ρ, assumed to be real, represents the radius of the helical waveform here. The first thing to notice is that whenever $\mathcal{M}_{++} = \mathcal{M}_{--} \neq 0$, there are no solutions of this form. This occurs when the off-diagonal matrix components in the original parametrization, $\mathcal{M}_{xy}$, are non-zero; that, in turn, occurs only in the case of non-harmonic, non-axisymmetric trapping, when $\partial_a \partial_b V(\mathbf{x})$ cannot be diagonalized. Simple

helical traveling waves cannot be sustained in such an asymmetric trapping configuration. Let us assume that we are dealing with usual trapping potentials, which are elliptical, so that these components $\mathcal{M}_{++}$ and $\mathcal{M}_{--}$ are zero. Substituting the ansatz into the equations of motion then leads to the expression

$$\omega(k) = \pm\frac{T_{(00)}(k)}{\bar{w}\Gamma}\frac{k^2}{\sqrt{1+\rho^2k^2}} \mp \begin{cases} \frac{T_{(01)}(k)}{\bar{w}\Gamma}\frac{\omega_x^2+\omega_y^2}{c_s^2} & \text{(harmonic trapping)} \\ \frac{\Gamma k^2}{16\pi^2}\left(f_{xx}+f_{yy}\right) & \text{(non-harmonic trapping)} \end{cases} . \tag{186}$$

Consider first what happens in the absence of trapping. The original dispersion relation for kelvon modes, $\omega \sim k^2 \log k$, is recovered in the low-momentum/small-radius limit $\rho k \ll 1$. In the opposite limit, when $\rho k \gg 1$, a new regime emerges with $\omega \sim k \log k$; this becomes approximately non-dispersive for low momentum and large radius ρ. For such large-amplitude Kelvin wave modes, which one may contemplate in the absence of trapping, the energy scales as

$$\omega(k) \simeq \pm\frac{\Gamma}{4\pi\rho}k\log(k\ell)\,. \tag{187}$$

This situation corresponds to the "self-pipe" analyzed by Horn *et al.* [49], in which the large-amplitude Kelvin wave acts as a solenoid with a nearly uniform velocity field aligned in the z direction inside the radius ρ and very little flow outside. The solenoid configuration itself travels with group velocity $v(k) \sim \frac{\Gamma}{\rho}\log k$.

In the case of harmonic trapping in the limit $\rho k \ll 1$, the original dispersion relation from linear analysis is only matched when the trap is perfectly circular, with $\omega_x = \omega_y$. Otherwise, we find $\omega \sim \left(c_s^2k^2 - \omega_x^2 - \omega_y^2\right)\log k$. This exhibits the usual enhanced logarithmic scaling at low momenta characteristic of harmonic trapping. There is no longer an unstable region for momenta between ω_x/c_s and ω_y/c_s in which propagating Kelvin waves are not supported. The opposite limit in which $\rho k \gg 1$ is not particularly sensible to consider in a trapped superfluid, since that would correspond to Kelvin wave solutions with radius

comparable to or greater than the size of the atomic cloud. The intermediate regime with non-negligible $\rho k \lesssim 1$ features a reduced group velocity for Kelvin waves compared to the case with negligible $\rho k \ll 1$.

Finally, when the trapping is non-harmonic, in the limit $\rho k \ll 1$ we recover the same dispersion relation when the trapping potential is perfectly symmetrical and $f_{xx} = f_{yy}$. If the trapping potential is oblate, however, we find $\omega \sim k^2 \left[4\pi \log(k\ell) + f_{xx} + f_{yy}\right]$. Again, there is no unstable regime for momenta at which the solution grows exponentially. Intermediate radii and momenta with $\rho k \lesssim 1$ again exhibit a reduced group velocity compared to the one found from the linearized analysis.

3.5 Three-dimensional Trapping and the Bending of Vortex Lines

We can attempt to extend this analysis by considering the effects of trapping in a third dimension, which is present in realistic experimental setups. For concreteness, we are imagining vortex lines that are more-or-less vertical (aligned with the z coordinate), but not necessarily straight. They may become slightly bent or curved due to the change in the trapping potential in the vertical direction. This means we must add mild z-dependence to the vortex line coordinates, since z-translation symmetry is no longer present. Our vortex line coordinates will now be parametrized as

$$\mathbf{X} = [X(t,z), Y(t,z), z] \ . \tag{188}$$

The trapping potential $V(\mathbf{x})$ also has explicit dependence on the coordinate z, in addition to the transverse coordinates. The effective action for vortex lines will be identical to the one we considered for Kelvin waves, Eq. (172), when we gave X and Y a slight z-dependence, but not the trapping potential. This effective action can now be written as

$$S_{\text{eff}}\left[\mathbf{X}\right] = \int dt\, dz\, \left[-\frac{\bar{n}\lambda}{2}\epsilon_{ab} X^a \dot{X}^b - T_{(00)}\sqrt{1+(\partial_z X^a)^2} - V_{\text{eff}}[\mathbf{X}(t,z)] \right] . \tag{189}$$

However, the expression for the effective potential must now be modified to account for three-dimensional trapping. The result we found in Eq. (150) is no longer valid.

To see what changes in the effective potential, we must go back to the expressions in Eqs. (140) and (141), the source terms for the phonon and hydrophoton fields due to interactions with the vortex line. These must be appropriately generalized for the case of three-dimensional trapping and vortex lines positions with z-dependence. As a result, we

must now use the expressions

$$J_A^i(\mathbf{x},t) = \bar{n}\lambda\,\delta^2\left(\mathbf{x}_\perp - \mathbf{X}_\perp(t,z)\right)\left[\delta_z^i + \delta_a^i\partial_z\dot{X}^a(t,z)\right]. \tag{190}$$

$$\begin{aligned} J_B^i(\mathbf{x},t) = {} & \bar{n}\lambda\epsilon_{ab}\delta^2\left(\mathbf{x}_\perp - \mathbf{X}_\perp(t,z)\right)\left[\dot{X}^b(t,z)\delta_a^i + \dot{X}^a(t,z)\partial_z X^b(t,z)\delta_z^i\right] \\ & - 2T_{(01)}\partial_i\left[\delta^2\left(\mathbf{x}_\perp - \mathbf{X}_\perp(t,z)\right)\sqrt{1+\left(\partial_z X^a(t,z)\right)^2}\right] \\ & - \bar{n}\partial_i V(\mathbf{x})\,. \end{aligned} \tag{191}$$

Although these are quite complicated expressions, to leading order very little changes. Following the same procedure as before, calculating contributions to the effective action from the diagrams in Fig. 7, we find that the resulting effective potential for vortex lines now has the form

$$V_{\text{eff}}(\mathbf{X}) = -\frac{2T_{(01)}}{mc_s^2}V(\mathbf{X})\sqrt{1+\left(\partial_z X^a\right)^2} - \frac{\bar{n}\lambda^2}{8\pi^2 m^2 c_s^2}\int d^2x_\perp \frac{V\left(x_\perp^a + X^a, z\right)}{x_\perp^2}\,. \tag{192}$$

We will again work with the assumption that the coordinates X^a are small, so that the vortex line does not stray far from the center of the cloud. This effective potential can then be expanded to quadratic order in X^a, and we can vary the action of Eq. (189) in order to find equations of motion for the vortex line coordinates. In addition, we consider approximately harmonic trapping along the z direction, focusing on the region where z is small near the center of the atomic cloud.

Assuming that the trapping along the z direction can be expressed in the form[5] $\frac{1}{2}m\omega_z^2 z^2$,

[5]In principle, we do not want our vortex lines to probe regions of divergent potential $z \to \infty$. If we wanted to be more careful about this, we could take the trapping along z to be an inverted Gaussian with small amplitude, which is roughly parabolic near the center of the trap, and solve the equations of motion approximately for regions of small z. Then the result is identical to what we find here.

the equations of motion in this case are

$$\begin{aligned} 0 = \bar{n}\lambda\epsilon_{ab}\dot{X}^b + \frac{2T_{(01)}}{mc_s^2}\partial_a\partial_b V\left(\mathbf{x}_\perp = 0, z\right) X^b \\ - T_{(00)}\partial_z^2 X^a - \frac{\omega_z^2 T_{(01)}}{c_s^2}\partial_z\left[z^2\partial_z X^a\right] . \end{aligned} \tag{193}$$

In this expression, $T_{(00)}$ and $T_{(01)}$ are understood to be the renormalized couplings in Eqs. (174) and (175). If we set all derivatives of X^a with respect to the z coordinate to zero, we see that the first line of this equation of motion is precisely the part that gave us precessional motion previously. As we will see, the second line will lead to solutions that allow the vortex lines to become kinked along the z direction. This set of two coupled differential equations can be solved using separation of variables. Let us choose the ansatz

$$\begin{pmatrix} X(t,z) \\ Y(t,z) \end{pmatrix} = \begin{pmatrix} \tilde{X}(t) \\ \tilde{Y}(t) \end{pmatrix} f(z) . \tag{194}$$

If we substitute this into the equations of motion, we immediately see that $\tilde{X}(t)$ and $\tilde{Y}(t)$ are the same precessing solutions with elliptical trajectories we found in Eq. (159) (but with a slightly different precession frequency), as long as the function $f(z)$ satisfies the differential equation

$$0 = \frac{d^2 f}{dz^2} + \frac{\omega_z^2 T_{(01)}}{c_s^2 T_{(00)}}\frac{d}{dz}\left(z^2\frac{df}{dz}\right) . \tag{195}$$

Although straight-line vortices still solve the equations of motion, we now have additional solutions for which $f(z)$ is simply the arctangent function. If we let $f_\pm$ be the limiting values we choose for the solution $f(z)$ as $z \to \pm R_z$ (where R_z is the spatial extent of the atomic cloud along the z axis), using Eqs. (174) and (175) we find that in the non-relativistic limit

$$f(z) = \frac{f_+ - f_-}{\pi}\arctan\left(\frac{\omega_z}{2c_s}z\right) + \frac{f_+ + f_-}{2} . \tag{196}$$

The solutions that we have found describe vortex lines precessing along elliptical orbits, but the vertical profile of the vortex lines is modulated by a function of the form in Eq. (196). The vortex lines can become kinked due to the trapping in the vertical direction. It is interesting to note that in this case, because of the form of the Kalb–Ramond term in the action, the precession frequency differs from the one we found previously in Eq. (158) by a factor of two thirds. For these solutions, we now have

$$\omega_p^{(3\mathrm{d})} = \frac{\Gamma}{4\pi c_s^2}\omega_x\omega_y \log\frac{R_\perp}{\ell}\,. \tag{197}$$

When the trapping is not harmonic, the situation is quite similar and bending will also occur, but we will not show it explicitly here, since the equations of motion will depend on the specific functional form of the trapping potential along the z-direction. It is interesting to note that the bending of vortex lines is observed experimentally—even in Fig. 5, for example. The simple arctangent profiles we found here demonstrate that the bending of vortex lines can be treated in our formalism. We could extend this analysis to look for non-linear solutions to the equations of motion, in which case we might discover other types of bent profiles (and possibly solitonic solutions). Ideally, we would also like to account for the effects of rapid rotation of the trap at the level of the effective action, which would certainly introduce more complicated bending of vortex lines, but we will leave this for future study.

3.6 Comparison to Experimental Results

We will now compare our theoretical results to the measurements of vortex precession conducted by Ku *et al.* [100]. The relevant equations are Eqs. (158) and (197), which we restate here for convenience:

$$\omega_p = \frac{\Gamma}{c_s^2}\omega_x\omega_y \log\frac{R_\perp}{\ell} \times \begin{cases} 3/8\pi & \text{(purely two-dimensional trapping)} \\ 1/4\pi & \text{(with trapping in the } z\text{-direction)} \end{cases} . \tag{198}$$

We are including the case of two-dimensional trapping (which we will call Model 1) because that was the result we initially published in [1], and it matches the precession frequency calculated by Svidzinsky and Fetter [95]. We would like to see how it will compare to data, although the experiment involved trapping in the z-direction. We expect that the modified expression relevant to three-dimensional trapping (which we call Model 2) will fare better when compared to experimental data. Recalling that the quantized circulation is given by $\Gamma \sim 2\pi\hbar/m$ (and integer multiples thereof) and the chemical potential is $\mu \sim mc_s^2$ in the non-relativistic limit, for symmetric traps with $\omega_\perp \sim \omega_x \simeq \omega_y$ we have

$$\frac{\omega_\perp}{\omega_p} \simeq \frac{\mu/(\hbar\omega_\perp)}{\log[\zeta\mu/(\hbar\omega_\perp)]} \times \begin{cases} 4/3 & \text{(Model 1)} \\ 2 & \text{(Model 2)} \end{cases} . \tag{199}$$

In this form, we have a definite prediction for the functional form of the normalized precession frequency $\omega_\perp/\omega_p$ as a function of the normalized chemical potential $\mu/(\hbar\omega_\perp)$, with a single free parameter ζ, which is to be determined by fitting to experimental data. In this form, our result is directly comparable to Fig. 3 in Ku *et al.* [100], where they report their measurements of vortex precession in trapped superfluid ^{6}Li over the BCS–BEC crossover region. Our fitted models are compared to their data in Fig. 10. The first thing to note is that the theoretical model proposed by Jackson *et al.* [94] (see Eq. (121)) does very poorly at fitting the data into the BCS region. In the case of Model 1, which is identical

to the results of Svidzinsky and Fetter [95], representing exactly two-dimensional trapping, the maximum likelihood estimator yields a value for the fit parameter ζ of 0.637 ± 0.045 (standard error), with a χ^2/d.o.f. value of 1.6. The fit is passable, but it is systematically high at low values of the chemical potential in the BCS region. For Model 2, representing our new result for precession with approximately harmonic trapping along the z-direction as well, the fit parameter ζ is 2.85 ± 0.33 (standard error), with a χ^2/d.o.f. value of 1.2. Model 2 fares much better at following the measurements at low chemical potential, although the overall fit is still not stellar. We cannot expect the model to work perfectly in this comparison because the measurements were taken over a range of energies that includes the complicated physics of the BCS–BEC phase transition, and we have also not accounted for possible finite temperature effects. Nonetheless, the comparison to data is illuminating, as it indicates that our second model is fairly successful even for this data set. More directly comparable future measurements, especially measurements that are taken with differently shaped trapping potentials, may shed more light on the success of our model and theoretical approach.

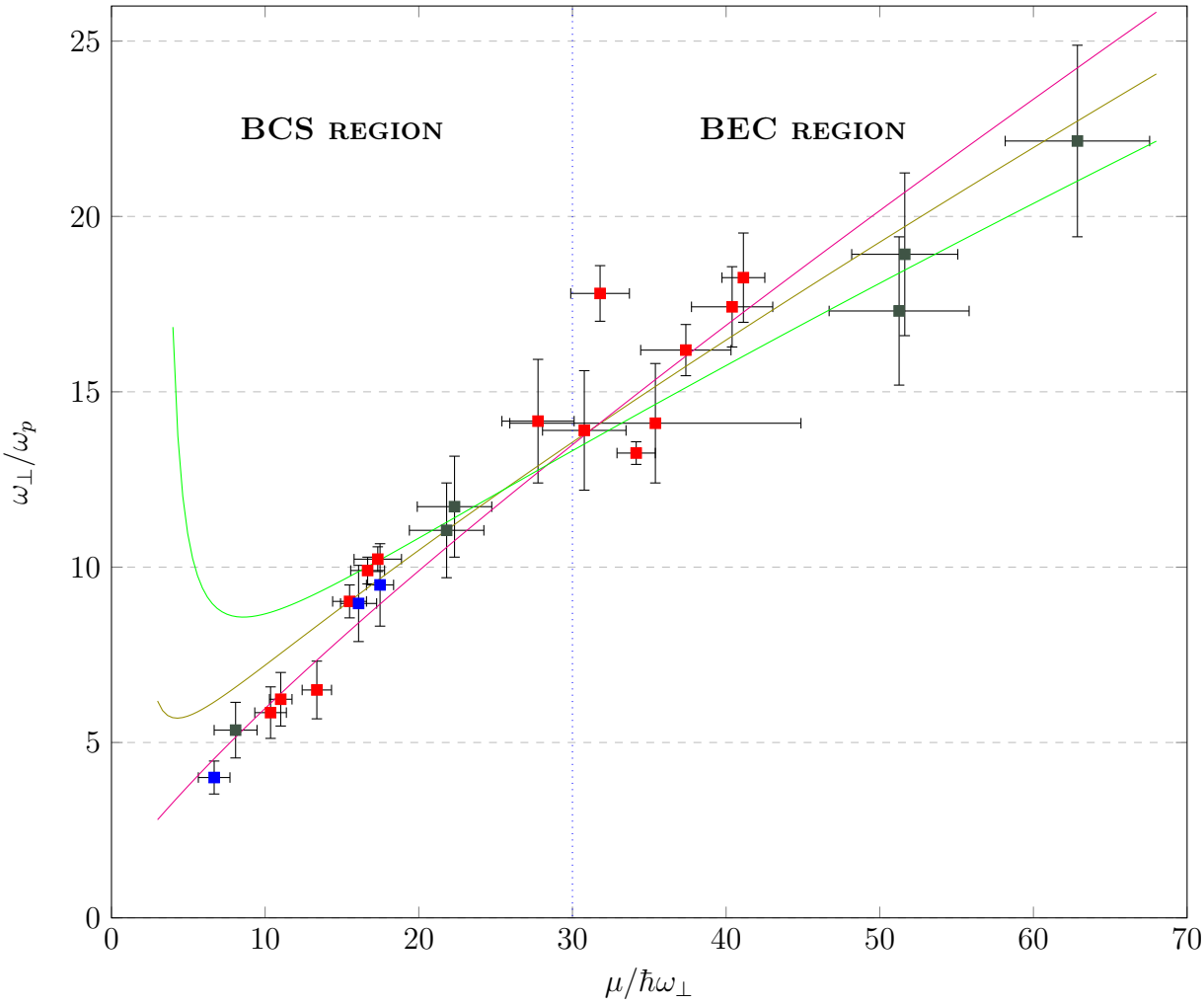

Figure 10: Experimental measurements of vortex precession frequency at different values of the normalized chemical potential, as reported in Ku *et al.* [100]. The measurement was carried out in trapped superfluid ^{6}Li over the BCS–BEC crossover region. The blue points correspond to frequency $\omega_z/2\pi = 5$ Hz; the red points are measured at $\omega_z/2\pi = 10$ Hz; and the teal points correspond to $\omega_z/2\pi = 23$ Hz. **Model 1**, fitted to this data set, is shown as the beige trend line; it is identical to the model proposed by Svidzinsky and Fetter [95]. **Model 2** is shown as the pink line. The green line is the best fit of the theoretical model proposed by **Jackson** *et al.* [94], based on Gross–Pitaevskii theory (see Eq. (121)).

3.7 Conclusion and Further Questions

In this analysis, we derived an effective action for vortex lines in trapped superfluids, Eq. (148), that is valid for any trapping potential that is confining in two dimensions. We have also worked out a relativistic generalization in Eq. (170). The result is an action principle that can be applied to study the dynamics of vortex lines in general trapping configurations. Here, we used it to find the precessional frequency of vortex lines in both harmonic and anharmonic trapping potentials. In the harmonic case, the frequency of precession around the center of the trap is logarithmically enhanced, scaling as $\omega_p \sim \Gamma \log(R_\perp/\ell)$. This result matches previous calculations from the Gross–Pitaevskii model, and it fares well when compared to experimental measurements reported in [100], particularly when the leading-order effects of trapping in the third dimension are accounted for. Even in traps where the potential is arbitrarily flat near the center, precession occurs in circular or elliptical orbits, but now with a frequency that scales as $\omega_p \sim \Gamma/R_\perp^2$. This is consistent with well-known behavior of vortex lines in flatter traps [109, 110]. Our result implies that this scaling of the precessional frequency will still be observed in a uniformly trapped, quasi-two-dimensional "superfluid in a box," of the type realized in [111–113], for example. Experiments show that vortex lines get mildly bent by the trap [100, 114, 115], and our EFT framework demonstrated that kinked profiles of vortex lines can be found already at linear order when mild trapping in the z-direction is introduced. We also took the opportunity to study the dispersion of Kelvin waves propagating along vortex lines in trapped condensates. We found that the presence of a trapping potential modifies the well-known $\omega \sim k^2 \log k$ dispersion law in different ways, depending on whether the trapping potential is harmonic or flatter-than-harmonic near the center of the atomic cloud.

Overall, our low-energy effective theory of vortex lines in trapped superfluids presents a robust and flexible alternative to analysis based on Gross–Pitaevskii theory, with rich possibilities for comparisons to experimental realizations and extensions to the study of other types of dynamics, besides precessional motion. Possible next steps include extending

the theory to account for general trapping configurations in three dimensions, incorporating the effects of rotation, and looking for curved vortex line profiles at non-linear order. Finite-temperature effects are also interesting to consider. Since we expect the string coupling $T_{(01)}$ to be positive, the effective vortex line potential we found in Eq. (150) is actually a negative quantity. This could lead to instabilities involving phonon interactions. We would expect a finite-temperature thermal bath of phonons to produce an effective friction for vortex line motion, gradually driving vortices to regions of lower effective potential. We would thus expect a precessing vortex line to slowly spiral outward away from the center of the atomic cloud, where the trapping potential is stronger. This is an effect considered in [96], and it would be interesting to see it come out of our effective field theory formulation. Other possible applications of the theory we have developed here include: studying the Brownian motion of vortex lines of the sort observed in [116]; expanding our theory to higher order in vortex line velocity in order to calculate anharmonicity in the oscillatory behavior of vortex lines (see [117]); calculating vortex–vortex interactions, scattering phenomena, and the excitation spectrum of a vortex lattice in a rotating superfluid (see [118, 119]); and carefully analyzing relativistic effects in our effective theory, which is in principle fully relativistic, and their relevance to the dynamics of neutron star interiors, which are expected to be dominated by superfluid components containing vortex lines pinned to impurities in the crust [120–126]. In particular, the possibility of using our language to describe the pinning and unpinning of superfluid vortices from a non-superfluid matter component is particularly intriguing, as it is one of the proposed mechanisms to explain glitching phenomena observed in millisecond pulsars [127, 128]. Vibrational instabilities of pinned vortex lines have also been proposed as mechanisms of generating starquakes and "wobble" phenomena in neutron stars [129]. Treating this in our formalism would involve generalizing it to finite-temperature superfluids with an ordinary fluid component and abandoning the simple straight-line parametrization of vortex lines, but it may well be feasible. We leave such intriguing possibilities for future studies.

4 Case Study 2: The Gravitational Mass of Sound Waves in Superfluids, Fluids, and Solids

4.1 Introduction: Do Sound Waves Carry Mass?

In this section, part of which follows our recent paper [2], we will apply effective field theory techniques to the study of perturbations in a wide variety of media. Our overarching goal will be to answer a single answer: Do sound waves carry mass? This may seem like a strange question to ask, since the conventional answer, at least according to common lore, is usually no. For instance, physics students learn from the popular undergraduate textbook *University Physics* [130] that such waves "transport energy, but not matter." Sound waves certainly carry energy and momentum, but the net mass transferred by sound waves is generally believed to vanish. This is a claim that is certainly true in the linear regime, but we would like to explore it further by studying sound waves within the formalism of the effective field theory of condensed matter systems. In particular, we would like to see if there is a gravitational mass associated with sound waves that appears at non-linear order.

Nicolis and Penco [131] first found results suggesting that sound carries non-zero net mass using an effective point-particle theory for phonons in a superfluid at zero temperature. They found that phonons, treated in a point-particle-like approximation, have an effective coupling to gravitational fields, which is determined by both the energy of the phonon and the equation of state of the superfluid. For ordinary equations of state, when the speed of sound in the superfluid increases with increasing mass density, this coupling to the gravitational field is equivalent to a *negative effective gravitational mass*, meaning that phonon trajectories tend to bend in the direction opposite to the gravitational field. On the Earth's surface, nearly horizontal phonon trajectories tend to bend upward with a radius of curvature of the order of c_s^2/g, where c_s is the sound speed and g is the gravitational acceleration. Other

excitations such as rotons were found to couple to gravitational fields somewhat differently in this effective point-particle theory, with positive or negative effective gravitational mass depending on their momentum.

In the case of phonon trajectories bending under the influence of a gravitational field, the effect Nicolis and Penco studied is, of course, completely equivalent to the refraction of sound waves due to pressure gradients, and it can be formulated in the same way as Snell's law. Since the pressure in a superfluid gains a dependence on depth in the presence of an external gravitational field, the speed of sound depends on depth as well, causing phonon trajectories to become curved in the geometric acoustics limit. Nonetheless, refraction is not the end of the story. An important point that was not fully appreciated by Nicolis and Penco is that since the effect is produced from a direct coupling between phonons and gravity in the effective Lagrangian, the same interaction must in turn lead to changes in the field equation for gravity. Thus, the phonon itself has an associated very small (and negative) gravitational mass, which sources very small changes in the gravitational field, and this gravitational source travels along with the phonon. It is also important to emphasize that this is a true gravitational mass and not a mere artifact of relativistic mass–energy equivalence; as we will see, this effect survives in the non-relativistic limit $c \to \infty$. We will also see that since this analysis applies equally well to classical waves, the generation of a (negative) gravitational mass associated with phonons is not a quantum effect.

Hints of the effect that we are studying have appeared before. We will find that the effective gravitational mass depends on a particular logarithmic derivative of the speed of sound with respect to the mean density that has been seen in other contexts in the study of fluid and superfluid excitations; it appeared relatively recently in a paper by Watanabe *et al.* [2013] about gapped Goldstone boson-like excitations (which they somewhat imprecisely term "massive Nambu–Golstone bosons") in relativistic systems at finite density, and as early as 1925 in Brillouin's classic study of long-range momentum transport by acoustic and elastic waves, or as he termed it, "*tensions de radiation.*" Non-linear effects giving rise to non-zero

total momentum associated with acoustic wave packets are also well-known, with authors such as Landau and Lifshitz [86] commenting that such effects imply a small transfer of matter, although there is no indication that these effects have been interpreted as a source of gravitational mass. We will build upon such precedents in this section and study the effect in detail.

After reviewing the effective point-particle theory developed by Nicolis and Penco [131], we will confirm their result explicitly by calculating the gravitational mass carried by a sound wave packet in a zero-temperature superfluid from effective field theory methods. This will involve extending the standard linear analysis of wave packets to non-linear order, as the non-zero net mass is a non-linear effect from the point of view of wave mechanics; this mass would be inferred to be zero at linear order. We will also extend this analysis to other condensed matter systems, including sound waves in ordinary fluids and both longitudinal and transverse waves in solids. In each case, we will find that in the non-relativistic limit, the gravitational mass associated with a sound wave packet traveling through a medium can be written as

$$M = -\frac{d\log c_s}{d\log \rho_m}\frac{E}{c_s^2}\,, \tag{200}$$

where c_s is the speed of sound, ρ_m is the background mass density in the medium, and E is the energy of the wave packet. A slightly generalized form of this equation holds for media with both longitudinal and transverse excitations. Thus, the gravitational mass is determined by the energy of the wave packet and the equation of state of the medium. Since the derivative $d\log c_s/d\log \rho_m$ is positive for typical equations of state, this mass turns out to be a negative quantity. The logarithmic derivative is understood to be a standard adiabatic one, and it is identical to the logarithmic derivative seen by Brillouin [132] in the study of general radiative stresses in fluids.

Initially, we will work in fully relativistic language and take the non-relativistic limit

later, in order to distinguish between relativistic and non-relativistic contributions to the equations of motion of phonons. In addition to confirming the result in Eq. (200) using low-energy effective field theory techniques involving Poincaré symmetry, we will also confirm this result for superfluids starting from Galilei symmetry alone, which corresponds to taking the non-relativistic limit from the outset. Furthermore, we will see that it is possible to derive analogous formulas indicating a net transfer of mass from ordinary classical hydrodynamics and the non-linear theory of elasticity in continuum mechanics, confirming that the phenomenon we are considering is not a relativistic or quantum effect in its origin, and it could have easily been discovered by the careful study of non-linear effects centuries ago.

Before proceeding, we must make a note of clarification about precisely what we mean by mass, or M, in Eq. (200). There is no problem with talking about mass in an unambiguous manner when we consider excitations that propagate through a Poincaré-invariant vacuum; in that case, the invariant mass is well-defined, and it determines the energy gap of the excitation. However, we are considering media that explicitly break invariance under Lorentz boosts. In such cases, boost symmetry no longer constrains the energy spectrum $E(p)$ of the excitation under consideration, so that there is no longer a clearly defined notion of an "invariant mass." However, a non-relativistic medium, in which its mass density is much greater than its energy density divided by c^2, certainly still has a definite total mass as a conserved quantity. In a non-relativistic medium, then, the mass M is understood to be the fraction of the total mass of the system that travels along with the excitation as it propagates through the medium, rather than the invariant mass that the excitation would have in a Poincaré-invariant vacuum. This, too, is a well-defined quantity. Note that it is still consistent with the symmetries of the system for gapless excitations—Goldstone modes, for which $E(p) \to 0$ as $p \to 0$—to carry non-zero net mass.

4.2 A Coarse-Grained Perspective: Effective Point-Particle Theory of Localized Collective Excitations

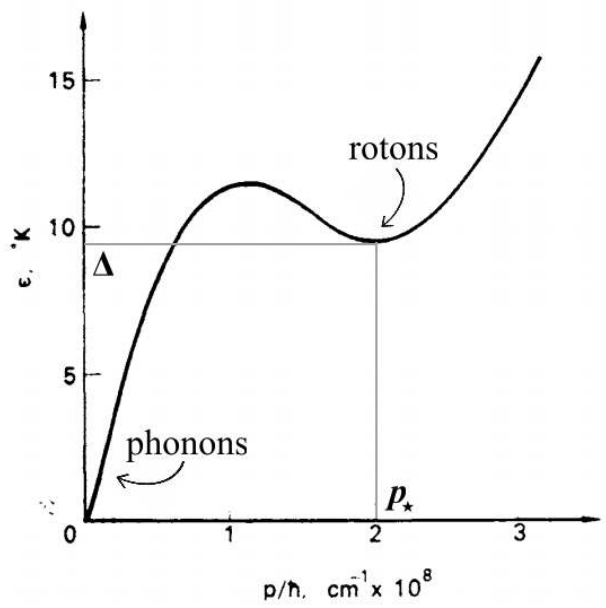

Figure 11: Schematic representation of the spectrum of excitations in superfluid helium-4, as first outlined by Landau. The low-momentum linear regime corresponds to the phonon spectrum, while rotons are around the local minimum $p \sim p_\star$. The roton energy gap is indicated by Δ, corresponding to $E(p_\star)$. Adapted from [133], reprinted from Landau [54].

Here, we will review the effective point-particle theory of excitations in a superfluid developed by Nicolis and Penco [131]. A typical energy spectrum of elementary excitations in superfluid helium-4 is shown in Fig. 11. There are two qualitatively different regions of the curve, corresponding to two different quasiparticles. Phonons appear in the low-momentum, linear regime of the dispersion curve, where

$$E_{\text{phonon}}(p) \simeq c_s p\,, \tag{201}$$

while excitations near the local minimum around $p \approx p_\star$, where

$$E_{\text{roton}}(p) \simeq \Delta + \frac{1}{2m_\star}(p - p_\star)^2\,, \tag{202}$$

are termed *rotons*. Elementary excitations, near the local maximum of the curve in Fig. 11 are sometimes called *maxons*. The equation of state, temperature, and chemical potential determine the precise values of c_s, Δ, and $m_\star$. Dimensionally, if m is the mass of helium-4 and a is the typical distance between atoms, of the same order as the Bohr radius, then we can say that $c_s \sim (ma)^{-1}$, $p_\star \sim a^{-1}$, $\Delta \sim (ma^2)^{-1}$, and $m_\star \sim m$. For our purposes, however, we will not be concerned with the roton or maxon regions of the spectrum of collective excitations, although they exhibit rich physics. For us, the phonons are of primary importance.

Following the approach of Nicolis and Penco [131], we are interested in developing a point-particle description for elementary excitations in the phonon regime of the dispersion curve. We will consider point particles to be highly localized wave packets of phonons that propagate with definite momenta, although the description is necessarily approximate. Our medium is characterized by a spontaneously broken internal $U(1)$ symmetry, as well as broken symmetry under boosts. Spacetime translations and rotations are preserved as symmetries. If we label particle states with three-momentum $\mathbf{p}$, the little group of $\mathbf{p}$ is simply the group of spatial rotations around $\mathbf{p}$. We need not add a helicity label to one-particle states, though, since phonons—quanta of longitudinal pressure waves—have zero helicity. In the phonon region of the dispersion curve, we can characterize all single-particle states by momentum $\mathbf{p}$, with no need for additional quantum numbers or degrees of freedom.

We take the Hamiltonian describing the dynamics of elementary excitations to simply have the form of the excitation spectrum shown in Fig. 11:

$$H(\mathbf{p}) = H\left(|\mathbf{p}|\right) = E\left(|\mathbf{p}|\right) \ . \tag{203}$$

We assume that the point-particle limit corresponds to a highly localized wave packet cen-

tered at position $\mathbf{x}$. The velocity is given by Hamilton's equations.

$$\dot{\mathbf{x}} = \frac{\partial H}{\partial \mathbf{p}}\,, \tag{204}$$

and the associated Lagrangian is found by performing a Legendre transformation in the standard manner.

$$L = \mathbf{p}\cdot\dot{\mathbf{x}} - H\left(|\mathbf{p}|\right) \equiv f(|\dot{\mathbf{x}}|)\,. \tag{205}$$

Note that this Lagrangian is symmetric under spatial translations and rotations, but not Galilean boosts, which is to be expected, since the superfluid medium breaks symmetry under boosts as well.

In the phonon region of the dispersion curve, we have

$$H(|\mathbf{p}|) \simeq c_s|\mathbf{p}|\,, \tag{206}$$

so that

$$\dot{\mathbf{x}} \simeq c_s\hat{\mathbf{p}} \tag{207}$$

by Hamilton's equation, where $\hat{\mathbf{p}}$ is the unit vector in the direction of the momentum $\mathbf{p}$, and the action becomes

$$S = \int dt\, f(|\dot{\mathbf{x}}|) \simeq \int dt\, p(\dot{\mathbf{x}}\cdot\hat{\mathbf{p}} - c_s)\,. \tag{208}$$

Imposing the condition that $\dot{\mathbf{x}}$ is parallel to $\hat{\mathbf{p}}$ from Eq. (207), Hamilton's equation, we find that

$$S \simeq \int dt\, p\left(|\dot{\mathbf{x}}| - c_s\right)\,. \tag{209}$$

The next step is to introduce long-wavelength bulk perturbations by allowing the Lagrangian to depend on invariant quantities built from the bulk degrees of freedom. We can easily implement this by allowing the Lagrangian to depend on the invariant quantity $\sqrt{X}$, which we introduced in Eq. (18). In addition the velocity $\dot{\mathbf{x}}$ will only appear in the combination $\dot{\mathbf{x}}-\mathbf{u}$, where $\mathbf{u}$ is the superfluid bulk velocity field introduced in Eq. (26), as dictated by Galilei invariance. Recall that the invariant $\sqrt{X}$ is equal to $\mu = \mu_0 + mc^2$ on the background, where μ is the "relativistic" chemical potential, μ_0 is the standard non-relativistic chemical potential, and m is the mass of the microscopic constituents of the superfluid. Note that $\mu_0 \ll mc^2$ generally. To leading order, the velocity field is given by

$$\mathbf{u} = -\mu c^2 \frac{\boldsymbol{\nabla}\pi}{\sqrt{X}} = -c^2 \boldsymbol{\nabla}\pi \,. \tag{210}$$

After introducing bulk perturbations into the point-particle action, we find

$$S[\mathbf{x}, p, \pi] \simeq \int dt\, p \left[|\dot{\mathbf{x}} - \mathbf{u}| - c_s \left(\sqrt{X} \right) \right] . \tag{211}$$

The precise functional form of the speed of sound as a function of the invariant $\sqrt{X}$ is determined by the equation of state.

The next step is to introduce a weak gravitational field into the metric via a Newtonian potential Φ in the non-relativistic limit $c \to \infty$.

$$g_{\mu\nu} = \eta_{\mu\nu} + \delta g_{\mu\nu} \,, \quad \delta g_{00} = -\frac{2\Phi}{c^2} \,, \quad \delta g_{\mu i} = \delta g_{i\mu} = 0 \,. \tag{212}$$

Then the invariant X becomes

$$X \to \mu^2 \left[\left(1 - \frac{2\Phi}{c^2} \right) (1 + \dot{\pi})^2 - c^2 \left(\boldsymbol{\nabla}\pi \right)^2 \right] , \tag{213}$$

and to quadratic order, we find

$$\begin{aligned}\sqrt{X} &\approx (\mu_0 + mc^2)\left[1 - \frac{\Phi}{c^2} + \dot{\pi} - \frac{c^2}{2}\left(\boldsymbol{\nabla}\pi\right)^2\right] \\ &\xrightarrow[c\to\infty]{} mc^2\left[1 + \frac{\mu_0 - m\Phi}{mc^2} + \dot{\pi} - \frac{c^2}{2}\left(\boldsymbol{\nabla}\pi\right)^2\right] .\end{aligned} \tag{214}$$

To leading order, the only effect of introducing the Newtonian potential Φ is to shift the non-relativistic chemical potential by $\mu_0 \to \mu_0 - m\Phi$. This is very similar to what we found in Eqs. (135) and (136) when introducing a trapping potential into the effective field theory of a superfluid condensate. To leading order, the trapping potential merely shifted the chemical potential (or the number density) in a linear manner, much like in Eq. (214). We can, in fact, interpret the gravitational potential as a sort of weak external trapping potential.

Returning now to the point-particle action and neglecting the bulk perturbation modes π, we see that introducing a gravitational field has the effect of shifting the sound speed in a position-dependent manner:

$$c_s\left(\mu_0\right) \to c_s\left(\mu_0 - m\Phi\right) . \tag{215}$$

To leading order, the action in Eq. (211) now becomes

$$S \to \int dt\, p\left[|\dot{\mathbf{x}}| - c_s\left(\mu_0 - m\Phi(\mathbf{x})\right)\right] . \tag{216}$$

Varying the action with respect to momentum p simply constrains the point particle to move at the speed of sound, which is now modulated by the gravitational potential. Varying the action with respect to position $\mathbf{x}$ gives the following equation of motion:

$$\frac{d\mathbf{p}}{dt} = p\frac{dc_s}{d(\mu_0/m)}\boldsymbol{\nabla}\Phi\,, \tag{217}$$

where, as before, we have $\mathbf{p} = p\dot{x}/|\dot{\mathbf{x}}|$. Now, comparing the equation of motion in Eq. (217)

to the standard force equation for a point particle in an ordinary Newtonian gravitational field, $d\mathbf{p}/dt = -M\boldsymbol{\nabla}\Phi$, where M is the particle's gravitational mass, we see that the effective net gravitational mass of a phonon with total momentum p is equal to

$$M = -p\frac{dc_s}{d(\mu_0/m)}\,. \tag{218}$$

Note that this quantity is negative for ordinary equations of state. We can also use thermodynamic relations to rewrite this in another form. Recall that from Eqs. (31) and (32) and $\mu = mc^2 + \mu_0$, we have

$$\rho \equiv mn = m\frac{dP}{d\mu} = \frac{dP}{d(\mu_0/m)}\,, \quad c_s^2 = \frac{c^2}{\mu}\frac{dP/d\mu}{d^2P/d\mu^2} \approx \frac{dP/d(\mu_0/m)}{d^2P/d(\mu_0/m)^2}\,. \tag{219}$$

Therefore, we find that

$$\frac{dc_s}{d(\mu_0/m)} = \frac{1}{c_s}\frac{d\log c_s}{d\log\rho}\,, \tag{220}$$

and using the fact that $E = c_s p$ in the phonon region of the dispersion curve, the net gravitational mass becomes

$$M = -\frac{d\log c_s}{d\log\rho}\frac{E}{c_s^2}\,. \tag{221}$$

This is precisely the formula anticipated in Eq. (200).

We can extend this analysis to fluids in a straightforward manner. Recall that the bulk dynamics of a fluid are described by a Lagrangian that is a function of the invariant $b = \sqrt{\det B^{IJ}}$—see Eq. (59). Using the expression [21]

$$b = (\det\partial\phi)\sqrt{1 - \frac{\mathbf{v}^2}{c^2}}\,, \quad \mathbf{v} = -(\partial\phi^T)^{-1}\cdot\dot{\boldsymbol{\phi}}\,, \tag{222}$$

where $(\partial\phi)^{IJ} \equiv \partial^I\phi^J$, and perturbing the metric by $\delta g_{00} = -2\Phi/c^2$, it is simple to verify that

the gravitational potential Φ does not enter the invariant b directly in the non-relativistic $c \to \infty$ limit. The gravitational potential only enters the metric determinant in the measure of the action integral. If we write an action for a fluid in a gravitational field, we find

$$S = -w_0 \int dt\, d^3x \sqrt{1 + \frac{2\Phi}{c^2}} f(b)\,. \tag{223}$$

Expanding in small fluctuations $\boldsymbol{\pi}$ to quadratic order and integrating by parts, we get

$$S_{\text{fluid}} \to w_0 b_0 \int dt\, d^3x \left[\boldsymbol{\pi} \cdot \boldsymbol{\nabla}\Phi + \frac{1}{2}\dot{\boldsymbol{\pi}}^2 - \frac{c_s^2}{2}\left(\boldsymbol{\nabla} \cdot \boldsymbol{\pi}\right)^2\right], \tag{224}$$

where we used $\boldsymbol{\phi} = b_0^{1/3}\left(\mathbf{x} + \boldsymbol{\pi}\right)$, $c_s^2 = b_0 f''(b_0)$, and the normalization condition $f'(b_0) = c^2$. The gravitational potential provides an external source for phonons of the form

$$\mathbf{J} = w_0 b_0 \boldsymbol{\nabla}\Phi\,, \tag{225}$$

which in turn shifts the VEV of $\boldsymbol{\nabla} \cdot \boldsymbol{\pi}$ to give

$$\langle \boldsymbol{\nabla} \cdot \boldsymbol{\pi} \rangle = -\frac{\Phi}{c_s^2}\,, \tag{226}$$

as can easily be deduced by convoluting the source term in Eq. (225) with the phonon propagator, $G_{ij}(\omega, \mathbf{k}) \sim \hat{\mathbf{k}}_i \hat{\mathbf{k}}_j / (\omega^2 - c_s^2 \mathbf{k}^2)$. Then, since $b = b_0\left(1 + \boldsymbol{\nabla} \cdot \boldsymbol{\pi} + \cdots\right)$, we immediately see that the background value of the invariant b is shifted by $-b_0\Phi/c_s^2$ in the presence of a gravitational field.

Finally, we can write an effective point-particle action for a sound wave packet in an ordinary fluid in the presence of a gravitational potential in a manner analogous to Eq. (216). To leading order, the result is

$$S \simeq \int dt\, p\left[|\dot{\mathbf{x}}| - c_s\left(b_0 - b_0\Phi/c_s^2(b_0)\right)\right]. \tag{227}$$

Varying the action with respect to the position of the point particle, $\mathbf{x}$, we immediately read off the equation of motion

$$\frac{d\mathbf{p}}{dt} = \frac{b_0}{c_s^2}\frac{dc_s}{db} p \boldsymbol{\nabla}\Phi \,. \tag{228}$$

As a result, the effective gravitational mass of a phonon in a fluid, computed in the point-particle approximation, is

$$M = -\frac{b_0}{c_s^2}\frac{dc_s}{db} p \,. \tag{229}$$

Note that in the non-relativistic limit, the density is proportional to the level of hydrostatic compression, so that $\rho \propto b$. For phonons in this fluid, we also have $E = c_s p$, so that we again obtain the result

$$M = -\frac{d\log c_s}{d\log \rho}\frac{E}{c_s^2} \,, \tag{230}$$

as expected.

For both longitudinal phonons and transverse excitations in a solid, the above analysis carries through almost without modification, since the gravitational potential does not enter into the additional invariants Y and Z in the non-relativistic $c \to \infty$ limit. The only difference is that only longitudinal bulk modes take on a shifted VEV in the presence of a gravitational field. In the case of a solid, we have the following relation instead of Eq. (226), to leading order:

$$\langle \boldsymbol{\nabla} \cdot \boldsymbol{\pi}_L \rangle = -\frac{\Phi}{c_L^2} \,. \tag{231}$$

As a result, depending on whether we are considering a longitudinal or transverse point

particle excitation propagating through the solid, the point-particle action is

$$S \simeq \int dt\, p \left[|\dot{\mathbf{x}}| - c_X \left(b_0 - b_0 \Phi / c_L^2(b_0) \right) \right] , \tag{232}$$

where $X = L$ for a longitudinal mode and $X = T$ for a transverse mode. As a result the effective gravitational mass of a phonon in a solid is

$$M_X = -\frac{d \log c_X}{d \log \rho} \frac{E_X}{c_L^2} , \tag{233}$$

where E_X is the energy carried by a wave packet of either longitudinal or transverse excitations. We will see that this is the appropriate generalization of Eq. (200) when we verify it more rigorously, without resorting to point-particle-like representations. The mass associated with each type of excitation is different, but the general structure of the expression is unchanged—the gravitational mass is negative, and it scales with the energy of the sound wave packet over the square of the longitudinal sound velocity. The constant of proportionality depends on the functional form of the velocity of longitudinal or transverse excitations as a function of the density, but it is generically a positive number of order one.

4.3 Superfluids at Zero Temperature

As we saw in Section 2.1, we can describe the dynamics of low-energy phonons in a superfluid at zero temperature using an effective field theory with a single scalar field ϕ. That scalar must take a VEV with a non-zero time derivative, which we wrote as $\langle\phi\rangle = \mu t$. Expanding the superfluid action to cubic order about the VEV, we found Eq. (30), an action for superfluid phonons π, corresponding to small fluctuations of the scalar about the time-dependent background. The action we found in Eq. (30) then allows us to compute the classical equation of motion for π, given by $\partial_\mu \left[P'(-c^2\partial_\nu\phi\partial^\nu\phi)\partial^\mu\phi\right] = 0$, to non-linear (quadratic) order in small fluctuations:

$$\ddot{\pi} - c_s^2\nabla^2\pi = c^2\left(1 - \frac{c_s^2}{c^2}\right)\dot{\pi}\nabla^2\pi + \frac{\partial}{\partial t}\left[c^2\left(1 - \frac{c_s^2}{c^2}\right)(\boldsymbol{\nabla}\pi)^2 - g\dot{\pi}^2\right], \tag{234}$$

where

$$c_s^2 = c^2\frac{dP/d\mu}{\mu d^2P/d\mu^2}, \quad g = \frac{c^2}{2c_s^2}\left(1 - \frac{c_s^2}{c^2}\right) - \frac{\mu}{c_s}\frac{dc_s}{d\mu}. \tag{235}$$

We can solve Eq. (234) to non-linear order by writing the phonon field as an expansion, $\pi = \pi_{(1)} + \pi_{(2)} + \cdots$, where $\pi_{(1)}(\mathbf{x}, t)$ is a localized wave packet solution to the linearized wave equation, $\ddot{\pi}_{(1)} - c_s^2\nabla^2\pi_{(1)} = 0$. The quadratic correction $\pi_{(2)}$ is then sourced by $\pi_{(1)}$ in turn. We can find the leading non-linear correction $\pi_{(2)}$ by solving the wave equation for $\pi_{(2)}$ in Eq. (234) with $\pi_{(1)}$ sourcing the quadratic terms on the right-hand side.

$$\ddot{\pi}_{(2)} - c_s^2\nabla^2\pi_{(2)} = \partial_t\left[c^2\left(1 - \frac{c_s^2}{c^2}\right)\left(\boldsymbol{\nabla}\pi_{(1)}\right)^2 - g\dot{\pi}_{(1)}^2 + \frac{c^2}{2c_s^2}\left(1 - \frac{c_s^2}{c^2}\right)\dot{\pi}_{(1)}^2\right]. \tag{236}$$

In order to determine the net mass associated with a phonon wave packet in a superfluid, we will also calculate the contribution to the energy–momentum tensor component T_{00} from solutions of the classical equations of motion, Eqs. (234) and (236). The energy–momentum tensor we are considering is the gravitational energy–momentum; we use gravity as a probe

to calculate the mass associated with sound waves because gravity couples only to mass in the non-relativistic limit. We already expanded T_{00} to quadratic order in small fluctuations in Section 2.1, resulting in Eq. (35). Recall that the expression is

$$T_{00} = \frac{\mu n c^2}{c_s^2}\left[\dot{\pi} + \frac{c^2}{2c_s^2}\left(1 - \frac{2\mu c_s}{c^2}\frac{dc_s}{d\mu}\right)\dot{\pi}^2 - \frac{c^2}{2}\left(1 - \frac{2c_s^2}{c^2}\right)(\boldsymbol{\nabla}\pi)^2\right]. \tag{237}$$

Since we are dealing with a localized phonon wave packet, our approach will involve integrating T_{00} over a volume containing the wave packet and averaging T_{00} over some time interval $\mathcal{T}$ that is much longer than the typical oscillation time, over which the linearized solution $\pi_{(1)}$ averages to zero; explicitly, $\mathcal{T} \gg 1/\omega$. After taking the non-relativistic limit, the leading contribution to $\frac{1}{c^2}\int d^3x\, T_{00}$ that survives when $c \to \infty$ can be interpreted as the net gravitational mass associated with the phonon wave packet.

In principle, both the linearized wave packet solution $\pi_{(1)}$ and the leading non-linear correction $\pi_{(2)}$ can contribute to the linear term in T_{00} proportional to $\dot{\pi}$. However, time averaging will make the contribution from $\pi_{(1)}$ vanish, since the term involves a time derivative and we are integrating over many oscillation times, over which the linear solution averages to zero. The contribution from the non-linear correction $\pi_{(2)}$ will also vanish after time averaging, since the time derivative eliminates constant terms in the quadratic source on the right-hand side of Eq. (236), leaving only oscillatory terms whose time derivatives also give zero after the time averaging procedure. Thus, the linear term in T_{00} does not contribute to the effective gravitational mass of the phonon wave packet.

Now, the quadratic terms in T_{00} are important, but only the linearized wave packet solution $\pi_{(1)}$ can contribute via the quadratic terms at this order in perturbation theory. Let us represent the combination of spatial integration and time averaging by the notation $\left\langle \int \dots \right\rangle$. We get

$$\left\langle \int T_{00} \right\rangle = \frac{\mu n c^4}{2c_s^2}\left[\frac{1}{c_s^2}\left(1 - \frac{2\mu c_s}{c^2}\frac{dc_s}{d\mu}\right)\left\langle \int \dot{\pi}_{(1)}^2 \right\rangle - \left(1 - \frac{2c_s^2}{c^2}\right)\left\langle \int (\boldsymbol{\nabla}\pi_{(1)})^2 \right\rangle\right]. \tag{238}$$

We can immediately relate the time-averaged, spatially integrated quantities $\left\langle \int \dot{\pi}_{(1)}^2 \right\rangle$ and $\left\langle \int (\boldsymbol{\nabla}\pi_{(1)})^2 \right\rangle$ for the linearized wave packet to the total energy of the wave packet. The total energy can be found in turn by time-averaging the value of the contribution of the linearized wave packet to the free Hamiltonian of the superfluid. Because the ground state spontaneously breaks the $U(1)$ symmetry associated with particle number, the Hamiltonian of the ground state in a superfluid at zero temperature is equal to

$$H = \int d^3x \, \left(T^{00} - \mu J^0 \right) \, , \tag{239}$$

where $J^\mu = 2P'(X)\partial^\mu \phi$ is the Noether current associated with the broken $U(1)$ symmetry. To quadratic order, the Hamiltonian is given by

$$H = \frac{\mu n c^2}{2c_s^2} \int d^3x \, \left[\dot{\pi}^2 + c_s^2 \left(\boldsymbol{\nabla}\pi \right)^2 \right] \, . \tag{240}$$

After time averaging and using the virial theorem, we obtain expressions for the total energy of the wave packet, E.

$$E = \frac{\mu n c^2}{c_s^2} \left\langle \int \dot{\pi}_{(1)}^2 \right\rangle = \mu n c^2 \left\langle \int (\boldsymbol{\nabla}\pi_{(1)})^2 \right\rangle \, . \tag{241}$$

Now combining the results of Eqs. (238) and (241), we find

$$\left\langle \int T_{00} \right\rangle = \left(1 - \frac{\mu}{c_s} \frac{dc_s}{d\mu} \right) E \, . \tag{242}$$

At zero temperature, we also have the thermodynamic relations $\mu n = \epsilon + P$ and $dP = n d\mu$, so we may rewrite this result as

$$\left\langle \int T_{00} \right\rangle = \left(1 - \frac{\epsilon + P}{c_s} \frac{dc_s}{dP} \right) E \, . \tag{243}$$

This expression is fully relativistic. In the non-relativistic limit, $\epsilon + P$ is approximately equal

to $mnc^2 = \rho_m c^2$, where ρ_m is the equilibrium mass density. Using $dP/d\rho_m = c_s^2$ and taking the $c \to \infty$ limit, we find that the net gravitational mass associated with the phonon wave packet is

$$M = \frac{1}{c^2} \left\langle \int T_{00} \right\rangle \simeq -\frac{\rho_m}{c_s} \frac{dc_s}{dP} E = -\frac{d \log c_s}{d \log \rho_m} \frac{E}{c_s^2} \,. \tag{244}$$

This is precisely the result obtained by Nicolis and Penco [131] from their effective point-particle theory. We have now confirmed this result explicitly from effective field theory methods, without resorting to any point-particle-like approximations.

In Section A, we show how the same result can be derived from the dual description of a superfluid in terms of a two-form field, and in Section B, we confirm the result for a single-phonon state in quantum field theory.

4.4 Fluids and Solids

In this section, we will show that an analogous result holds in both fluids and solids using a similar effective field theory approach. We will consider a solid first and then specialize to the case of a fluid, since a fluid is simply a very symmetric solid from the effective field theory point of view—see our discussion of solids in Section 2.3. Recovering the effective theory of a fluid from that of a solid is simply a matter of neglecting derivatives of the Lagrangian density with respect to all invariant quantities except for the determinant of the matrix B^{IJ}, which is compatible with symmetry under volume-preserving diffeomorphisms.

Recall that in the effective field theory of a solid, the Lagrangian is built out of three scalar fields ϕ^I associated with the co-moving (or Lagrangian) coordinates labeling volume elements in the solid. These scalars take VEVs that are aligned with the physical spatial (or Eulerian) coordinates, $\langle \phi^I \rangle \propto x^I$. The Lagrangian is a generic function of three linearly independent $SO(3)$ invariants built out of $B^{IJ} = \partial_\mu \phi^I \partial^\mu \phi^J$, which we choose to be $b = \sqrt{\det B}$, $Y = (\mathrm{tr}\, B^2)/(\mathrm{tr}\, B)^2$, and $Z = (\mathrm{tr}\, B^3)/(\mathrm{tr}\, B)^3$. Phonons π^I are introduced to the theory by considering small fluctuations about the VEV, $\phi^I = \sqrt[3]{b_0}(x^I + \pi^I)$. Expanding to cubic order in these small fluctuations leads to the cubic action for phonons in a solid, Eq. (78), with associated longitudinal and transverse sound speeds and non-linear coupling constants defined in Eqs. (79) to (87). We can take the variation of the action in Eq. (78) with respect to the fluctuation fields π^I in order to obtain the following non-linear equations of motion:

$$\ddot{\pi}_i - c_L^2 \partial_i \boldsymbol{\nabla} \cdot \boldsymbol{\pi} - c_T^2 \left(\nabla^2 \pi_i - \partial_i \boldsymbol{\nabla} \cdot \boldsymbol{\pi} \right) = \partial_j A_{ij} + \partial_t B_i \,, \tag{245}$$

where the tensor A_{ij} is given by

$$\begin{aligned} A_{ij} = {} & g_1\delta_{ij}\dot{\boldsymbol{\pi}}^2 + g_2\dot{\pi}_i\dot{\pi}_j + 3g_3\delta_{ij}\left(\boldsymbol{\nabla}\cdot\boldsymbol{\pi}\right)^2 + g_4\delta_{ij}(\partial_k\pi_l)^2 + 2g_4\partial_j\pi_i\boldsymbol{\nabla}\cdot\boldsymbol{\pi} \\ & + g_5\delta_{ij}\left(\boldsymbol{\nabla}\times\boldsymbol{\pi}\right)^2 + 2g_5\partial_j\pi_i\boldsymbol{\nabla}\cdot\boldsymbol{\pi} - 2g_5\partial_i\pi_j\boldsymbol{\nabla}\cdot\boldsymbol{\pi} + g_6\partial_i\pi_k\partial_j\pi_k \\ & + g_6\partial_k\pi_i\partial_k\pi_j + 3g_7\partial_i\pi_k\partial_k\pi_j\,, \end{aligned} \tag{246}$$

and the vector B_i is similarly formed from quadratic combinations of field π_i, although the explicit form of B_i is not relevant for the rest of this calculation. Here, B_i appears only as a full time derivative in the equations of motion, which we will average over a time interval much longer that the period of oscillation of solutions to the linear wave equation. Since B_i is quadratic in the oscillatory fields, the time average of $\partial_t B_i$ will vanish in this procedure and we can drop it.

We will now proceed to computing the effective gravitational mass associated with a localized wave packet of longitudinal or transverse phonons in a solid. It will be related to the energy–momentum tensor component T_{00}, which we found to quadratic order in small fluctuations in Eq. (89). For convenience, we choose to take the non-relativistic limit right away. This is useful because apart from $\partial f/\partial b$, the derivatives of $f(b, Y, Z)$ with respect to its arguments are all of the same order as c_L^2 or c_T^2, and combinations of these derivatives appear in the definitions of the non-linear couplings $g_1, g_2, \ldots, g_7$, as well as the prefactors of the surviving quadratic terms in Eq. (89) after spatially integrating T_{00}. The only relevant $\mathcal{O}(c^2)$ term that we must consider in the non-relativstic limit is

$$T_{00} \simeq c^2 w_0 b_0 \boldsymbol{\nabla}\cdot\boldsymbol{\pi}\,. \tag{247}$$

Clearly, if there is an $\mathcal{O}(c^0)$ contribution from the wave packet to $\boldsymbol{\nabla}\cdot\boldsymbol{\pi}$ after integrating over a volume containing the wave packet and averaging in time, we will find a non-zero total gravitational mass. With our formulation of this effective theory, the linear term contributes to the mass density, but quadratic and higher-order terms contribute only to the energy

density and not the mass density. Using the notation $\langle \int \dots \rangle$ to denote time-averaging and spatial integration once again, we will find the gravitational mass from

$$M = w_0 b_0 \left\langle \int \boldsymbol{\nabla} \cdot \boldsymbol{\pi} \right\rangle . \tag{248}$$

At first glance, one may be tempted to say that the gravitational mass must be zero, since the spatial integration of a divergence produces a boundary term, which seems like it vanishes for integrals over large volumes. This is true only for wave packet solutions to the linearized equations of motion, however, since those can be taken to be highly localized. The non-linear corrections from the quadratic equations of motion, Eq. (245), can lead to non-zero contributions to M at this order in perturbation theory. Accordingly, we separate the fluctuation field into $\boldsymbol{\pi} = \boldsymbol{\pi}_{(1)} + \boldsymbol{\pi}_{(2)} + \cdots$, where $\boldsymbol{\pi}_{(1)}$ solves the equations of motion at linear order, and $\boldsymbol{\pi}_{(2)}$ is sourced in turn by $\boldsymbol{\pi}_{(1)}$. Substituting a linear wave packet $\boldsymbol{\pi}_{(1)}$ into the right-hand side of Eq. (245) can in principle give rise to a non-linear correction $\boldsymbol{\pi}_{(2)}$ that scales as $1/|\mathbf{x}|^2$ at large distances, so that a finite contribution to M in Eq. (248) is indeed possible.

In order to calculate this contribution, we will take the divergence of the equation of motion Eq. (245) and solve for the divergence of the non-linear correction $\Psi \equiv \boldsymbol{\nabla} \cdot \boldsymbol{\pi}_{(2)}$, which solves a wave equation sourced by the linearized solution $\boldsymbol{\pi}_{(1)}$,

$$\left(\partial_t^2 - c_L^2 \nabla^2\right) \Psi = \partial_i \partial_j A_{ij} + \partial_t \boldsymbol{\nabla} \cdot \mathbf{B} \,, \tag{249}$$

where A_{ij} and $\mathbf{B}$ are understood to be functions of the linear wave packet solution $\boldsymbol{\pi}_{(1)}$ only at this order in perturbation theory. We then take the time average of this equation over an interval much longer than $1/\omega$, over which the full time derivative terms average to zero.

We are thus left with

$$\nabla^2\langle\Psi\rangle = -\frac{1}{c_L^2}\langle\partial_i\partial_j A_{ij}\rangle\,. \tag{250}$$

This is a simple Poisson's equation. It can be solved in a straightforward way by Green's function methods. After integrating over a volume in space containing the wave packet, we obtain the expression

$$\left\langle\int\Psi\right\rangle = \frac{1}{4\pi c_L^2}\int d^3x\, d^3y\, \frac{\left\langle\partial_i^{(y)}\partial_j^{(y)}A_{ij}(\mathbf{y})\right\rangle}{|\mathbf{x}-\mathbf{y}|}\,. \tag{251}$$

Further integration by parts[6] leads immediately to the result

$$\left\langle\int\boldsymbol{\nabla}\cdot\boldsymbol{\pi}\right\rangle \simeq -\frac{1}{3c_L^2}\left\langle\int A_{ii}\right\rangle\,. \tag{252}$$

This allows us to proceed with calculating the gravitational mass in Eq. (248). All that remains is the computation of $\left\langle\int A_{ii}\right\rangle$. The full form of A_{ij} is written out in Eq. (246), and it must be understood as a function of the linear wave packet solution $\boldsymbol{\pi}_{(1)}$. For convenience, we split this linear solution into longitudinal (L) and transverse (T) components—$\boldsymbol{\pi}_{(1)} = \boldsymbol{\pi}_L + \boldsymbol{\pi}_T$, where $\boldsymbol{\nabla}\times\boldsymbol{\pi}_L = 0$ and $\boldsymbol{\nabla}\cdot\boldsymbol{\pi}_T = 0$. The total energies of the longitudinal and transverse components of the linearized wave packet solution are given by their respective

[6]In this integration by parts, we must also use the following distributional identity:

$$\partial_i\partial_j\frac{1}{|\mathbf{x}|} = \frac{1}{|\mathbf{x}|^3}\left(3\hat{\mathbf{x}}_i\hat{\mathbf{x}}_j - \delta_{ij}\right) - \frac{4\pi}{3}\delta_{ij}\delta^3(\mathbf{x})\,.$$

The first term on the right-hand side must be interpreted as a 3-dimensional type of principal part, in the sense of removing an infinitesimally small ball centered at the origin. It integrates to zero if the integral is taken over any spherical volume about the origin.

contributions to the Hamiltonian. In this case, the resulting expressions are

$$E_L = \frac{w_0 b_0}{2} \int d^3x \, \left[\dot{\boldsymbol{\pi}}_L^2 + c_L^2 \left(\boldsymbol{\nabla} \cdot \boldsymbol{\pi}_L \right)^2 \right] , \tag{253}$$

$$E_T = \frac{w_0 b_0}{2} \int d^3x \, \left[\dot{\boldsymbol{\pi}}_T^2 + c_T^2 \left(\boldsymbol{\nabla} \times \boldsymbol{\pi}_T \right)^2 \right] , \tag{254}$$

respectively. Time averaging and using the virial theorem gives

$$E_L = w_0 b_0 \left\langle \int \dot{\boldsymbol{\pi}}_L^2 \right\rangle = w_0 b_0 c_L^2 \left\langle \int (\boldsymbol{\nabla} \cdot \boldsymbol{\pi}_L) \right\rangle , \tag{255}$$

$$E_T = w_0 b_0 \left\langle \int \dot{\boldsymbol{\pi}}_T^2 \right\rangle = w_0 b_0 c_T^2 \left\langle \int (\boldsymbol{\nabla} \times \boldsymbol{\pi}_T) \right\rangle . \tag{256}$$

Finally, combining Eqs. (246), (248), (252), (255) and (256), as well as the definitions of the non-linear coupling constants in Eqs. (81) to (87), we find that a number of apparently miraculous algebraic cancellations lead to the surprisingly simple result

$$\begin{aligned} M &\simeq -\frac{w_0 b_0^2}{c_L^2} \left[c_L c_L' \left\langle \int (\boldsymbol{\nabla} \cdot \boldsymbol{\pi})^2 \right\rangle + c_T c_T' \left\langle \int (\boldsymbol{\nabla} \times \boldsymbol{\pi})^2 \right\rangle \right] \\ &= -\frac{b_0}{c_L^2} \left[\frac{c_L'}{c_L} E_L + \frac{c_T'}{c_T} E_T \right] . \end{aligned} \tag{257}$$

Note that longitudinal and transverse phonons propagate at different sound speeds generally—see Eq. (88). Therefore, if we consider a localized wave packet of phonons made up of both longitudinal and transverse components, it will separate over time into two different unmixed localized wave packets. These will have different masses in general. Recall that $c_L' = \partial c_L / \partial b$ and $c_T' = \partial c_T / \partial b$, and in the non-relativistic limit, the overall mass density ρ_m in the solid is directly proportional to b, the level of compression or dilation. When we exchange the derivatives with respect to b for derivatives with respect to ρ_m, these must be taken in the absence of shear stresses, corresponding to hydrostatic compression. We then find that the mass of a wave packet consisting of phonons of either component—longitudinal

(L) or transverse (T)—is equal to

$$M_X = -\frac{d\log c_X}{d\log \rho_m}\frac{E}{c_L^2}\,, \tag{258}$$

where $X = L, T$. As expected, this result is identical to the one we found in Eq. (233) using the effective point-particle theory of a highly localized phonon wave packet in a solid.

The extension of this result to a sound wave packet in a perfect fluid is immediate. Following our prescription, we set the derivatives f_Y and f_Z to zero in the action for phonons, Eq. (78), when varying it to find the equations of motion. There are no longer transverse modes and the transverse sound speed c_T is zero. Following the same steps as above leads to a single mass for (longitudinal) phonons,

$$M = -\frac{d\log c_s}{d\log \rho_m}\frac{E}{c_s^2}\,, \tag{259}$$

where c_s is the speed of sound in the fluid. This, too, is precisely the same result we found for phonons in a fluid using the effective point-particle theory—see Eq. (230). We have thus verified both results using more rigorous effective field theory methods, without relying on a point-particle-like approximate representation for the sound wave packet.

4.5 Fluids with Galilei Symmetry

Low-energy physicists who study condensed matter phenomena and fluid dynamics typically do not work with relativistic systems. From that point of view, deriving the results that we have been considering from a fully relativistic starting point may seem gratuitous, and it is nice to demonstrate that similar results can be deduced from a completely non-relativistic starting point. This would demonstrate once again that the "gravitational mass" of sound waves that we are calculating is not in any way a consequence of relativistic mass–energy equivalence. In this section we will show that the sound wave packets carry a net mass in a non-relativistic fluid without dissipation. In order to do so, we will develop an effective theory of a dissipationless fluid that lives in a spacetime whose fundamental symmetries are not the Poincaré, but translations, spatial rotations, and Galilei boosts, rather than Lorentz boosts. Granted, this does not describe the exact symmetries of any real-world system, but it is an approximation that is relevant for low-energy physics.

To begin, we will largely follow the notation and setup of Schakel [134], reviewing how to construct invariant combinations of fields under Galilean transformations. There is a single degree of freedom that we will use to construct the theory, namely the velocity potential $\phi(\mathbf{x}, t)$, which is related to the bulk velocity field by $\mathbf{u} = \boldsymbol{\nabla}\phi$. Under a Galilei boost with small velocity $\mathbf{v}$, we find the following transformation properties for ϕ:

$$\mathbf{x} \to \mathbf{x} - \mathbf{v}t\,, \tag{260}$$

$$\partial_t \to \partial_t + \mathbf{v} \cdot \boldsymbol{\nabla}\,, \tag{261}$$

$$\boldsymbol{\nabla}\phi(\mathbf{x}, t) \to \boldsymbol{\nabla}\phi(\mathbf{x}, t) - \mathbf{v}\,, \tag{262}$$

$$\phi(\mathbf{x}, t) \to \phi(\mathbf{x}, t) - \mathbf{v} \cdot \mathbf{x} + f(t)\,. \tag{263}$$

The function $f(t)$ can be determined by taking inspiration from Bernoulli's principle in standard hydrodynamics in the absence of a gravitation field, $\dot{\phi} + \frac{1}{2}u^2 + h = 0$, where h is the enthalpy per unit mass; indeed, in a perfect, dissipationless fluid with mass conservation, the

quantity $\dot{\phi}$ can be interpreted as $-\mu/m$ where μ is the (non-relativistic) chemical potential. The enthalpy per mass h should remain invariant under a Galilean transformation. Using the above Galilei transformations and requiring that h remains invariant, we find that

$$\frac{df}{dt} = \frac{1}{2}v^2 \implies f(t) = \frac{1}{2}v^2 t\,, \tag{264}$$

where $\mathbf{v}$ is the velocity of the Galilei boost[7].

The only Galilei-invariant combination that we must consider at lowest order in the derivative expansion is therefore proportional to $\dot{\phi} + \frac{1}{2}(\boldsymbol{\nabla}\phi)^2$. We will choose to work with the invariant quantity

$$X \equiv -\dot{\phi} - \frac{1}{2}(\boldsymbol{\nabla}\phi)^2\,. \tag{265}$$

The Lagrangian is a generic function of this invariant quantity. We write the action as

$$S = \int dt\, d^3x\, F(X)\,. \tag{266}$$

Since dimensional analysis shows that F has dimensions of energy density and X has dimensions of chemical potential per unit mass, $F'(X)$ must have units of mass density. We will define $F' \equiv \rho_m$ on the background value of $X = 0$, and we will see that ρ_m is the background mass density. Let us expand the action to cubic order in derivatives of ϕ, as usual. The resulting action is

$$S_3 = \frac{\rho_m}{2c_s^2}\int dt\, d^3x\, \left[\dot{\phi}^2 - c_s^2(\boldsymbol{\nabla}\phi)^2 + \dot{\phi}(\boldsymbol{\nabla}\phi)^2 - \frac{1 - 2c_s c_s'}{3c_s^2}\dot{\phi}^3\right]\,, \tag{267}$$

[7]There is, of course, no need to include an integration constant, since ϕ is a velocity potential.

where the sound speed is

$$c_s^2 = \frac{F'}{F''}\,, \tag{268}$$

and the prime ($'$) symbol represents differentiation with respect to X. We will also note that the non-linear equation of motion of ϕ is

$$\left(\partial_t^2 - c_s^2\nabla^2\right)\phi = -\frac{1}{2}\partial_t\left[(\boldsymbol{\nabla}\phi)^2 - \frac{1-2c_sc_s'}{c_s^2}\dot{\phi}^2\right] - \boldsymbol{\nabla}\cdot\left(\dot{\phi}\boldsymbol{\nabla}\phi\right)\,. \tag{269}$$

Next, recall that thermodynamically, $\mu = \partial H/\partial n$, where H is the Hamiltonian and n is the number density of microscopic constituents of the fluid. Since we have the thermodynamic interpretation $\mu/m = -\dot{\phi}$ and mass density ρ is equal to mn, it is clear that ϕ and ρ are canonically conjugate variables. We can therefore calculate the mass density from the Lagrangian by simple differentiation:

$$\rho = -\frac{\partial F[X(\partial\phi)]}{\partial\dot{\phi}}\,. \tag{270}$$

Expanding to quadratic order in ϕ, we find

$$\delta\rho \equiv \rho - \rho_m = -\frac{\rho_m}{c_s^2}\left[\dot{\phi} + \frac{1}{2}(\boldsymbol{\nabla}\phi)^2 - \frac{1-2c_sc_s'}{2c_s^2}\dot{\phi}^2\right]\,. \tag{271}$$

Now, we consider a localized wave packet solution ϕ and find its contribution to the density perturbation $\delta\rho$. Time averaging over an interval much longer than the oscillation time $1/\omega$ and integrating over volume will give the net mass that travels along with the wave packet ϕ—*i.e.* $M = \left\langle\int\delta\rho\right\rangle$. We can solve the equation of motion Eq. (269) to non-linear order by separating ϕ into a linearized wave equation solution $\phi_{(1)}$ and a non-linear correction $\phi_{(2)}$, sourced by $\phi_{(1)}$ itself. As in the case of the relativistic superfluid, we find that $\left\langle\int\dot{\phi}_{(1)}\right\rangle = \left\langle\int\dot{\phi}_{(2)}\right\rangle = 0$ as a result of time averaging. We can relate the quadratic part

of $\langle \int \delta\rho \rangle$ to the energy E of the wave packet via the Hamiltonian,

$$H = \frac{\rho_m}{2c_s^2} \int d^3x \, \left[\dot{\phi}^2 + c_s^2 (\boldsymbol{\nabla}\phi)^2 \right] . \tag{272}$$

Using the virial theorem, we see that

$$E = \frac{\rho_m}{c_s^2} \left\langle \int \dot{\phi}^2 \right\rangle = \rho_m \left\langle \int (\boldsymbol{\nabla}\phi)^2 \right\rangle . \tag{273}$$

Combining Eqs. (271) and (273) gives the net mass that travels along with the wave packet,

$$M = -\frac{c_s'}{c_s} E \, . \tag{274}$$

Since X can be identified with h, the enthalpy density, and to leading order, $\delta h = c_s^2 \delta\rho/\rho_m$, we can exchange the derivative with respect to X for a logarithmic (adiabatic) derivative with respect to mass density. This yields

$$M \simeq -\frac{d \log c_s}{d \log \rho_m} \frac{E}{c_s^2} \, , \tag{275}$$

as expected. This is the same result we discovered in the effective point-particle theory and using relativistic field theoretic methods.

4.6 The Mass of Sound Waves in Classical Fluid Dynamics

We will now show that a similar result can be derived by performing an analogous non-linear analysis of density perturbations in the framework of classical fluid dynamics. The interpretation of the mass displaced by a sound wave as gravitational mass is not immediately obvious from the classical framework, but we will see that the result is quantitatively identical to the one derived using field theoretic methods. The fact that the same expression can be derived directly from classical fluid dynamics confirms that the gravitational mass we are calculating is not a quantum phenomenon or relativistic effect.

There is a long history of studying non-linear effects of this sort within fluid dynamics, and many similar calculations have been carried out. The calculation of a net momentum carried by sound waves at non-linear order is a standard result derived by Landau and Lifshitz [86]. A completely analogous procedure is used when calculating the radiation pressure of mechanical waves at non-linear order—see, for example, [135]. In our language, that would correspond to calculating $\left\langle \int T_{ii} \right\rangle$, rather than $\left\langle \int T_{00} \right\rangle$. Nevertheless, to our knowledge, the exact quantity that we are considering—the negative gravitational mass associated with a sound wave packet—has not been worked out in the context of classical fluid dynamics.

Our starting point will be the ordinary Euler equations of classical fluid dynamics, which govern adiabatic, inviscid flow. Equally, we could start from the Navier–Stokes equations and assume zero viscosity and thermal conductivity. In our case, we will consider the incompressible Euler equations in Lagrangian form, rather than Eulerian form:

$$\dot{\rho} + \boldsymbol{\nabla} \cdot (\rho \mathbf{v}) = 0 \,, \tag{276}$$

$$\dot{\mathbf{v}} + (\mathbf{v} \cdot \boldsymbol{\nabla})\, \mathbf{v} = -\frac{\boldsymbol{\nabla} p}{\rho} \,. \tag{277}$$

In the equations above, ρ is the mass density, $\mathbf{v}$ represents the velocity field, and p is the pres-

sure. Our approach will be to consider a steady background in hydrostatic equilibrium and a small density perturbation $\delta\rho$, which takes the form of a localized wave packet. We organize the density perturbations as a second-order perturbative expansion, with corresponding perturbations in the velocity field and the pressure.

$$\rho = \rho_0 + \delta\rho_{(1)} + \delta\rho_{(2)} + \cdots \,, \tag{278}$$

$$\mathbf{v} = \mathbf{v}_{(1)} + \mathbf{v}_{(2)} + \cdots \,, \tag{279}$$

$$p = p_0 + \delta p_{(1)} + \delta p_{(2)} + \cdots \,, \tag{280}$$

where $\dot{\rho}_0 = 0$ and $\dot{p}_0 = 0$. Although the full non-linear relationship between ρ and p is determined by the equation of state, we can use the thermodynamic identity $dp/d\rho = c_s^2(\rho)$ in order to relate ρ and p perturbatively, order by order.

$$\delta p_{(1)} = c_s^2 \delta\rho_{(1)} \,, \tag{281}$$

$$\delta p_{(2)} = c_s^2 \delta\rho_{(2)} + c_s c_s' \left(\delta\rho_{(1)}\right)^2 \,, \tag{282}$$

where $c_s' \equiv dc_s/d\rho$. Both c_s and c_s' are implicitly evaluated on the background in the above equations.

Now, we substitute Eqs. (278) to (282) into Eqs. (276) and (277). To first order, the result is

$$\rho_0 \boldsymbol{\nabla} \cdot \mathbf{v}_{(1)} = -\delta\dot{\rho}_{(1)} \,, \tag{283}$$

$$\rho_0 \dot{\mathbf{v}}_{(1)} = -c_s^2 \boldsymbol{\nabla} \delta\rho_{(1)} \,. \tag{284}$$

Of course, differentiating Eq. (283) with respect to time and substituting Eq. (284) gives the ordinary wave equation,

$$\delta\ddot{\rho}_{(1)} = c_s^2 \nabla^2 \delta\rho_{(1)} \,. \tag{285}$$

We take $\delta\rho_{(1)}$ to be a localized wave packet solution to the linear equations of motion. Taking the curl of Eq. (284) gives $\boldsymbol{\nabla}\times\mathbf{v} = \text{const}$, and we can take that constant value to be zero. In other words, the fluid flow is irrotational to first order in our perturbative expansion. Taking the time derivative of Eq. (284), substituting Eq. (283), and introducing a velocity potential via $\mathbf{v}_{(1)} = \boldsymbol{\nabla}\phi_{(1)}$, we find a second wave equation for the first-order velocity potential

$$\ddot{\phi}_{(1)} = c_s^2\nabla^2\phi_{(1)}\,. \tag{286}$$

We will also take $\phi_{(1)}$ to be a localized wave packet solution of this linear equation, with $\mathbf{v}_{(1)}$ defined accordingly as its gradient. The nonlinear corrections $\delta\rho_{(2)}$ and $\mathbf{v}_{(2)}$ are sourced in turn by the linear solutions $\delta\rho_{(1)}$ and $\mathbf{v}_{(1)}$ in the Euler equations. After some algebraic manipulation we find a sourced wave equation for the non-linear correction to the density perturbation:

$$\begin{aligned}\delta\ddot{\rho}_{(2)} - c_s^2\nabla^2\delta\rho_{(2)} = \rho_0\boldsymbol{\nabla}\cdot\left[\left(\mathbf{v}_{(1)}\cdot\boldsymbol{\nabla}\right)\mathbf{v}_{(1)}\right] - \frac{c_s^2}{\rho_0}\left(1-\frac{2\rho_0 c_s'}{c_s}\right)\boldsymbol{\nabla}\cdot\left(\delta\rho_{(1)}\boldsymbol{\nabla}\delta\rho_{(1)}\right)\\ - \partial_t\left(\mathbf{v}_{(1)}\cdot\boldsymbol{\nabla}\delta\rho_{(1)} - \frac{1}{\rho_0}\delta\rho_{(1)}\delta\dot{\rho}_{(1)}\right)\,.\end{aligned} \tag{287}$$

In order to find the net mass that travels with the sound wave packet, we will perform the usual set of operations: solve the non-linear equations of motion, average in time over an interval much larger than the typical oscillation time $1/\omega$, and integrate $\delta\rho = \delta\rho_{(1)}+\delta\rho_{(2)}$ over a volume containing the wave packet. The resulting quantity will have the interpretation of the net mass that travels with the sound wave. As a first step, we will time-average Eq. (287), which has the effect of removing total time derivative terms, since they produce combinations of oscillatory terms that average to zero. Reintroducing the velocity potential, we find that the time-averaged equation of motion can be written as

$$\nabla^2\left\langle\delta\rho_{(2)}\right\rangle = -\left\langle\nabla^2 F\right\rangle\,, \tag{288}$$

where we introduced the function

$$F\left(\mathbf{x},t\right)=\frac{\rho_0}{2c_s^2}\left[\boldsymbol{\nabla}\phi_{(1)}\left(\mathbf{x},t\right)\right]^2-\frac{1}{2\rho_0}\left(1-\frac{2\rho_0 c_s'}{c_s}\right)\left[\delta\rho_{(1)}\left(\mathbf{x},t\right)\right]^2 . \tag{289}$$

We can easily solve the time-averaged equation of motion Eq. (288) using Green's function methods. Integrating the solution over a volume containing the wave packet, we obtain the expression

$$\left\langle\int\delta\rho_{(2)}\right\rangle=\frac{1}{2\rho_0}\left(1-\frac{2\rho_0 c_s'}{c_s}\right)\left\langle\int\left(\delta\rho_{(1)}\right)^2\right\rangle-\frac{\rho_0}{2c_s^2}\left\langle\int\left(\boldsymbol{\nabla}\phi_{(1)}\right)^2\right\rangle . \tag{290}$$

We know that the Lagrangian for a fluid with barotropic, inviscid, irrotational flow is given by $L=\int d^3x\,\left[\frac{1}{2}\rho\left(\boldsymbol{\nabla}\phi\right)^2-e(\rho)\right]$, where the internal energy density e is related to the density by $e''(\rho)=c_s^2(\rho)/\rho$. Notice, then that in Eq. (290), all the terms on the right-hand side other than $-\frac{c_s'}{c_s}\left\langle\int\left(\delta\rho_{(1)}\right)^2\right\rangle$ are precisely the Lagrangian of density perturbations in such a fluid, averaged over time and divided by c_s^2, to leading order in the perturbative expansion. Those terms must therefore average to zero over time. We are left with

$$\left\langle\int\delta\rho_{(2)}\right\rangle=-\frac{c_s'}{c_s}\left\langle\int\left(\delta\rho_{(1)}\right)^2\right\rangle . \tag{291}$$

Using the virial theorem, we can show that the total energy (or time-averaged Hamiltonian) associated with density perturbations in such a fluid must be equal to

$$E=\rho_0\left\langle\int\left(\boldsymbol{\nabla}\phi_{(1)}\right)^2\right\rangle=\frac{c_s^2}{\rho_0}\left\langle\int\left(\delta\rho_{(1)}\right)^2\right\rangle \tag{292}$$

to leading order, where $\phi_{(1)}$ and $\delta\rho_{(1)}$ are wave packet solutions of the wave equation. Thus, combining Eqs. (291) and (292), we find that the net mass M associated with a sound wave

packet in a fluid is given by

$$M = -\frac{\rho_0 c_s'}{c_s^3} E = -\frac{d \log c_s}{d \log \rho} \frac{E}{c_s^2} \,. \tag{293}$$

This is the same now-familiar result for the net gravitational mass associated with a sound wave packet in the fluid that we have derived using several different methods. It is a useful cross-check which confirms that the effect we are studying has nothing to do with relativity; in fact, this effect has been hidden in plain sight in classical fluid dynamics for centuries, since the time of Euler.

4.7 The Mass of Sound Waves in Classical Elasticity Theory

Just as we derived the result for the net mass that travels with sound waves in a fluid from classical fluid dynamics, we can verify the result we obtained in isotropic solids using the classical theory of elasticity in continuum mechanics, which also proves to be a useful cross-check. We will slightly adapt the notation and exposition in Marder [136] and Landau *et al.* [75] to review the basic setup of the non-linear theory of elasticity in isotropic solids.

We begin by considering a solid in which material points are located in some reference state with coordinates $\mathbf{x}$. Elastic deformation causes the material points to be displaced to a set of new positions with coordinates $\mathbf{s}(\mathbf{x})$. The main degrees of freedom in this theory are the displacements $\mathbf{u}$, defined as

$$\mathbf{u}(\mathbf{x}) = \mathbf{s}(\mathbf{x}) - \mathbf{x}\,. \tag{294}$$

The change in square distance between a material point originally located at $\mathbf{x}$ and its nearest neighbor originally at $\mathbf{x} + d\mathbf{x}$ induced by the elastic deformation is given by

$$\begin{aligned} \frac{1}{2}\left[|\mathbf{s}(\mathbf{x}+d\mathbf{x}) - \mathbf{s}(\mathbf{x})|^2 - dx^2\right] &= \frac{1}{2}(g_{ij} - \delta_{ij})dx_i dx_j \\ &\equiv e_{ij}dx_i dx_j\,, \end{aligned} \tag{295}$$

where the extra factor of $1/2$ is included by convention. e_{ij} is generally known as the non-linear strain (or Lagrangian stress) tensor, and the metric g_{ij} is defined as

$$g_{ij} \equiv \frac{\partial \mathbf{s}}{\partial x_i} \cdot \frac{\partial \mathbf{s}}{\partial x_j}\,. \tag{296}$$

In terms of the displacements $\mathbf{u}$, this metric can also be written as

$$\begin{aligned} g_{ij} &= \delta_{ij} + \partial_i u_j + \partial_j u_i + \partial_i u_k \partial_j u_k \\ &\equiv \delta_{ij} + 2e_{ij} \,, \end{aligned} \tag{297}$$

where the partial derivatives ∂_i are taken with respect to material point positions x_i. In the theory of linear elasticity, the quadratic term in e_{ij} is neglected, allowing for a simplified analysis of the dynamics of elastic waves in the solid. However, the non-linear part will be important for us here.

The behavior of elastic waves in solids can be studied by minimizing a free energy functional $\mathcal{F}$. If we were interested in linear elasticity only, we would write a free energy functional that is quadratic in the strain tensor. We would not include any terms linear in the strain, so that the ground state will correspond to the undistorted solid, for which $e_{ij} = 0$. Therefore, in linear elasticity, we write the free energy functional as

$$\mathcal{F} = \frac{1}{2} \int d^3x \, e_{ij} K_{ijkl} e_{kl} = \frac{1}{2} \int d^3x \, e_{ij} \sigma_{ij} \,, \tag{298}$$

where $\sigma_{ij} \equiv K_{ijkl} e_{kl}$ is the stress tensor and K_{ijkl} is the elastic modulus tensor of rank 4 [75]. Since the strain is symmetric under interchange of indices, the tensor K_{ijkl} can generally be assumed to be symmetric under $i \leftrightarrow j$, $k \leftrightarrow l$, and $ij \leftrightarrow kl$ permutations. Any further constraints on the form of K_{ijkl} are imposed by the symmetry point group of the solid. We will be particularly interested in the case of an isotropic solid, and the tensor K_{ijkl} for an isotropic solid can be written in the form

$$K_{ijkl} = \lambda \delta_{ij} \delta_{kl} + \mu \left(\delta_{ik} \delta_{jl} + \delta_{il} \delta_{jk} \right) \,, \tag{299}$$

which keeps the elastic energy invariant under $SO(3)$ rotations. The parameters λ and μ are known as the Lamé constants of the solid.

When working to non-linear (cubic) order with the full Lagrangian stress tensor, there are additional cubic terms in the Lagrangian stress that can be added to the free energy functional. The conventional approach—see, for example, Landau *et al.* [75]—is to add to the elastic energy functional[8] three independent cubic scalar combinations in the strain, usually $(\mathrm{tr}\, e)^3$, $(\mathrm{tr}\, e)(\mathrm{tr}\, e^2)$, and $\mathrm{tr}\, e^3$, in addition to the quadratic scalars $\mathrm{tr}\, e^2$ and $(\mathrm{tr}\, e)^2$, since those scalar combinations are invariant under rotations. However, a functional involving both quadratic and cubic invariants in the strain is no longer going to have $e_{ij} = 0$ as its ground state in general. If our theory is to describe elastic waves as perturbations around the lowest-energy configuration of a general isotropic solid, we must introduce a new ground state $u_i \propto x_i, e_{ij} \propto \delta_{ij}$ around which to introduce small fluctuations[9]. Instead of doing this, we can eschew the standard elasticity formalism involving the strain tensor and take the completely equivalent approach of building quadratic and cubic invariants directly from the metric tensor g_{ij}, in which case the ground state is unchanged—$g_{ij} \propto \delta_{ij}$. Furthermore, we can take inspiration from our approach to studying a solid in the relativistic effective field theory treatment of Section 2.3. As before, we introduce an overall scaling parameter b_0 and write

$$\mathbf{s}(\mathbf{x}) = \sqrt[3]{b_0}\,[\mathbf{x} + \mathbf{u}(\mathbf{x})]\ . \tag{300}$$

Assuming the solid is isotropic, we build three linearly independent $SO(3)$ rotational

[8]It is no longer accurate to call it free energy in this case, since anharmonic effects give rise to adiabatic motion.

[9]Note that Landau *et al.* [75] build the elastic energy functional from quadratic and cubic invariants of the non-linear strain tensor $e_{ij} = \partial_i u_j + \partial_j u_i + \partial_i u_k \partial_j u_k$ when analyzing anharmonic vibrations, without giving $\mathbf{u}$ a non-zero VEV. The resulting theory does not describe the ground state of the most general solid, and it does not fully reproduce the dynamics of elastic waves at non-linear order.

invariants from the metric $g_{ij} = \partial_i s_k \partial_j s_k$, which we choose to be

$$b = \sqrt{\det g}\,, \quad Y = \frac{\mathrm{tr}\, g^2}{(\mathrm{tr}\, g)^2}\,, \quad Z = \frac{\mathrm{tr}\, g^3}{(\mathrm{tr}\, g)^3}\,. \tag{301}$$

The elastic energy density will then be a function of these three invariants, which can be Taylor expanded to reproduce contributions to the elastic energy from all possible invariant combinations of the strain to arbitrary order in perturbation theory. We choose to write the most general elastic energy of an isotropic solid as

$$\mathcal{F} = \rho_0 \int d^3x\, f(b, Y, Z)\,. \tag{302}$$

We pulled out an overall factor of ρ_0, the equilibrium mass density in the solid. Expanding to cubic order in small displacements $\mathbf{u}$, the elastic energy becomes

$$\begin{aligned}\mathcal{F} \to \rho_0 b_0 \int d^3x \Bigg[&\frac{c_L^2 - c_T^2}{2}(\boldsymbol{\nabla}\cdot\mathbf{u})^2 + \frac{c_T^2}{2}(\partial_i u_j)^2 + g_3(\boldsymbol{\nabla}\cdot\mathbf{u})^3 + g_4(\boldsymbol{\nabla}\cdot\mathbf{u})(\partial_i u_j)^2 \\ &+ g_5(\boldsymbol{\nabla}\cdot\mathbf{u})(\boldsymbol{\nabla}\times\mathbf{u})^2 + g_6 \partial_i u_j \partial_i u_k \partial_j u_k + g_7 \partial_i u_j \partial_j u_k \partial_k u_i \Bigg]\,,\end{aligned} \tag{303}$$

where the constants $c_L^2, c_T^2, g_3, g_4, g_5, g_6, g_7$ have precisely the same form as in the relativistic theory—see Eqs. (79), (80) and (83) to (87).

Let us now introduce time dependence into the theory. While displacements are occurring, material points move with velocities $\dot{\mathbf{s}} \equiv \partial_t \mathbf{s}(\mathbf{x}, t) \propto \partial_t \mathbf{u}(\mathbf{x}, t)$. There is an associated kinetic energy density at each material point given by $\rho_0 \dot{s}^2/2$, where ρ_0 is the mean mass density of the solid at equilibrium. We can use this to define a total kinetic energy and a Lagrangian associated with elastic deformations:

$$\mathcal{L} \equiv \mathcal{T} - \mathcal{F}\,, \tag{304}$$

$$\mathcal{T} = \rho_0 b_0 \int d^3x\, \frac{1}{2}\dot{u}^2 \tag{305}$$

is the total kinetic energy. The b_0 factor is included since we want the Lagrangian to scale uniformly with dilations or compressions of the reference state of the solid, as an extensive quantity. We can use Eq. (303) and vary the cubic Lagrangian with respect to the small displacements $\mathbf{u}$ to find non-linear (quadratic) equations of motion for displacements. The result is

$$\rho_0 \ddot{u}_i - \left(c_L^2 - c_T^2\right) \partial_i \left(\boldsymbol{\nabla} \cdot \mathbf{u}\right) - c_T^2 \nabla^2 u_i = \partial_j A_{ij} \,, \tag{306}$$

where A_{ij} has exactly the same form as Eq. (246) if we identify $\mathbf{u}$ with $\boldsymbol{\pi}$, but with the couplings g_1 and g_2 set to zero. As before, this equation can be solved non-linearly by defining a perturbative expansion $\mathbf{u} = \mathbf{u}_{(1)} + \mathbf{u}_{(2)} + \cdots$, where $\mathbf{u}_{(1)}$ solves the linearized equations of motion, and $\mathbf{u}_{(2)}$ is sourced by $\mathbf{u}_{(1)}$. The linear equations of motion show that c_L and c_T are indeed the longitudinal and transverse sound velocities, respectively.

In order to find the mass that travels with a localized elastic wave packet in this solid, we must simply calculate $M \simeq \rho_0 b_0 \langle \int \boldsymbol{\nabla} \cdot \mathbf{u} \rangle$, since at leading order $\boldsymbol{\nabla} \cdot \mathbf{u} \sim e_{ii}$ encodes the density of displaced material points due to the presence of compressional elastic waves. Mass M must include a factor of b_0 because it scales linearly with volume, as does b_0. Again, we use $\langle \int \dots \rangle$ to denote the combination of time averaging and spatial integration over a volume containing the wave packet. At linear order, the quantity $\langle \int \boldsymbol{\nabla} \cdot \mathbf{u} \rangle$ is zero, since a plane wave packet can be made arbitrarily localized. However, the non-linear correction will contribute a non-zero quantity to this net mass. Following the same procedure as before, we solve the time-averaged non-linear equation of motion Eq. (306) for $\langle \boldsymbol{\nabla} \cdot \mathbf{u}_{(2)} \rangle$ using Green's function methods in order to calculate the mass M. The exact same cancellations occur as in Section 2.3, and the result is the same:

$$M = -\frac{b_0}{c_L^2} \left[\frac{c_L'}{c_L} E_L + \frac{c_T'}{c_T} E_T \right] , \tag{307}$$

where E_L and E_T are now the contributions of longitudinal and transverse elastic waves,

respectively, to the Hamiltonian $\mathcal{H} = \mathcal{T} + \mathcal{F}$, averaged over time. Noting that b is proportional to e_{ii}, which is proportional in turn to the change in the mass density induced by the elastic wave packet in the solid, we find that the net mass that travels with longitudinal (L) and transverse (T) waves is once again given by

$$M_X = -\frac{d \log c_X}{d \log \rho_m} \frac{E_X}{c_L^2} \,, \tag{308}$$

for $X = L, T$. Thus we see that this net mass associated with elastic waves is a completely classical effect, contained within the ancient theory of elasticity in continuum mechanics; it could have been calculated by Cauchy, had he known to look for it.

4.8 Discussion and Implications

In this section, we have repeatedly shown that sound waves carry a net mass in a variety of media: superfluids, ordinary fluids, and solids. The mass associated with a localized sound wave packet truly is a gravitational one, in the sense that it is not only affected by gravity, but it also *sources* gravity in turn. This mass happens to be negative, as a fraction of the total mass of the system, meaning that sound gets refracted in direction opposite to the gravitational field; we showed that phonons float, though typically very slowly. This effect is tied to the non-linear interactions of phonons in condensed matter systems, and it would have been invisible from a purely linear wave analysis. The net gravitational mass associated with sound waves is still a very small quantity, but it has a direct scaling with the energy carried by the sound wave, with a coefficient of proportionality that is completely determined by the equation of state of the medium. Let us pause to consider the implications.

A direct consequence of equations of motion such as Eq. (217) for localized phonon wave packets is that in a stratified medium, where the speed of sound depends on a single spatial coordinate z in a gravitational field, an analogue of Snell's law holds for sound waves: $c_s^{-1}(z)\sin\theta = \text{const}$, where θ is the angle of the phonon's net momentum with respect to the z axis. Instead of traveling along straight trajectories, nearly horizontal localized phonon trajectories gradually curve upward in a downward gravitational field, with radius of curvature comparable to $R \sim c_s^2/g$. In seawater, for example, this curvature radius is of order $R \sim 10^2$ km, which implies that they are refracted by one degree every couple of seconds, while in superfluid helium, nearly horizontal phonons are refracted by 10 degrees in a comparable period of time. The refraction of phonons in stratified media implies that uniform sound radiation will spread in a very, very slightly not-quite-spherical manner—Huygens' principle for sound waves would have to be ever-so-slightly modified. Technically, this would lead to systematic corrections that could be accounted for in technologies such as sonar [137], but these are negligible effects over distances much smaller than the radius of curvature of phonon trajectories.

It may seem as though the effect we are considering is so small that is undetectable in ordinary experimental conditions. Consider, for instance, a phonon in superfluid helium-II that is highly energetic, say, with momentum of order $k \sim 1$ keV ~ 0.5 Å^{-1}, which is starting to get close to the "maxon" region of the excitation spectrum (see Fig. 1). Assuming $d \log c_s / d \log \rho$ is of order 1, the mass associated with the phonon is of the same order as a single helium atom, or 1 GeV. A lower-momentum phonon would displace a mass that is a fraction of the mass of a helium atom. Note that this does not contradict the fact that particle number is strictly integral in a superfluid condensate, since a generic single phonon state in the condensate corresponds to a many-body wave-function solution to the Schrödinger equation that is delocalized over much of the system.

Is this rather subtle effect potentially detectable in realistic experimental setups, then? Since the mass of a sound wave scales as E/c_s^2, we can either consider media with low sound speeds or highly energetic phenomena for the most optimistic experimental realizations. Very slow sound speeds have been observed in ultracold atomic gases and Bose–Einstein condensates. Let us take as an example a dilute rubidium or cesium Bose–Einstein condensate. An expression for the sound velocity at peak density in such a condensate was first given by Bogolyubov [138]. It is typically of order $c_s \sim \sqrt{4\pi\hbar^2 n_0 a_s / m^2}$, where n_0 is the peak number density, a_s is the scattering length in the medium, and m is the mass of atoms in the condensate. With a peak density of order 10^{19} m^{-3}, a scattering length around 10 Å, and mass of order 10^{-25} kg, this gives a sound speed on the order of $c_s \sim 1$ mm/s. Indeed, such velocities of sound have been measured experimentally in dilute sodium Bose–Einstein condensates [139]. For an energetic phonon with maximum momentum $k \sim 1/a_s$ in such a medium, the displaced mass can be as high as $M \sim 10^4$ GeV/c^2, and for an atomic cloud with roughly 50 thousand cesium atoms, this amounts to between 0.1% and 1% of the total mass of the condensate [140]. Although the displaced mass is a small fraction of the total, it is certainly not negligibly small. Ultracold Bose–Einstein gases offer an interesting potential avenue for studying this effect experimentally, especially because trapping configurations can

be tuned to simulate strong gravitational fields.

At the other extreme, we can consider highly energetic events involving macroscopic sound waves that propagate over large distances; seismic waves from earthquakes are an ideal candidate. Consider an extremely powerful earthquake with Gutenberg–Richter magnitude around 9. Such an earthquake is expected to radiate about 10^{18} J in seismic energy. Using a typical p-wave velocity of around 5000 km/s [141], this corresponds to a net displaced mass of approximately 10^{11} kg, or a change in gravitational acceleration of the order of $\delta g \sim 10$ fGal. With current technology, mobile atomic gravimeters can be used to measure changes in gravitational acceleration up to the 10 pGal level [142–144], so an improvement in sensitivity of around three orders of magnitude would be required to make such a measurement[10]. Still, given the rate of improvement of atomic clock technology, such measurements may become possible in the not-too-distant future.

Besides concrete measurements that can be done on Earth, we can consider the theoretical implications of this result for the dynamics of neutron stars, which are believed to have superfluid matter in their interiors [126, 145–147]. The behavior of phonons in strong gravitational fields has implications for phonon-mediated transport properties in neutron stars. The sound speed is expected to be relativistic in such settings [125, 148], but this is not a problem since our formalism is fully relativistic and we need not approximate beyond Eq. (243). Slightly generalized results hold for media with relativistic sound velocities.

Another conclusion that can be drawn from our result, which is beautiful to consider but almost certainly undetectable, is that since sound waves generate gravitationl fields, they gravitate with each other. Two wave packets propagating in parallel through a medium will both have negative gravitational mass, and since like charges attract in gravity, their trajectories will slowly begin to converge over time.

[10]Of course, we hope that the opportunity to make such measurements in the aftermath of a magnitude 9 earthquake will never arise!

5 Beyond EFT: UV Completion of a Perturbative Solid

5.1 Overview

So far, we have been exploring the power of effective field theories to model the low-energy dynamics of condensed matter systems. It is clearly a powerful framework, with the potential to describe observable macroscopic phenomena, such as vortex precession in trapped superfluids, as well as subtle non-linear effects like the net gravitational mass of phononic excitations. However, the formalism of effective field theory has built-in limitations from the outset. The theories we have been considering are valid when describing low-energy phenomena or the interaction of long-wavelength excitations with external sources, representing non-perturbative phenomena such as vortices. Such effective theories have associated cutoff length scales that limit the regime of validity of perturbation theory, obscuring the short-distance physics of condensed matter systems. One way to move beyond this obvious limitation would be to study a UV-complete (renormalizable) theory with a non-trivial fixed point that reduces to the effective theory at low energies after integrating out certain heavier degrees of freedom. Although this is not a uniquely defined task, symmetry considerations can help guide us when trying to formulate a UV completion of an effective field theory. If done successfully for the effective theory of a solid, which is necessarily homogeneous in our formulation, it would allow us to ask a simple yet intriguing question: Must all solids that appear to be homogeneous at long distances eventually break homogeneity at short distances, as seems to be the case in nature for all the real-world solids with which we are familiar? Or, stated conversely, can one formulate a state in relativistic quantum field theory that appears to be a homogeneous solid at long distances, yet is still perfectly homogeneous at short distances? How would such solids behave, and what peculiar properties must such solids have, if any? All such questions can be answered by finding UV completions of a low-energy effective theory of a perturbative solid. Moreover, such UV completions would allow us to

study more technical questions about the dynamics of the system at shorter wavelengths, the renormalization of the theory and its running couplings, how symmetry-breaking processes at low energies might be connected to the symmetries of the UV-complete theory, and what possible candidates for holographic dual theories of solids we may consider. It could lead to the discovery of additional constraints on the couplings in the low-energy theory, from the requirement of properties such as subluminality, positivity, and stability in the UV theory.

A common approach to finding UV completions for general effective theories is to embed them into linear sigma models by introducing additional heavy "radial modes" and restoring the broken internal symmetries. This is achieved by adding modes with masses around the strong-coupling scale in the low-energy effective theory. If G is a broken symmetry group, H is an unbroken subgroup, $g \in G$, $h \in H$, and $\boldsymbol{\pi}$ are a set of associated Goldstone modes, then the radial modes $\boldsymbol{\rho}$ transform linearly under g as $\boldsymbol{\rho} \to h\left(\boldsymbol{\pi}, g\right)\boldsymbol{\rho}$, thus restoring the broken symmetry and realizing a UV completion of the dynamics of the Goldstones. A major obstacle in UV completing low-energy effective theories of condensed matter, however, is the spontaneous breaking of space-time symmetries, especially space-time translations. Indeed, Endlich *et al.* [149] demonstrated that this process of embedding effective theories into linear sigma models generally fails when the spontaneously broken symmetries are not internal, but space-time symmetries. Since all condensed matter systems spontaneously break some of the Poincaré symmetries, we must look for other options to UV-complete their effective theories and study symmetry breaking at high energies.

One popular avenue for exploring the properties of condensed matter at strong coupling and transcending the limitations of the low-energy effective theories involves holography. Holographic AdS dual models have been studied for systems realizing the properties of superconductors/superfluids [56], fluids and solids [57, 150–152], and even supersolids [153]. Finding candidate theories of condensed matter systems that have holographic duals can be somewhat more of an art than a science, however, since it is not always straightforward to find well-defined, renormalizable theories that realize the appropriate symmetry-breaking

patterns. Holographic methods are very effective for getting an idea about what happens to condensed matter systems at quantum criticality, when standard field theoretic approaches fail. These methods are also computationally tractable, lending themselves to the calculation of transport properties in various media at strong coupling and finite temperature. One of the primary difficulties in constructing a holographic dual theory that realizes the symmetry-breaking pattern of a solid arises from the non-compactness of the subgroup of translations in the Poincaré group. Since the holographic dictionary demands that global boundary theory symmetries become gauge symmetries in the bulk, finding a gauged companion for global translation symmetry is not an easy task. For this reason, in [150], Esposito *et al.* resorted to building a theory of a conformal solid on a sphere, working out a holographic dual description, and then taking a flat-space limit. We will take inspiration from this approach here. Rather than relying on holographic methods, however, we will explore somewhat different questions and issues surrounding how to find a UV completion for the effective theory of solids. We will explore a class of renormalizable, Lorentz-invariant interacting quantum field theories, including that of a solid on a sphere, and implement symmetry-breaking patterns paralleling those of an isotropic solid. We will see to what extent each of these theories is an appropriate description of a solid, with the hope that one of them might provide a viable renormalizable theory that can be used as a dual theory in the holographic framework. In each case, we will integrate out gapped modes in order to obtain a low-energy effective theory of gapless Goldstones, which should resemble, at least in part, the one we studied previously in Section 2.3.

As we have seen in Section 2.3, an isotropic solid can be treated in effective field theory as a continuous, homogeneous medium at large distances. Its properties and dynamics can be modeled by considering the motion of volume elements, represented by three scalar fields $\phi^I(\mathbf{x}, t)$. In the case of a fluid (which is just a highly symmetric solid from the effective field theory point of view), the coordinates ϕ^I can be thought of as the co-moving Lagrangian coordinates. These coordinates can be chosen so that in the ground state of the solid, they

become aligned with the physical coordinates, $\langle \phi^I \rangle = \alpha x^I$, where the constant α encodes the degree of uniform compression or dilation of the solid. It is clear that this ground state configuration breaks symmetry under both spatial translations and rotations, though. In this section, we will consider a solid that is both homogeneous and isotropic, so we require that that the theory possesses an internal $ISO(3)$ symmetry [16, 74, 150] under which the scalars ϕ^I transform as

$$\phi^I \to O^I{}_J \, \phi^J + a^I \,, \tag{309}$$

where a^I is a constant vector and $O^I{}_J$ is an $SO(3)$ rotation matrix. An isotropic solid, then, can be defined as a system that spontaneously breaks internal translations and rotations, as well as boosts, down to a diagonal subgroup. The overall symmetry breaking pattern is $ISO(3,1) \times ISO(3) \to ISO(3)$. This diagonal subgroup enforces the homogeneity and isotropy of the resulting state.

In the effective field theory of solids, we postulated a Lagrangian density that is a generic function of three linearly independent Poincaré and internal $ISO(3)$ invariants constructed from the scalar fields ϕ^I, which are the lowest-order invariants in the derivative expansion. We introduced fluctuations about the VEV and expanded the action to obtain a perturbative theory of phonons in the solid. In this section, we want to go beyond this approach. We will try several different methods to formulate a UV-complete theory that realizes the same symmetry-breaking pattern as the perturbative homogeneous solid. We will then integrate out heavy degrees of freedom in order to obtain a low-energy theory of weakly coupled phonons in a solid. In spite of the disparate starting points, we will find that in every case, after integrating out heavy modes, the resulting low-energy theories are the same; this common "theoretical fixed point" associated with isotropic solids has a highly peculiar structure, enjoying an enhanced $SO(3) \times SO(3)$ symmetry, in which space-time coordinates and internal indices may be rotated independently. The velocity of propagation of

transverse excitations in this theory is always luminal, while longitudinal phonons propagate at a subluminal velocity as long as the original UV theory is stable. These turn out to be common features of effective theories of isotropic solids that are homogeneous at both long and short distances. The theory that emerges must describe a rather extraordinary solid!

Note on conventions: Unlike in the prior sections, we will not be interested in studying the non-relativistic limit of these theories. Accordingly, we set $c = \hbar = 1$. We continue to work in metric signature $(-,+,+,+)$. We will also use X to represent the combination of fields $\mathrm{tr}\, B^{IJ} = \mathrm{tr}\left(\partial_\mu \phi^I \partial^\mu \phi^J\right)$, rather than the combination in the effective theory of a superfluid.

5.2 Isotropic Limit of a Cubic Solid

It is not immediately obvious how to formulate a theory of an isotropic solid with renormalizable interactions. Instead, let us begin by writing a theory of a system that has the symmetries of an anisotropic, cubic solid. Approximate isotropy can then be recovered by restricting to a particular set of coupling constants in the theory for which the anisotropies become negligible. We will build the Lagrangian from a set of three complex scalar fields $\Phi^I(x)$, with $I = 1, 2, 3$. The Lagrangian will have internal $U(1) \times U(1) \times U(1)$ symmetry and $\Phi^I \leftrightarrow \Phi^J$ permutation symmetry. The most general Lorentz invariant and renormalizable action that is compatible with the above symmetries is [154]

$$\begin{aligned} S = &- \int d^4x \sum_I \left[\left|\partial\Phi^I\right|^2 - m^2 \left|\Phi^I\right|^2 + \frac{\lambda_1}{2} \left|\Phi^I\right|^4 \right] \\ &- \int d^4x \, \frac{\lambda_2}{2} \sum_{I \neq J} \left|\Phi^I\right|^2 \left|\Phi^J\right|^2 , \end{aligned} \tag{310}$$

where the parameters m^2, λ_1, and λ_2 are arbitrary constants for now. The sign of the mass term was chosen for later convenience, so that the potential would have a Mexican hat-like form for positive m^2.

Next, we implement symmetry breaking by looking for complex scalar field configurations that break the internal $U(1)^3$ symmetry by a non-trivial VEV. In order to do so, we redefine the complex scalar fields Φ^I in terms of six real scalars, ρ^I and ϕ^I:

$$\Phi^I(x) = \rho_I(x) e^{i\phi^I(x)} . \tag{311}$$

This field decomposition separates the complex scalars into heavy radial modes ρ_I and light phases ϕ^I, which undergo constant shifts under the internal $U(1)^3$ transformations of Φ^I. The permutation symmetry has the same effect of permuting $\phi^I \leftrightarrow \phi^J$. These phases ϕ^I are nothing other than the nondimensionalized co-moving coordinates of volume elements in a solid, and their symmetry properties indicate that the solid has cubic symmetry. In terms

of these new real scalar fields, the action of Eq. (310) becomes

$$\begin{aligned} S = &- \int d^4x \sum_I \left[(\partial \rho_I)^2 - m^2 \rho_I^2 + \rho_I^2 \left(\partial \phi^I \right)^2 \right] \\ &- \int d^4x \left[\frac{\lambda_1}{2} \sum_I \rho_I^4 + \frac{\lambda_2}{2} \sum_{I \neq J} \rho_I^2 \rho_J^2 \right] . \end{aligned} \tag{312}$$

Our next goal is to integrate out the heavy radial modes ρ_I, leaving only a low-energy effective theory for the light fields ϕ^I, representing co-moving coordinates in the solid. In order to integrate out the heavy fields, it will be convenient to introduce the following notation:

$$\begin{aligned} \boldsymbol{\rho^2} &\equiv \begin{pmatrix} \rho_1^2 \\ \rho_2^2 \\ \rho_3^2 \end{pmatrix} , \quad \boldsymbol{b} \equiv \begin{pmatrix} B^{11} - m^2 \\ B^{22} - m^2 \\ B^{33} - m^2 \end{pmatrix} , \\ \boldsymbol{\Lambda} &\equiv \begin{pmatrix} \lambda_1 & \lambda_2 & \lambda_2 \\ \lambda_2 & \lambda_1 & \lambda_2 \\ \lambda_2 & \lambda_2 & \lambda_1 \end{pmatrix} . \end{aligned} \tag{313}$$

As in Sections 2.2 and 2.3, we have $B^{IJ} = \partial_\mu \phi^I \partial^\mu \phi^J$. Since the radial fields are heavy and we are going to integrate them out, we can neglect derivatives of ρ_I, leaving the action in the simple form

$$S \simeq - \int d^4x \left(\boldsymbol{\rho^2} \cdot \boldsymbol{b} + \frac{1}{2} \boldsymbol{\rho^2} \cdot \boldsymbol{\Lambda} \cdot \boldsymbol{\rho^2} \right) . \tag{314}$$

Varying this action with respect to $\boldsymbol{\rho^2}$ gives the equation of motion for the heavy radial mode,

$$\boldsymbol{\rho^2} \simeq - \boldsymbol{\Lambda}^{-1} \cdot \boldsymbol{b} . \tag{315}$$

Substituting this classical solution for the radial mode back into the action, we find the following effective action for the light scalar fields ϕ^I:

$$S_{\text{eff}} = \frac{1}{2}\int d^4x\, \boldsymbol{b}\cdot\boldsymbol{\Lambda}^{-1}\cdot\boldsymbol{b}\,. \tag{316}$$

Inverting the matrix $\boldsymbol{\Lambda}$ and introducing the notation $X \equiv \operatorname{tr} B^{IJ}$, we can rewrite this effective action as

$$S_{\text{eff}} = -\int d^4x\, \left[m^2\,(\xi - 2\xi')\,X + \frac{1}{2}\xi' X^2 + (\xi+\xi')\,\tau^{IJKL}B^{IJ}B^{KL}\right], \tag{317}$$

where the parameters ξ and ξ' are defined as

$$\xi \equiv \frac{\lambda_1+\lambda_2}{(\lambda_1-\lambda_2)(\lambda_1+2\lambda_2)}\,, \quad \xi' \equiv \frac{\lambda_2}{(\lambda_1-\lambda_2)(\lambda_1+2\lambda_2)} \tag{318}$$

and the tensor τ^{IJKL} is given by

$$\tau^{IJKL} \equiv \sum_{M=1}^{3}\delta^I_M\delta^J_M\delta^K_M\delta^L_M\,. \tag{319}$$

The effective action Eq. (317) describes a theory of a solid, but it is clearly not isotropic. Anisotropies are produced by the third term proportional to τ^{IJKL}, which is a consequence of cubic symmetry. While the term preserves the original permutation symmetry and shift symmetry of the ϕ^I fields, it is not invariant under arbitrary rotations. Since we are interested in generating an effective theory of a solid that is isotropic at long distances, we must tune the coupling parameters λ_1 and λ_2 so that the final term is negligibly small. We cannot make $\xi+\xi'$ strictly equal to zero, since that corresponds to precisely those couplings λ_1 and λ_2 which make the matrix $\boldsymbol{\Lambda}$ singular (*i.e.* the original theory becomes strongly coupled).

However, we can study the regime in which

$$\lambda_1 + 2\lambda_2 \ll \lambda_1 - \lambda_2 \,, \tag{320}$$

since this ordering between the couplings would entail that

$$\begin{aligned} \xi + \xi' = \frac{1}{\lambda_1 - \lambda_2} \ll -\frac{1}{3(\lambda_1 + 2\lambda_2)} \simeq \xi' \\ \sim \frac{1}{\lambda_1 + 2\lambda_2} = \xi - 2\xi' \,, \end{aligned} \tag{321}$$

and the anisotropic term involving τ^{IJKL} is subleading compared to the first two terms in the effective action Eq. (317). We are then left with the effective action

$$S_{\text{eff}} = -\frac{m^2}{\lambda_1 + 2\lambda_2} \int d^4x \, \left[X - \frac{1}{6m^2} X^2 + \mathcal{O}\left(\frac{\lambda_1 + 2\lambda_2}{\lambda_1 - \lambda_2} \right) \right] . \tag{322}$$

This action is completely isotropic to leading order if we expand in powers of the parameter $(\lambda_1 + 2\lambda_2)/(\lambda_1 - \lambda_2)$, which is small in the regime we are considering. If we canonically normalize the fields by performing the rescaling $\phi^I \to \sqrt{\frac{\lambda_1 + 2\lambda_2}{2m^2}} \phi^I$, we find that the effective action becomes

$$S_{\text{eff}} = -\int d^4x \, \left[\frac{1}{2} X - \frac{\lambda}{4m^4} X^2 \right] , \tag{323}$$

to leading order, where we defined $\lambda \equiv (\lambda_1 + 2\lambda_2)/6$. This action has a peculiar structure with enhanced symmetry in both the kinetic term and the quartic term. In particular, we see that the action in this limit is still invariant under internal rotations $\phi^I \to O^I{}_J \phi^J$, where $O^I{}_J$ is an $SO(3)$ matrix, as well as spatial rotations. We will see that this action reappears in unexpected contexts throughout the following sections. Note that under this rescaling, we have the VEV $\langle \phi^I \rangle = \alpha' x^I$, where $\alpha' = \sqrt{\frac{m^2}{3\lambda}} \alpha$.

Let us now consider the behaviors of phonons in this low-energy effective theory. Phonons

are introduced in the usual manner, by fluctuating the ϕ^I scalar fields about the ground state configuration. Letting $\phi^I = \alpha' \left(x^I + \pi^I\right)$ as before, and recalling that $X = -\dot{\boldsymbol{\phi}}^2 + (\partial_i \phi_j)^2$, we obtain the phonon action

$$\begin{aligned} S = \frac{\alpha^2(m^2-\alpha^2)}{3\lambda} \int d^4x \left[\frac{1}{2}\dot{\boldsymbol{\pi}}^2 + \frac{1-c_L^2}{2} \left(\boldsymbol{\nabla}\cdot\boldsymbol{\pi}\right)^2 - \frac{1}{2}(\partial_i \pi_j)^2 \right. \\ \left. - \frac{1-c_L^2}{2} \left(\boldsymbol{\nabla}\cdot\boldsymbol{\pi}\right) \dot{\boldsymbol{\pi}}^2 + \frac{1-c_L^2}{2} \left(\boldsymbol{\nabla}\cdot\boldsymbol{\pi}\right) \left(\partial_i \pi_j\right)^2 \right]. \end{aligned} \tag{324}$$

From the first line of Eq. (324) we can immediately see that the longitudinal (L) and transverse (T) velocities of sound are

$$c_L^2 = 1 - \frac{2\alpha^2}{3(m^2-\alpha^2)}\,, \quad c_T^2 = 1\,. \tag{325}$$

Indeed, this is a theory of a highly peculiar isotropic solid in which the transverse excitations propagate luminally, while the longitudinal phonons always propagate at a different velocity, since we always have $\alpha^2 > 0$. The inequality of Eq. (88) is not satisfied by the velocities of sound in this case. Moreover, requiring stability and subluminality of the longitudinal modes produces additional constraints on the parameters of the theory; in particular, we have the conditions

$$\frac{3}{5}m^2 > \alpha^2 > 0\,, \quad \lambda_1 + 2\lambda_2 > 0\,. \tag{326}$$

As we will show below, these conditions are consistent with those that are found by requiring the stability of the UV theory. The luminal speed of transverse excitations is a direct consequence of the fact that the effective action in Eq. (323) depends only on the trace of B^{IJ}. In order for the transverse sound speed to be subluminal, the effective action must include other linearly independent $SO(3)$ invariants, such as $\mathrm{tr}\, B^2$ and $\mathrm{tr}\, B^3$. Integrating out heavy modes from the theory that we started with in Eq. (310) does not produce any additional terms of that sort in the effective action after we take the isotropic limit.

Let us briefly turn back to the UV theory that we started with and consider what its stability implies for the allowed regions of the parameter space $\{\lambda_1, \lambda_2, m^2, \alpha^2\}$. Substituting the (non-rescaled) VEV $\langle \phi^I \rangle = \alpha x^I$ into the equation of motion for the radial modes, Eq. (315), we find that on the background,

$$\langle \rho_I^2 \rangle = \frac{m^2 - \alpha^2}{\lambda_1 + 2\lambda_2} \tag{327}$$

for all $I = 1, 2, 3$. The internal consistency of our analysis and stability of the UV theory then requires that this VEV be strictly positive. The requirement of positivity can be achieved in three different ways:

1. $m^2 > \alpha^2 > 0$ and $\lambda_1 + 2\lambda_2 > 0$: In this situation, the $\alpha^2 \to 0$ limit (in which the solid background is not present) is stable against perturbations. Since we have $m^2 > 0$, spontaneous symmetry breaking occurs in the UV theory regardless of the value of α^2. Increasing the value of α^2, which is positive by definition, reduces the value of the VEV of the radial modes, thus driving the fields closer to the center of the Mexican hat-like radial potential.

2. $\alpha^2 > m^2 > 0$ and $\lambda_1 + 2\lambda_2 < 0$: In this case, taking the limit $\alpha^2 \to 0$ also results in $m^2 \to 0$. The vacuum in this limit is not perturbatively stable. This case is not a viable one for achieving positivity and stability in the UV theory.

3. $m^2 < 0$ and $\lambda_1 + 2\lambda_2 < 0$: Although the vacuum in the $\alpha^2 \to 0$ limit is perturbatively stable, the opposite sign of the mass term implies that spontaneous symmetry breaking does not take place; $\langle \phi^I \rangle = \alpha x^I$ is no longer an actual VEV, as the potential in this case is unbounded from below.

We can also study the stability of the ground state in the UV theory against small perturbations by considering the mass matrix of the heavy radial modes. A negative eigenvalue in the mass matrix would produce an instability of the low-energy effective theory that

results from integrating out the radial modes. The mass matrix is readily calculated from the Lagrangian:

$$M_{IJ}^{(\rho)} = -\frac{1}{2}\frac{\partial^2 \mathcal{L}}{\partial \rho_I \partial \rho_J} = 2\langle \rho_I^2 \rangle \Lambda^{IJ} \,. \tag{328}$$

(No summation is implied over repeated indices in the above expression.) Since we have already established that the VEV of ρ_I^2 must be strictly positive, the mass matrix of the radial modes will have all positive eigenvalues as long as the matrix $\mathbf{\Lambda}$, defined in Eq. (313), also has all positive eigenvalues. The eigenvalues of $\mathbf{\Lambda}$ are precisely $\lambda_1 - \lambda_2$ (doubly degenerate) and $\lambda_1 + 2\lambda_2$. Therefore, we see that requiring positive eigenvalues of the mass matrix of radial modes eliminates all possibilities except the first one for achieving positivity of the VEV $\langle \rho_I^2 \rangle$—the case where $m^2 > \alpha^2 > 0$ and $\lambda_1 + 2\lambda_2 > 0$. Since in the isotropic limit, $\lambda_1 + 2\lambda_2 \ll \lambda_1 - \lambda_2$, there is no trouble with the other eigenvalue. The condition $m^2 > \alpha^2 > 0$ is less stringent than the tachyon-free condition, Eq. (325), in the low-energy effective theory of phonons; stability of the UV theory guarantees subluminality of longitudinal modes in the low-energy theory.

One question that arises from this analysis is whether the regime in which the theory is approximately isotropic corresponds to a natural choice of couplings, in the sense that fine-tuning in the UV theory is not required to achieve the inequality $\lambda_1 + 2\lambda_2 \ll \lambda_1 - \lambda_2$. In a subsequent section—see Section 5.5—we will consider this question in more detail. It turns out that the choice of couplings that leads to approximate isotropy in the low-energy effective theory is not entirely natural, but there are subtleties arising from a highly unusual renormalization group (RG) flow in the UV theory of the cubic solid. We will return to this matter.

5.3 Flat Limit of a Spherical Solid

In this section, we will consider a different possible UV theory of a solid. Inspired by the setup of Esposito *et al.* [150], we will study a theory of a homogeneous and isotropic solid living on a three-dimensional hypersurface of a 3-sphere with radius r. By focusing in on a small patch of the surface that is much smaller in extent than the radius r of the 3-sphere (formally, taking the limit of large radius r), we hope to obtain an effective theory of an isotropic solid in flat three-dimensional space. We will now build the UV theory from an $SO(4)$ multiplet of complex scalar fields Φ^I that live in this space. The action must be invariant under $SO(4)$ spatial rotations, since the isometry group of the 3-sphere is $SO(4)$, as well as internal rotations of the Φ^I fields, which are in the fundamental representation of the internal $SO(4)$ symmetry group. In this case, the overall symmetry-breaking pattern of a solid on a hypersurface of the 3-sphere is $SO(4) \times SO(4) \to SO(4)$. Throughout this section, we will use upper-case Latin indices $I, J, \ldots$ to represent indices ranging over $1, 2, 3, 4$, while lower-case indices $i, j, \ldots$ range over $1, 2, 3$.

We choose to describe the curved space we are considering using the round metric on the 3-sphere,

$$ds^2 = -dt^2 + r^2 \left[d\theta_1^2 + \sin^2 \theta_1 \left(d\theta_2^2 + \sin^2 \theta_2 d\theta_3^2 \right) \right] , \tag{329}$$

where θ_1 and θ_2 range over $[0, \pi)$ and θ_3 ranges over $[0, 2\pi)$. Our starting point will be the most general action of a renormalizable theory with Lorentz invariance and internal $SO(4)$ symmetry:

$$S = - \int dt \, d^3\theta \, \sqrt{-g} \left[\frac{1}{2} \left| \partial \mathbf{\Phi} \right|^2 - \frac{m^2}{2} \left| \mathbf{\Phi} \right|^2 + \frac{\lambda}{4} \left| \mathbf{\Phi} \right|^4 \right] . \tag{330}$$

Derivatives ∂_i are taken with respect to the angular coordinates θ_i for $i = 1, 2, 3$. Again, we have chosen the sign of the mass term for convenience in implementing symmetry breaking.

With this choice, if m^2 and λ are positive, the ground state of the complex scalar fields spontaneously breaks internal and spatial rotational symmetry down to a diagonal subgroup by picking out a particular direction; if m^2 is negative, $SO(4) \times SO(4)$ symmetry is not broken spontaneously.

When spontaneous symmetry breaking occurs, the VEV of the scalar fields $\mathbf{\Phi}(\boldsymbol{\theta}, t)$ becomes aligned with some direction $\hat{\mathbf{r}}(\boldsymbol{\theta})$. We choose to express this VEV as

$$\langle \mathbf{\Phi}(\boldsymbol{\theta}, t) \rangle = \bar{\rho} \hat{\mathbf{r}}(\boldsymbol{\theta}) = \bar{\rho} \mathbf{R}(\boldsymbol{\theta}) \cdot \hat{\mathbf{x}}_4 \,, \tag{331}$$

where $\mathbf{R}(\boldsymbol{\theta})$ is an $SO(4)$ rotation matrix. If we represent the generators of $SO(4)$ by $T^{IJ}_{KL} = \delta^I_K \delta^J_L - \delta^I_K \delta^J_L$, then we can write any general $SO(4)$ rotation as

$$\mathbf{R}(\boldsymbol{\theta}) = \exp\left[\left(\theta_3 - \frac{\pi}{2}\right) \mathbf{T^{34}}\right] \exp\left[\left(\theta_2 - \frac{\pi}{2}\right) \mathbf{T^{24}}\right] \exp\left[\left(\theta_1 - \frac{\pi}{2}\right) \mathbf{T^{14}}\right] . \tag{332}$$

Substituting the VEV in Eq. (331) into the equations of motion for $\mathbf{\Phi}$ gives

$$\bar{\rho}^2 = \frac{m^2 - 3/r^2}{\lambda} \,. \tag{333}$$

Note that this expression is always positive if m^2 and λ are also positive in the large radius limit ($r \gg 1/m$), which we ultimately wish to implement. Although $\bar{\rho}^2$ becomes negative when $r < \sqrt{3}/m$, we are not interested in this regime. As before, we can decompose the fields $\mathbf{\Phi}$ into a heavy radial mode ρ and three light angular modes ϕ_i by writing

$$\mathbf{\Phi}(\boldsymbol{\theta}, t) = \mathbf{R}\left[\mathbf{\Theta}(\boldsymbol{\theta}, t)\right] \cdot \boldsymbol{\rho}(\boldsymbol{\theta}, t) \,, \tag{334}$$

where we defined

$$\boldsymbol{\rho}(\boldsymbol{\theta}, t) \equiv \rho(\boldsymbol{\theta}, t) \hat{\mathbf{x}}_4 \,, \quad \Theta_i(\boldsymbol{\theta}, t) \equiv \frac{\pi}{2} - \phi_i(\boldsymbol{\theta}, t) \,. \tag{335}$$

In the ground state, we have $\langle\rho\rangle = \bar{\rho}$ and $\langle\phi_i\rangle = \frac{\pi}{2} - \theta_i$. In order to integrate out the heavy mode, it is useful to introduce a "covariant derivative" $(\mathbf{D}_\mu)_{IJ} = \partial_\mu \delta_{IJ} + (\mathbf{R}^{-1} \cdot \partial_\mu \mathbf{R})_{IJ}$. With this notation, we can rewrite the action of Eq. (330) in the form

$$\begin{aligned} S &= -\int dt\, d^3\theta\, \sqrt{-g} \left[\frac{1}{2} \left| \mathbf{D}(\boldsymbol{\Theta}) \cdot \boldsymbol{\rho} \right|^2 - \frac{m^2}{2}\rho^2 + \frac{\lambda}{4}\rho^4 \right] \\ &= -\int dt\, d^3\theta\, \sqrt{-g} \left\{ \frac{1}{2}(\partial\rho)^2 + \frac{1}{2}\rho^2 \left[\partial \mathbf{R}^{-1}(\boldsymbol{\Theta}) \cdot \partial \mathbf{R}(\boldsymbol{\Theta}) \right]_{44} - \frac{m^2}{2}\rho^2 + \frac{\lambda}{4}\rho^4 \right\} . \end{aligned} \tag{336}$$

Now, our goal is to integrate out the heavy radial degree of freedom ρ and take the large radius limit to obtain a low-energy effective theory of a flat isotropic solid. At low energies, we can neglect the kinetic energy of the radial mode and vary the action of Eq. (336) with respect to ρ^2 to find the approximate classical solution to the equation of motion of the radial mode. This procedure yields

$$\rho^2 \simeq \frac{m^2 - \left[\partial \mathbf{R}^{-1}(\boldsymbol{\Theta}) \cdot \partial \mathbf{R}(\boldsymbol{\Theta}) \right]_{44}}{\lambda} . \tag{337}$$

To a first approximation at low energy, the effective action for angular modes $\boldsymbol{\phi}$ that results from substituting this classical solution back into Eq. (336) is

$$S_{\text{eff}} \simeq -\int dt\, d^3\theta\, \sqrt{-g} \left\{ \frac{m^2}{2\lambda} \left(\partial \mathbf{R}^{-1} \cdot \partial \mathbf{R} \right)_{44} - \frac{1}{4\lambda} \left[\left(\partial \mathbf{R}^{-1} \cdot \partial \mathbf{R} \right)_{44} \right]^2 \right\} , \tag{338}$$

where the rotation matrices $\mathbf{R}$ are understood to be functions of $\boldsymbol{\Theta}(\boldsymbol{\phi})$.

We have not done anything yet to restrict to a small approximately flat patch of the three-dimensional hypersurface, which formally corresponds to taking the large radius limit. We therefore focus on a small region of the hypersurface much smaller than r in diameter[11]. We also change coordinates via $\theta_i = \frac{\pi}{2} - \frac{x_i}{r}$, where x_i are coordinates in the three-dimensional

[11] One need not worry about contributions of boundary terms to the action when changing the limits of integration, since any boundary terms will be sub-leading in the large radius limit. If the diameter of the flat patch is of order $\bar{x}$, any contributions from boundary terms will be of order $\mathcal{O}(\bar{x}^2/r^2)$.

tangent space at the center of the small patch. We perform an expansion in powers of $\frac{x_i}{r}$ when $|\mathbf{x}| \ll r$, which amounts to taking the large radius limit. The induced metric in the patch becomes Minkowski to leading order, $g_{\mu\nu} = \eta_{\mu\nu} + \mathcal{O}(x^2/r^2)$, allowing us to map the approximately flat patch directly onto the flat tangent space. We are not actually taking the $r \to \infty$ limit, however, since the free parameter r^{-1} plays a role analogous to the parameter α in the theory of the cubic solid; it must be finite and positive, and its value is related to the precise boundary conditions we use in this procedure. Expanding the rotation matrices in this limit gives $\mathbf{R}(\boldsymbol{\Theta}) = \mathbb{1} - \phi_i(\mathbf{x}, t)\mathbf{T}^{i4} + \mathcal{O}(x^2/r^2)$, so we find

$$\left[\partial \mathbf{R}^{-1}(\boldsymbol{\Theta}) \cdot \partial \mathbf{R}(\boldsymbol{\Theta})\right]_{44} \to X + \mathcal{O}(x^2/r^2)\,, \tag{339}$$

where $X = \eta^{\mu\nu}\partial_\mu \boldsymbol{\phi} \cdot \partial_\nu \boldsymbol{\phi}$. Let us now canonically normalize the fields ϕ_i by performing the rescaling $\boldsymbol{\phi} \to \sqrt{\frac{\lambda}{m^2}}\boldsymbol{\phi}$. This has the effect of transforming the effective action in Eq. (338) into a much more familiar form,

$$S_{\text{eff}} \simeq -\int d^4x \left[\frac{1}{2}X - \frac{\lambda}{4m^4}X^2\right], \tag{340}$$

where we kept only the leading-order contribution in the large radius limit. This is precisely the same effective action that we found in Eq. (323) for the isotropic limit of the cubic solid; the resulting effective theory is identical.

We can expand in small fluctuations about the ground state in the usual way to find the effective action for phonons in this theory, $\phi_i = (x_i + \pi_i)/r'$, where $r' = \sqrt{\frac{\lambda}{m^2}}r$. Upon identifying $r^{-1} \sim \alpha$, the resulting phonon action will be identical to Eq. (324), up to an overall normalization constant. The dynamics of phonons are unchanged; in this case, we also have luminal propagation of transverse modes and subluminal longitudinal modes. The values of the velocities of sound are again given by Eq. (325), and much of the stability analysis carries through with little modification. In this case, we have $m^2 > 3/r^2 > 0$ and $\lambda > 0$ as stability criteria of the UV theory. This also ensures that the longitudinal sound

speed

$$c_L^2 = 1 - \frac{2}{3(m^2 r^2 - 1)} \tag{341}$$

remains subluminal in the low-energy effective theory of phonons. In fact, we now have the added condition that $c_L^2 > 2/3$, which means that the longitudinal excitations are quite relativistic.

5.4 Wigner–Inönü Group Contraction of an $SO(4)$ Theory

We will now present a third method of obtaining a UV theory that exhibits the same symmetry-breaking pattern as a solid using a procedure known as Wigner–Inönü group contraction [155], which allows one to start from the Lie algebra of the $SO(4)$ group and take the limit of a certain parameter in order to change the structure constants and obtain the algebra of the $ISO(3)$ group. Let us briefly review how this works. We first separate the generators $\mathbf{T}^{\boldsymbol{IJ}}$ of $SO(4)$ into those that transform as tensors and those that transform as vectors under the subgroup $SO(3)$. We will again use upper-case indices for $1, 2, 3, 4$ and lower-case indices for $1, 2, 3$. The complete commutation relations of the $\mathbf{so}(4)$ algebra can be written as

$$\left[\mathbf{T}^{\boldsymbol{ij}}, \mathbf{T}^{\boldsymbol{kl}}\right] = \delta^{ik}\mathbf{T}^{\boldsymbol{jl}} + \delta^{jl}\mathbf{T}^{\boldsymbol{ik}} - \delta^{il}\mathbf{T}^{\boldsymbol{jk}} - \delta^{jk}\mathbf{T}^{\boldsymbol{il}}\,, \tag{342}$$

$$\left[\mathbf{T}^{\boldsymbol{ij}}, \mathbf{T}^{\boldsymbol{k4}}\right] = \delta^{ik}\mathbf{T}^{\boldsymbol{j4}} - \delta^{jk}\mathbf{T}^{\boldsymbol{i4}}\,, \tag{343}$$

$$\left[\mathbf{T}^{\boldsymbol{i4}}, \mathbf{T}^{\boldsymbol{j4}}\right] = \mathbf{T}^{\boldsymbol{ij}}\,. \tag{344}$$

The idea of Wigner–Inönü group contraction in this case is that if we rescale the generator $\mathbf{T}^{\boldsymbol{i4}} = \zeta\mathbf{P}^{\boldsymbol{i}}$ and formally take the limit $\zeta \to \infty$, then the $\mathbf{so}(4)$ algebra becomes isomorphic to the $\mathbf{iso}(3)$ algebra upon identifying $\mathbf{P}^{\boldsymbol{i}}$ as the generators of shifts and $\mathbf{T}^{\boldsymbol{ij}}$ as the generators of $SO(3)$ rotations.

The UV theory that we will now consider lives in flat (Minkowski) space-time with $3+1$ dimensions from the outset, and the $SO(4)$ symmetry will be only an internal symmetry. We take Φ^I to be a set of scalar fields in the fundamental representation of $SO(4)$. We start with the same action as in the case of the solid on the sphere, except the background space-time

is now flat:

$$S = -\int d^4x \left[\frac{1}{2}\left|\partial\mathbf{\Phi}\right|^2 - \frac{m^2}{2}\left|\mathbf{\Phi}\right|^2 + \frac{\lambda}{4}\left|\mathbf{\Phi}\right|^4\right] . \tag{345}$$

This is the most general renormalizable action for the $SO(4)$ multiplet $\mathbf{\Phi}$ that is invariant under internal $SO(4)$ rotations. Under the action of an $SO(4)$ transformation with rescaled generators and transformation parameters θ^{IJ}, the multiplet Φ^I transforms as

$$\Phi^i \to \Phi^i + \theta^{ji}\Phi^j - \frac{1}{\zeta}\theta^{i4}\Phi^4 , \tag{346}$$

$$\Phi^4 \to \Phi^4 + \frac{1}{\zeta}\theta^{i4}\Phi^i . \tag{347}$$

We can decompose the fields Φ^I into a single heavy mode ρ and three light modes ϕ_i by taking $\Phi^i(x) = \rho(x)\phi_i(x)$ and $\Phi^4(x) = \zeta\rho(x)$, where neither ρ nor ϕ_i depends implicitly on the large parameter ζ. From Eq. (346), we see that like the co-moving coordinates of a solid, the fields ϕ_i transform as vectors under $ISO(3)$, with the transformation parameters θ^{ji} and θ^{i4} associated with spatial rotations and constant shifts, respectively. If we formally take the limit $\zeta \to \infty$, then the field ρ becomes an $ISO(3)$ scalar, provided that it does not scale with ζ in any way; clearly it is invariant under the modified $SO(4)$ transformation up to order $\mathcal{O}(1/\zeta^2)$.

Returning now to the original action Eq. (345), we proceed by breaking the internal $SO(4)$ symmetry with a large VEV, $\langle\mathbf{\Phi}\rangle = \zeta\bar{\rho}\hat{\mathbf{x}}_4$. Substituting this VEV back into the equations of motion derived from Eq. (345) gives $\bar{\rho} = \sqrt{m^2/(\lambda\zeta^2)}$ as the value of the heavy mode in the ground state of the solid. Since we want the VEV of the heavy mode ρ to be of order $\mathcal{O}(\zeta^0)$, so that it scales independently of the large group contraction parameter, we must rescale the Lagrangian parameters m^2 and λ in such a manner that the combination m^2/λ is of order $\mathcal{O}(\zeta^2)$. In order to integrate out the heavy mode, it will be convenient to

rewrite the fields Φ^I as follows:

$$\boldsymbol{\Phi}(x) = \zeta \boldsymbol{\mathcal{O}}(x) \cdot \boldsymbol{\rho}(x)\,, \tag{348}$$

$$\boldsymbol{\mathcal{O}}(x) \equiv \exp\left[-\frac{1}{\zeta}\phi_i(x)\mathbf{T}^{\boldsymbol{i4}}\right]\,, \tag{349}$$

where we again defined the vector $\boldsymbol{\rho}(x) \equiv \rho(x)\hat{\mathbf{x}}_4$. Just as we did in the case of the solid on the sphere, we can define a covariant derivative $(\mathbf{D}_\mu)_{ij} \equiv \partial_\mu \delta_{ij} + \left(\boldsymbol{\mathcal{O}}^{-1} \cdot \partial_\mu \boldsymbol{\mathcal{O}}\right)_{ij}$ and use it to rewrite the action as

$$\begin{aligned} S &= -\zeta^2 \int d^4x \, \left[\frac{1}{2}\left|\mathbf{D}(\boldsymbol{\phi}) \cdot \boldsymbol{\rho}\right|^2 - \frac{m^2}{2}\rho^2 + \frac{\lambda\zeta^2}{4}\rho^4\right] \\ &= -\zeta^2 \int d^4x \, \left[\frac{1}{2}(\partial\rho)^2 + \frac{1}{2}\rho^2\left(\partial\boldsymbol{\mathcal{O}}^{-1} \cdot \partial\boldsymbol{\mathcal{O}}\right)_{44} - \frac{m^2}{2}\rho^2 + \frac{\lambda\zeta^2}{4}\rho^4\right]\,. \end{aligned} \tag{350}$$

After neglecting the kinetic term of the heavy mode at low energy and integrating it out, we find the effective action for $\boldsymbol{\phi}$,

$$S_{\text{eff}} \simeq -\int d^4x \, \left\{\frac{m^2}{2\lambda}\left(\partial\boldsymbol{\mathcal{O}}^{-1} \cdot \partial\boldsymbol{\mathcal{O}}\right)_{44} - \frac{1}{4\lambda}\left[\left(\partial\boldsymbol{\mathcal{O}}^{-1} \cdot \partial\boldsymbol{\mathcal{O}}\right)_{44}\right]^2\right\}\,. \tag{351}$$

Finally, we let $\zeta \gg 1$ and expand in inverse powers of ζ, in order to recover an $ISO(3)$ symmetry in the effective action. In the large ζ limit, to leading order we have

$$\left(\partial\boldsymbol{\mathcal{O}}^{-1} \cdot \partial\boldsymbol{\mathcal{O}}\right)_{44} \simeq \frac{1}{\zeta^2}X\,, \tag{352}$$

where $X = \partial_\mu\boldsymbol{\phi}\cdot\partial^\mu\boldsymbol{\phi}$ as usual. The next correction is of order $\mathcal{O}(1/\zeta^3)$ and can be neglected. Before simply substituting Eq. (352) back into the effective action Eq. (351), however, we must remember that the parameters m^2 and λ are not independent of ζ, so it is necessary to consider the large ζ limit more carefully. We can remove dependence on ζ by rescaling the parameters: $m^2 = \tilde{m}^2\zeta^a$ and $\lambda = \tilde{\lambda}\zeta^b$. The rescaled mass $\tilde{m}$ and coupling $\tilde{\lambda}$ do not depend on ζ, while a and b are exponents that must be determined. We already established that

$m^2/\lambda \sim \zeta^2$, so $a - b = 2$. The first term in the effective action Eq. (351) therefore starts at order $\mathcal{O}(\zeta^0)$, while the second term goes as $\mathcal{O}\left(\zeta^{-b-4}\right)$. The only choice that keeps the second term finite and of the same order as the kinetic energy is $b = -4$ and $a = -2$. Any other choice leads to a trivial effective theory. After rescaling the fields $\phi_i \to \sqrt{\tilde{\lambda}/\tilde{m}^2}\phi_i$ so that they are canonically normalized, the effective action takes on the familiar form

$$S_{\text{eff}} = -\int d^4x \left[\frac{1}{2}X - \frac{\tilde{\lambda}}{4\tilde{m}^4}X^2\right] + \mathcal{O}(1/\zeta^2)\,, \tag{353}$$

matching the low-energy theories found in Eqs. (323) and (340) up to renaming of the parameters λ and m. Introducing fluctuations about the VEV via $\phi_i = \alpha(x_i + \pi_i)$ leads to the same low-energy effective theory of phonons in the solid as we found in Eq. (324), and the sound velocities are the unchanged. The longitudinal modes are subluminal as long as $\tilde{m}^2 > \alpha^2 > 0$ and $\tilde{\lambda} > 0$, conditions that are guaranteed by the stability of the UV theory from which we began our analysis.

5.5 Puzzles of the Cubic Solid: Naturalness and Renormalization

In this section, we revisit the theory of the cubic solid that we analyzed in Section 5.2. Our goal here will be to study the isotropic regime and understand whether the isotropic limit

$$\lambda_1 + 2\lambda_2 \ll \lambda_1 - \lambda_2 \tag{354}$$

is natural, *i.e.* the extent to which it may require fine-tuning of parameters in the UV theory. From the point of view of the low-energy effective field theory of phonons in the isotropic limit, there are no terms that spoil isotropy, nor any mechanism for generating further anisotropic terms. However, the running of coupling constants in the UV theory may well spoil the limit in Eq. (354), rendering it unstable and adding anisotropic terms to the effective theory that would have to be removed via a fine-tuning of coupling parameters. If the isotropic limit does turn out to be stable, how does it emerge from the UV theory? We will now consider such questions.

The most straightforward way to approach this issue is to simply compute the beta functions of the coupling constants in the UV theory. This is done in Section C. If we define

$$\begin{aligned} \lambda &\equiv \frac{\lambda_1 + 2\lambda_2}{6}\,, \quad \beta \equiv \frac{d\lambda}{d\log\mu}\,, \\ \lambda' &\equiv \lambda_1 - \lambda_2\,, \quad \beta' \equiv \frac{d\lambda'}{d\log\mu}\,, \end{aligned} \tag{355}$$

where μ is a running energy scale, then the leading-order beta functions associated with these couplings are found to be

$$\beta = \frac{63\lambda^2 + 6\lambda\lambda' + \lambda'^2}{36\pi^2}\,, \tag{356}$$

$$\beta' = \frac{3\lambda'(4\lambda + \lambda')}{8\pi^2}\,. \tag{357}$$

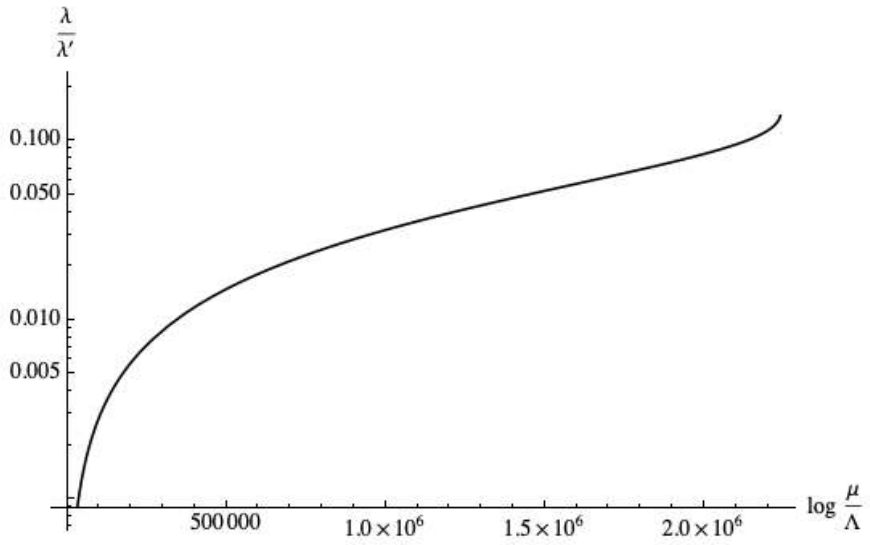

Figure 12: Ratio between the couplings λ and λ', calculated numerically from Eqs. (386) and (387) with initial values $\lambda(0) = 10^{-12}$, $\lambda'(0) = 10^{-5}$, corresponding to approximately isotropic initial conditions at low energy. Λ is a reference energy scale at which the isotropic limit is a very good approximation—e.g. some scale at which the low-energy effective theory of phonons in the isotropic solid breaks down. Evidently, the running spoils isotropy in the far UV, so fine-tuning is needed, although the deviation from the isotropic limit Eq. (354) is mild over a very large range of energies.

Evidently, the short answer is that the limit $\lambda \ll \lambda'$ is unnatural and requires fine-tuning in the UV. At this order there are no non-trivial fixed points[12]. The beta functions show that the running of λ and λ' will eventually spoil the isotropy condition Eq. (354) at high-enough energies, and this is easily verified numerically—see Fig. 12. Nonetheless, the fact that the isotropic limit is spoiled very mildly over a large range of energies suggests that there may be more to this story.

Recall the action that we found after separating the fields into heavy radial modes and light phases, Eq. (312). It can be written in the form

$$S = -\int d^4x \left[\sum_I (\partial \rho_I)^2 + \sum_I b_I \rho_I^2 + \frac{1}{2} \sum_{I,J} \Lambda_{IJ} \rho_I^2 \rho_J^2 \right] . \tag{358}$$

[12]At two-loop order, however (see Section C), there are three non-trivial fixed points—explicitly, with $\{\lambda, \lambda'\} \simeq \{4.39, 26.3\}$, $\{11.5, 0\}$, and $\{-9.69, 90.6\}$—but there are none with $\lambda = 0$ or $0 < \lambda \ll \lambda'$, corresponding to the isotropic regime.

It will be convenient for us to perform the following field redefinitions involving the heavy radial modes:

$$\xi_1 = \sqrt{\lambda}(\rho_1 + \rho_2 + \rho_3)\,, \quad \xi_2 = \frac{1}{\sqrt{\lambda}}(-\rho_1 + \rho_2)\,, \quad \xi_3 = \frac{1}{\sqrt{\lambda}}(-\rho_1 + \rho_3)\,. \tag{359}$$

With these field redefinitions, we get the following expression for the action:

$$\begin{aligned} S = -\frac{1}{3}\int d^4x \Bigg[& \frac{1}{\lambda}(\partial\xi_1)^2 - \frac{1}{\lambda}\xi_1^2(m^2 - \operatorname{tr} B/3) + \frac{1}{3\lambda}\xi_1^4 - 2\xi_1\xi_2(\operatorname{tr} B/3 - B^{22}) \\ & - 2\xi_1\xi_3(\operatorname{tr} B/3 - B^{33}) + \frac{4(\lambda' + 3\lambda)}{9}\xi_1^2\left(\xi_2^2 + \xi_3^2 - \xi_2\xi_3\right) + 2\lambda(\partial\xi_2)^2 \\ & + 2\lambda(\partial\xi_3)^2 - 2\lambda\partial\xi_2\cdot\partial\xi_3 - \lambda\xi_2^2(2m^2 - \operatorname{tr} B/3 - B^{22}) \\ & - \lambda\xi_3^2(2m^2 - \operatorname{tr} B/3 - B^{33}) + 2\lambda\xi_2\xi_3(m^2 - 2\operatorname{tr} B/3 + B^{11}) \\ & + \frac{2\lambda\lambda'}{9}\xi_1(2\xi_2^3 + 2\xi_3^3 - \xi_2^2\xi_3 - \xi_2\xi_3^2) + \frac{\lambda^2(\lambda' + 12\lambda)}{9}(\xi_2^4 - \xi_3^4)\Bigg] \\ \equiv\ & \lambda^{-1}S_{-1} + \lambda^0 S_0 + \cdots\,, \end{aligned} \tag{360}$$

where the matrix B^{IJ} is defined in the usual way in terms of the light fields ϕ^I. In this action, all the fields are generically of order $\mathcal{O}(\lambda^0)$ with this particular normalization. Although it is a somewhat clunky expression, there are several important points to take note of here. First of all, the leading-order piece S_{-1} that scales as λ^{-1} in the small λ limit is completely isotropic. The first anisotropic terms involving B^{22} and B^{33} start at $\mathcal{O}(\lambda^0)$. There are three massive modes associated with ξ_1, ξ_2, and ξ_3, but their masses are not all of the same order in small λ. This can be seen by studying the equations of motion for the heavy fields ξ_1, ξ_2, and ξ_3 produced by varying this action. If we neglect the kinetic terms at low energy, the equations of motion can be solved order-by-order in powers of the parameter λ. Although there are numerous possible solutions to these equations of motion, we make use of the fact that $\lambda > 0$ to ensure stability and $\rho_I > 0$ by definition. This greatly constrains the solution

space, leading to the unique non-trivial background solutions

$$\bar{\xi}_1 = \sqrt{\frac{3m^2 - \operatorname{tr} B}{2}}\,, \tag{361}$$

$$\bar{\xi}_2 = \frac{3}{\lambda'}\sqrt{\frac{1}{2(3m^2 - \operatorname{tr} B)}}\left(B^{11} - B^{22}\right)\,, \tag{362}$$

$$\bar{\xi}_3 = \frac{3}{\lambda'}\sqrt{\frac{1}{2(3m^2 - \operatorname{tr} B)}}\left(B^{33} - B^{11}\right)\,, \tag{363}$$

Introducing fluctuations about these background solutions via $\xi_i = \bar{\xi}_i + \sigma_i$, we obtain an action for fluctuations of the radial modes of the form

$$\begin{aligned} S[\boldsymbol{\sigma}] \supset -\frac{1}{3}\int d^4x \Bigg\{ & \frac{1}{\lambda}(\partial\sigma_1)^2 + \frac{2(3m^2 - \operatorname{tr} B)}{3\lambda}\sigma_1^2 + \frac{2}{3}\left(5X - 7B^{22} - 8B^{33}\right)\sigma_1\sigma_2 \\ & - \frac{2}{3}\left(7\operatorname{tr} B - 8B^{22} - 13B^{33}\right)\sigma_1\sigma_3 + 2\lambda\left[(\partial\sigma_2)^2 + (\partial\sigma_3)^2 - \partial\sigma_2\cdot\partial\sigma_3\right] \\ & + \frac{2\lambda'(3m^2 - \operatorname{tr} B)}{9}\left(\sigma_2^2 + \sigma_3^2 - \sigma_2\sigma_3\right) + \mathcal{O}(1/\lambda)\left[\sigma_1 \text{ interactions}\right] \\ & + \mathcal{O}(\lambda^0)\left[\text{interactions involving } \sigma_1, \sigma_2, \sigma_3\right] \Bigg\} \left[1 + \mathcal{O}(\lambda)\right] \end{aligned} \tag{364}$$

There is kinetic mixing between the modes σ_2 and σ_3, and mass mixing occurs between all the modes. However, it is apparent that there is a hierarchy between the eigenvalues of the mass matrix. To leading order in small λ, we have

$$m_1^2 \sim m^2\,, \quad m_{23}^2 \sim \frac{\lambda'}{\lambda}m^2 \sim \frac{\lambda'}{\lambda}m_1^2\,. \tag{365}$$

In other words, as long as we are in the isotropic regime $\lambda \ll \lambda'$, the modes σ_2 and σ_3 are much heavier than σ_1. Also, since their kinetic terms appear only in S_1, we can neglect their kinetic energy at scales $\mu \ll \sqrt{\lambda'/\lambda}\, m$ and the fields become non-dynamical. They can be integrated out to yield an effective action for σ_1 and the light fields ϕ_i. The resulting effective action is dominated by the isotropic part S_{-1}, so as long as we stay far below the energy scale m_{23}, isotropy is preserved, even at scales comparable to σ_1, where one of the

radial modes participates in the dynamics. This explains why isotropy is barely spoiled by the running of the coupling constants over an exponentially large range of energies beyond the cutoff of the low-energy phonon theory. There is a quasi-isotropic regime involving one of the three radial modes, σ_1, and fine-tuning to achieve isotropy is only required above much higher energy scales corresponding to the eigenvalues of the mass matrix of the two other modes, σ_2 and σ_3.

As we have seen, this theory exhibits a highly unusual renormalization group flow. Fine-tuning is required in the far UV to enter an approximately isotropic regime. However, two of the three heavy radial modes can be integrated out, so that from the point of view of the "near-UV" theory involving only the lightest of the three radial modes, the isotropic regime $\lambda \ll \lambda'$ becomes "natural." Further renormalization group flow towards the IR does not produce sizable corrections that spoil the isotropic configuration.

5.6 Conclusion and Further Questions

In this section, we studied a number of different renormalizable, Lorentz invariant theories that allow for the spontaneously breaking of spatial rotations and translations, in order to assess whether they can serve as viable UV completions of the effective theory of phonons in a homogeneous, isotropic solid, and in order to find whether such a solid that appears homogeneous at long distances can be described by a state in relativistic quantum field theory that is also homogeneous at short distances, unlike typical solids with which we are familiar in nature. We discovered that such theories can in fact be formulated, but they are quite peculiar solids. In the process, we also managed to shed light on various possible methods to implement the spontaneous symmetry breaking of non-compact translations in a consistent manner. We studied the low-energy limit of three particular theories of homogeneous, isotropic solids and discovered that they all converge on a sort of "theoretical fixed point," a common effective action for phonons with an enhanced symmetry, involving only the invariant structure $X = \operatorname{tr} B^{IJ}$ and its square. The other invariants we considered in Section 2.3, namely $Y \propto \operatorname{tr} B^2$ and $Z \propto \operatorname{tr} B^3$, are absent. As a result, the excitations in the isotropic solid that this theory describes are highly unusual—in particular, the transverse excitations exhibit luminal propagation. Stability of the UV theories always ensures subluminal propagation of the longitudinal phonons.

We also studied how isotropy and homogeneity of the low-energy theory of solids might be spoiled by radiative corrections and the running of couplings from the renormalization of the UV theory. We saw that the isotropic low-energy limit of the cubic solid is not, in fact, stable against anisotropic corrections appearing at high energies, and the theory appears to be unnaturally fine-tuned. Nonetheless, approximate isotropy is preserved over a vast range of energies beyond the cutoff scale of the low-energy effective theory thanks to a hierarchical ordering between the mass matrix eigenvalues of heavy radial modes in the UV theory. Fine-tuning is still required in the far UV, but once isotropy is implemented after integrating out the heaviest of the radial modes, it is preserved by renormalization group flow all the way

down to the IR limit.

It would be interesting to investigate why the common effective theory that we found arises from the simple UV completions that we have considered, and how these UV theories might be deformed in order to produce the operators Y and Z in the low energy limit. In the absence of these invariants, it is impossible to move away from the limit in which transverse excitations propagate at the speed of light. It is unclear what modifications we can make to the UV theories to this end, but we leave this question for future study. We also hope to use these methods and the insights gained from this study to understand how to arrive at UV-completions of other effective theories of condensed matter and how to construct their holographic duals.

6 Summary and Outlook

In this work, we have demonstrated the power of techniques of high-energy physics in answering concrete questions about low-energy phenomena in condensed matter. Effective field theory provides a unified and beautiful approach to studying physical systems on the basis of their symmetries and symmetry-breaking patterns, exploiting the independence of long-wavelength phenomena from short-wavelength degrees of freedom. This allows for simple and efficient calculation of perturbative dynamics in any condensed matter system. The approach is flexible by construction, leaving most parameters of the effective theory to be fixed by measurements, so that it is easy to make contact with experimental research.

We reviewed the effective theories of a variety of condensed matter systems in considerable detail, including superfluids, ordinary fluids, solids, and supersolids. We also integrated vortex lines into the formalism of the effective field theory of superfluids. As a first direct application, we used this theoretical framework to study a very concrete experimental question: at what frequency do vortex lines in trapped ultracold atomic gases tend to precess around the center of an atomic cloud? We used our formalism to work out the precession frequency at different chemical potentials and demonstrated that it matches prior theoretical results from the Gross–Pitaevskii model, as well as experimental measurements of the precession frequency in fermionic superfluid condensates. We found that the precession frequency is logarithmically enhanced when the trapping potential is harmonic, recovering the well-known scaling $\omega_p \sim \Gamma \log(R_\perp/\ell)$, where ω_p is the precession frequency, Γ is the quantized circulation, $R_\perp$ is the transverse size of the atomic cloud, and ℓ is an ultraviolet cutoff length scale comparable to the healing length in the condensate. We extended previous calculations by accounting for the effects of trapping in three dimensions, demonstrating improved agreement with experimental data. As we saw, trapping along the third dimension also allows for kinked configurations of vortex lines. Moreover, we found that our calculations were directly applicable to the behavior of propagating Kelvin waves along vortex lines in trapped condensates, a phenomenon that has not been studied previously using effective field theory.

It turns out that the phonon-mediated interaction between vortex lines and the trapping potential leads to significant modifications in the dispersion relation of Kelvin waves, with distinct dispersive behavior appearing in the case of harmonic and non-harmonic trapping.

As a second case study, we considered a much broader set of questions concerning how gravitational fields affect sound waves in a wide variety of condensed matter systems. By studying non-linear dynamics of phonons, we were able to show that in superfluids, ordinary fluids, and solids, localized sound wave packets have an associated net gravitational mass that travels with them, so that sound waves are both affected by gravity and sources for gravity. In each case, the mass associated with sound waves, calculated as a fraction of the total mass of the medium, is *negative*, meaning that phonons float in a medium stratified under gravity; this has the same effect as acoustic refraction in a medium with a density gradient. The added insight that the associated mass is a gravitational source, and that it is transported by sound waves, is completely novel, however, and rather surprising. The mass of a sound wave packet scales as energy over the velocity of sound squared, and the constant of proportionality is completely determined by the equation of state. We confirmed this effect in several different media, using both field theoretic methods and classical methods, such as Eulerian fluid dynamics and non-linear elasticity theory; clearly, the effect we discovered is not an artifact of mass–energy equivalence in our relativistic EFT framework, nor is it a quantum effect. This is a robust result, and it has potential experimental implications for experiments involving ultracold atomic or molecular condensates, in which the velocity of sound is very low. The effect is also potentially detectable from highly energetic seismic events, and if the relativistic effects were studied in more detail, it could lead to improved understanding of phonon-mediated transport properties in relativistic media under strong gravitational fields, such as nuclear superfluid in neutron stars.

Finally, we turned to the issue of ultraviolet completion of low-energy effective theories of condensed matter and studied how the effective theory of a homogeneous and isotropic solid can be derived from a renormalizable theory that realizes the symmetry-breaking pattern of

a homogeneous solid. We discovered that it is indeed possible to find states that appear to be homogeneous solids at long distances, yet are also homogeneous at short distances, unlike the solids with inhomogeneous microscopic structure commonly found in nature. Due to the distinct challenges associated with the spontaneous breaking of space-time translations, we were forced to consider indirect procedures leading from UV theories to an isotropic flat solid. These included: a specific isotropic limit of a theory of a cubic solid; the flat-space (or large-radius) limit of a hyperspherical solid; and an $SO(4)$ theory that realizes the symmetry-breaking pattern of a solid via Wigner–Inönü group contraction. In each situation, we found a common low-energy effective theory which describes an isotropic solid, but not the standard one found by traditional methods. The limiting low-energy theory is one that has enhanced symmetry and transverse phonons that propagate at the velocity of light. We studied the stability of this effective theory against anisotropic corrections from the renormalization of the cubic solid UV theory, finding that fine-tuning is needed in the far UV, but after integrating out only some of the heavier radial modes, isotropy is preserved by RG flow toward the IR. Questions remain about how this unusual low-energy theory arises, and whether more normal isotropic solids can be realized by some deformations of the UV theories we considered. Nonetheless, we discovered that particular solids that appear homogeneous at long distances can in fact be described by the low-energy limit of a homogeneous state at short distances, and the methods we investigated may prove to be fruitful in further studies of UV completions of effective theories and how the holographic duals of condensed matter systems may be constructed.

Overall, this thesis is just a starting point that opens up many possibilities in the study of condensed matter using EFT methodology. There are numerous possible questions about the dynamics and properties of superfluid condensates, vortices, sound waves, and weakly coupled condensed matter systems that we have not addressed. Most importantly, the flexibility of EFT implies that the same methods we developed in this thesis can be adapted to study physical systems in completely different settings, from inflationary cosmology to

quark matter. What we have been developing, in our modest way, are some building blocks of a unified framework for understanding physics at all energy scales, both high and low.

Appendices

A Mass of Superfluid Sound Waves in the Dual Two-Form Theory

In this appendix, we demonstrate how to find the mass associated with superfluid phonons from the dual theory of a superfluid as a two-form field—see Section 2.1.2. The action expanded to cubic order in bulk fluctuations is given by Eq. (50). From the thermodynamic identifications in Eq. (43), we note that the 00 component of the energy–momentum tensor is simply equal to $T_{00} = -G(Y)$. This can be expanded to quadratic order in the fluctuation fields $\mathbf{A}$ and $\mathbf{B}$. The leading order piece in the non-relativistic limit is $T_{00} = -\bar{w}\boldsymbol{\nabla}\cdot\mathbf{B}$. Additional contributions are suppressed by factors of c_s^2/c^2. We can also use the cubic action to find equations of motion for the bulk fields. The hydrophoton equation of motion is a simple constraint equation, which can be solved to yield

$$\boldsymbol{\nabla}\times\mathbf{A} = \left(1-\frac{c_s^2}{c^2}\right)(\boldsymbol{\nabla}\cdot\mathbf{B})\,\dot{\mathbf{B}} + \mathcal{O}\left(B^3\right)\,. \tag{366}$$

Since $\boldsymbol{\nabla}\times\mathbf{A}$ starts at quadratic order in phonons $\mathbf{B}$, we can neglect it in any expression containing $\left(\dot{\mathbf{B}}-\boldsymbol{\nabla}\times\mathbf{A}\right)^2$. Next, let us consider the equation of motion for the phonon field calculated to quadratic order,

$$\ddot{B}_i - c_s^2\partial_i\boldsymbol{\nabla}\cdot\mathbf{B} = \partial_i\mathcal{F} + \partial_t\mathcal{G}_i\,, \tag{367}$$

where

$$\mathcal{F} = \frac{\bar{g}c_s^2}{2}(\boldsymbol{\nabla}\cdot\mathbf{B})^2 - \frac{1}{2}\left(1-\frac{c_s^2}{c^2}\right)\dot{\mathbf{B}}^2\,, \tag{368}$$

and the precise expression of $\mathcal{G}_i$ is unimportant for our purposes. It is a quadratic combination of fields whose time derivative will vanish once we average the equations of motion over

a long period of time.

We now follow the usual procedure of time averaging the equations of motion and integrating over a volume containing a localized phonon wave packet in order to find the leading-order contribution of the wave packet to the associated mass $M = \left\langle \int T_{00} \right\rangle / c^2$, in the limit $c \to \infty$. We will also express time-averaged, integrated quadratic combinations of fields in terms of the energy of the phonon wave packet, which in this case is

$$E = \frac{\bar{w}}{c^2} \left\langle \int \dot{\mathbf{B}}^2 \right\rangle = \frac{\bar{w} c_s^2}{c^2} \left\langle \int (\boldsymbol{\nabla} \cdot \mathbf{B})^2 \right\rangle . \tag{369}$$

Applying this procedure to Eq. (367), we find

$$\left\langle \int \boldsymbol{\nabla} \cdot \mathbf{B} \right\rangle = -\frac{1}{c_s^2} \left\langle \int \mathcal{F} \right\rangle = \frac{c^2}{2\bar{w} c_s^2} \left(1 - \frac{c_s^2}{c^2} - \bar{g} \right) E \, . \tag{370}$$

Using the expression for the cubic coupling $\bar{g}$ in Eq. (51) and substituting into T_{00}, we immediately find that the mass of the wave packet is

$$M = -\frac{2\bar{n}^2}{c_s^3} \frac{dc_s}{d(\bar{n}^2)} E = -\frac{d \log c_s}{d \log \rho_m} \frac{E}{c_s^2} \, , \tag{371}$$

where we used $\bar{n} \propto \rho_m$. This is the same result we found in Section 4.3 using the scalar field theory to which the two-form theory is dual. This is a useful consistency check to go through.

B Mass of a Single Phonon Quantum State

We can also approach the problem of finding the mass associated with phononic excitations in a superfluid using second quantization formalism. The idea is simple: We quantize the phonon field π, promote T_{00} to an operator as well, and compute its expectation value for a single-phonon quantum state. We define phonon annihilation and creation operators $a_{\mathbf{k}}$ and $a_{\mathbf{k}}^{\dagger}$ that have a commutator with the usual normalization,

$$\left[a_{\mathbf{k}}, a_{\mathbf{k}'}^{\dagger}\right] = (2\pi)^3 2\omega_{\mathbf{k}} \delta^3 \left(\mathbf{k} - \mathbf{k}'\right) . \tag{372}$$

$\omega_{\mathbf{k}}$ is the energy of a phonon with momentum $\mathbf{k}$, determined by the dispersion relation. From the Hamiltonian of the effective theory, which we wrote in Eq. (240), we see that π must have the following expression in terms of these operators

$$\pi\left(\mathbf{x}, t\right) = \frac{c_s}{c\sqrt{\mu n}} \int \frac{d^3k}{(2\pi)^3 2\omega_{\mathbf{k}}} \left[a_{\mathbf{k}} e^{i\mathbf{k}\cdot\mathbf{x} - i\omega_{\mathbf{k}} t} + a_{\mathbf{k}}^{\dagger} e^{-i\mathbf{k}\cdot\mathbf{x} + i\omega_{\mathbf{k}} t}\right] . \tag{373}$$

This expression for the field π can then be substituted into Eq. (35) for T_{00} to quadratic order in π. It is obvious that the expectation value of π for a single phonon state $|\mathbf{k}\rangle = a_{\mathbf{k}}^{\dagger} |0\rangle$ vanishes, so $\langle \mathbf{k}' | \dot{\pi} | \mathbf{k} \rangle$ is equal to zero. The operators $\dot{\pi}^2$ and $(\boldsymbol{\nabla}\pi)^2$ have non-zero expectation values, however. These can be calculated from Eqs. (372) and (373) and integrated over volume to find

$$\int d^3x \, \langle \mathbf{k}' | \dot{\pi}^2 | \mathbf{k} \rangle = \frac{\omega_{\mathbf{k}} c_s^2}{\mu n c^2} \langle \mathbf{k}' | \mathbf{k} \rangle , \tag{374}$$

$$\int d^3x \, \langle \mathbf{k}' | \left(\boldsymbol{\nabla}\pi\right)^2 | \mathbf{k} \rangle = \frac{\omega_{\mathbf{k}}}{\mu n c^2} \langle \mathbf{k}' | \mathbf{k} \rangle . \tag{375}$$

Using these expectation values with Eq. (35) to calculate the expectation value of T_{00} between single phonon states, we once again find the expression

$$\begin{aligned} \int d^3x \, \langle \mathbf{k}' | \, T_{00} \left(\mathbf{x}, t \right) | \mathbf{k} \rangle &= \left(1 - \frac{\mu}{c_s} \frac{dc_s}{d\mu} \right) \omega_{\mathbf{k}} \langle \mathbf{k}' | \mathbf{k} \rangle \\ &\equiv M_{\mathbf{k}} c^2 \langle \mathbf{k}' | \mathbf{k} \rangle \ . \end{aligned} \tag{376}$$

This is completely analogous to Eq. (242), and it leads to the same result in the non-relativistic limit:

$$M_{\mathbf{k}} = - \frac{d \log c_s}{d \log \rho_m} \frac{\omega_{\mathbf{k}}}{c_s^2} \, . \tag{377}$$

This quantity can be interpreted as the mass associated with a single phonon quantum state of momentum $\mathbf{k}$, as long as $c_s \ll c$ and $\mathbf{k}$ is in the phonon region of the excitation spectrum of the superfluid.

C Running of Couplings in the Theory of the Cubic Solid

This appendix will explain how we arrived at the expressions for the beta functions in Eqs. (356) and (357) when studying the renormalization of the theory of the cubic solid. A similar (though somewhat less involved) calculation was carried out in Kleinert & Schulte-Frohlinde [156], and we will follow a similar plan and notation. It is convenient to Euclideanize the action of Eq. (310) and rewrite the complex scalars Φ in terms of pairs of real scalars ϕ: $\Phi^1 = (\phi_1 + i\phi_2)/\sqrt{2}$, $\Phi^2 = (\phi_3 + i\phi_4)/\sqrt{2}$, $\Phi^3 = (\phi_5 + i\phi_6)/\sqrt{2}$. Then forming a multiplet $\boldsymbol{\phi} = \{\phi_1, \phi_2, \ldots, \phi_6\}$, the Euclidean action of the UV theory in $d = 4 - \epsilon$ dimensions, including counterterms, can be written as

$$\begin{aligned} S_E = -\int d^d x_E \Bigg[& \frac{1+\delta_\phi}{2} \sum_i (\boldsymbol{\nabla}\phi_i)^2 + \frac{1+\delta_M}{2} M^2 \boldsymbol{\phi}^2 \\ & + \frac{1+\delta_1}{8} \lambda_1 \tilde{\mu}^\epsilon \left(\phi_1^2 + \cdots + \phi_6^2 + 2\phi_1^2\phi_2^2 + 2\phi_3^2\phi_4^2 + 2\phi_5^2\phi_6^2\right) \\ & + \frac{1+\delta_2}{4} \lambda_2 \tilde{\mu}^\epsilon \left[\left(\phi_1^2 + \phi_2^2\right)\left(\phi_3^2 + \cdots + \phi_6^2\right) + \left(\phi_3^2 + \phi_4^2\right)\left(\phi_5^2 + \phi_6^2\right)\right] \Bigg]. \end{aligned} \tag{378}$$

The Feynman rules of this theory can be expressed succinctly as

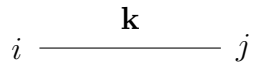

$\sim \quad \delta_{ij} \left(\mathbf{k}^2 + M^2\right)^{-1}$

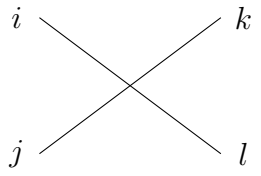

$\sim \quad -\lambda_{ijkl} = \sum_{n=1}^{3} \hat{\lambda}_n \tau^{(n)}_{ijkl} \tilde{\mu}^\epsilon$

$\sim \quad -\delta_{ij}\delta_M M^2$

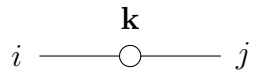

$\sim \quad -\delta_{ij}\delta_\phi \mathbf{k}^2$

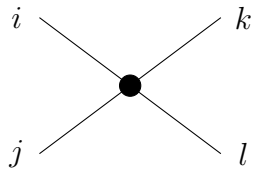

$\sim \quad \sum_{n=1}^{3} \hat{\lambda}_n \hat{\delta}_n \tau^{(n)}_{ijkl} \tilde{\mu}^\epsilon$

We defined $\hat{\lambda}_1 = \hat{\lambda}_2/2 \equiv 3\lambda_1$, $\hat{\lambda}_3 \equiv 6\lambda_2$, $\hat{\delta}_1 = \hat{\delta}_2 \equiv \delta_1$, and $\hat{\delta}_3 \equiv \delta_2$, as well as the tensors

$$\begin{aligned}
\tau^{(1)}_{ijkl} &= \delta^1_i\delta^1_j\delta^1_k\delta^1_l + \delta^2_i\delta^2_j\delta^2_k\delta^2_l + \cdots + \delta^6_i\delta^6_j\delta^6_k\delta^6_l \,, \\
\tau^{(2)}_{ijkl} &= \frac{1}{6}\left(\delta^1_i\delta^1_j\delta^2_k\delta^2_l + \delta^1_i\delta^2_j\delta^1_k\delta^2_l + 4 \text{ permutations}\right) \\
&\quad + (1 \to 3, 2 \to 4) + (1 \to 5, 2 \to 6) \,, \\
\tau^{(3)}_{ijkl} &= \frac{1}{6}\left(\delta^1_i\delta^1_j\delta^3_k\delta^3_l + \delta^1_i\delta^3_j\delta^1_k\delta^3_l + 4 \text{ permutations}\right) + (3 \to 4) + (3 \to 5) \\
&\quad + (3 \to 6) + (1 \to 2, 3 \to 4) + (1 \to 2, 3 \to 5) + (1 \to 2, 3 \to 6) \\
&\quad + (1 \to 6) + (1 \to 6) + (1 \to 5, 3 \to 4) + (1 \to 6, 3 \to 4) \,.
\end{aligned} \tag{379}$$

The two-loop beta functions of the couplings λ_1 and λ_2 can be determined from the counterterms δ_1 and δ_2 in the standard manner (and we work to two-loop order to find possible non-trivial fixed points that are not apparent at one-loop order). We choose to use dimensional regularization and modified minimal subtraction ($\overline{\text{MS}}$). Finding the counterterms to quadratic order in the couplings involves computing the following diagrams:

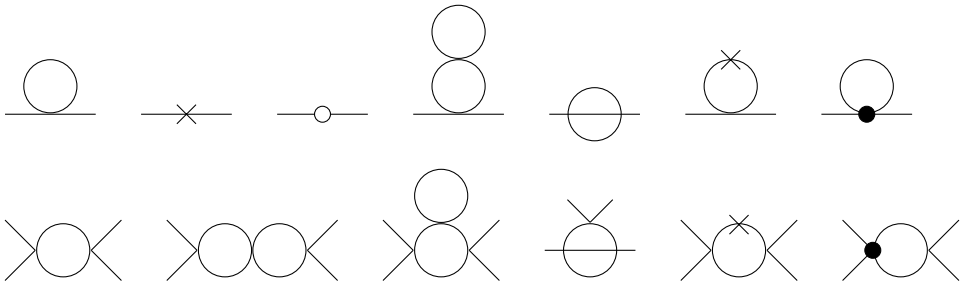

We will spare the reader the tedious details of the calculation, and simply state the resulting counterterms at two-loop order.

$$\delta_M = \frac{\lambda_1 + \lambda_2}{4\pi^2\epsilon} - \frac{13\lambda_1^2 + 8\lambda_1\lambda_2 + 13\lambda_2^2}{128\pi^4\epsilon} + \frac{7\lambda_1^2 + 8\lambda_1\lambda_2 + 7\lambda_2^2}{64\pi^4\epsilon^2} \,, \tag{380}$$

$$\delta_\phi = -\frac{\lambda_1^2 + \lambda_2^2}{256\pi^4\epsilon} \,, \tag{381}$$

$$\lambda_1\delta_1 = \frac{5\lambda_1^2 + 2\lambda_2^2}{8\pi^2\epsilon} - \frac{8\lambda_1^3 + 3\lambda_1\lambda_2^2 + 2\lambda_2^3}{64\pi^4\epsilon} + \frac{25\lambda_1^3 + 18\lambda_1\lambda_2^2 + 6\lambda_2^3}{64\pi^4\epsilon^2} \,, \tag{382}$$

$$\delta_2 = \frac{4\lambda_1 + 3\lambda_2}{8\pi^2\epsilon} - \frac{3\lambda_1^2 + 6\lambda_1\lambda_2 + 4\lambda_2^2}{64\pi^4\epsilon} + \frac{18\lambda_1^2 + 18\lambda_1\lambda_2 + 13\lambda_2^2}{64\pi^4\epsilon^2} \,. \tag{383}$$

It is then straightforward to calculate the two-loop beta functions β_1 and β_2 associated with the couplings λ_1 and λ_2, respectively, from these counterterms. The result is

$$\beta_1 = \frac{5\lambda_1^2 + 2\lambda_2^2}{8\pi^2} - \frac{15\lambda_1^3 + 5\lambda_1\lambda_2^2 + 4\lambda_2^3}{64\pi^4}\,, \tag{384}$$

$$\beta_2 = \frac{4\lambda_1\lambda_2 + 3\lambda_2^2}{8\pi^2} - \frac{5\lambda_1^2\lambda_2 + 12\lambda_1\lambda_2^2 + 7\lambda_2^3}{64\pi^4}\,. \tag{385}$$

Taking an appropriate linear combination of these beta functions to find the running of $\lambda = (\lambda_1 + 2\lambda_2)/6$ and $\lambda' = \lambda_1 - \lambda_2$ yields the expressions

$$\beta = \frac{63\lambda^2 + 6\lambda\lambda' + \lambda'^2}{36\pi^2} - \frac{2592\lambda^3 + 396\lambda^2\lambda' + 147\lambda\lambda'^2 + 20\lambda'^3}{1728\pi^4}\,, \tag{386}$$

$$\beta' = \frac{3\lambda'(4\lambda + \lambda')}{8\pi^2} - \frac{\lambda'(1008\lambda^2 + 384\lambda\lambda' + 43\lambda'^2)}{576\pi^4}\,. \tag{387}$$

References

[1] A. Esposito, R. Krichevsky, and A. Nicolis. "Vortex precession in trapped superfluids from effective field theory." *Physical Review A*, Sep 2017. **96**: 033615. doi:10.1103/PhysRevA.96.033615.

[2] A. Esposito, R. Krichevsky, and A. Nicolis. "Gravitational Mass Carried by Sound Waves." *Physical Review Letters*, Mar 2019. **122**: 084501. doi:10.1103/PhysRevLett.122.084501.

[3] D. B. Kaplan. "Effective Field Theories." In "Beyond the Standard Model 5. Proceedings, 5th Conference, Balholm, Norway, April 29-May 4, 1997," 1995 `arXiv:nucl-th/9506035`.

[4] S. Dubovsky, L. Hui, A. Nicolis, and D. T. Son. "Effective field theory for hydrodynamics: Thermodynamics, and the derivative expansion." *Physical Review D*, Apr 2012. **85**: 085029. doi:10.1103/PhysRevD.85.085029.

[5] A. V. Manohar. "Effective field theories." *Lecture Notes in Physics*, 1997. **479**: 311–362. doi:10.1007/BFb0104294.

[6] J. F. Donoghue. "General relativity as an effective field theory: The leading quantum corrections." *Physical Review D*, Sep 1994. **50**: 3874–3888. doi:10.1103/PhysRevD.50.3874.

[7] K. S. Stelle. "Classical gravity with higher derivatives." *General Relativity and Gravitation*, Apr 1978. **9(4)**: 353–371. doi:10.1007/BF00760427.

[8] C. M. Will. "The confrontation between general relativity and experiment." *Living Reviews in Relativity*, Jun 2014. **17(1)**: 4. doi:10.12942/lrr-2014-4.

[9] H. Georgi. "Effective Field Theory." *Annual Review of Nuclear and Particle Science*, 1993. **43(1)**: 209–252. doi:10.1146/annurev.ns.43.120193.001233.

[10] A. Pich. "Effective field theory: Course." In "Probing the Standard Model of Particle Interactions. Proceedings, Summer School in Theoretical Physics, NATO Advanced Study Institute, 68th Session, Les Houches, France, July 28-September 5, 1997. Pt. 1, 2," 1998 pages 949–1049. `arXiv:hep-ph/9806303`.

[11] S. Hartmann. "Effective field theories, reductionism and scientific explanation." *Studies in History and Philosophy of Science Part B: Studies in History and Philosophy of Modern Physics*, 2001. **32(2)**: 267 – 304. doi:10.1016/S1355-2198(01)00005-3.

[12] T. Appelquist and J. Carazzone. "Infrared singularities and massive fields." *Physical Review D*, May 1975. **11**: 2856–2861. doi:10.1103/PhysRevD.11.2856.

[13] Y. Nambu. "Quasi-Particles and Gauge Invariance in the Theory of Superconductivity." *Physical Review*, Feb 1960. **117**: 648–663. doi:10.1103/PhysRev.117.648.

[14] J. Goldstone. "Field theories with superconductor solutions." *Il Nuovo Cimento (1955-1965)*, Jan 1961. **19(1)**: 154–164. doi:10.1007/BF02812722.

[15] J. Goldstone, A. Salam, and S. Weinberg. "Broken Symmetries." *Physical Review*, Aug 1962. **127**: 965–970. doi:10.1103/PhysRev.127.965.

[16] A. Nicolis, R. Penco, F. Piazza, and R. Rattazzi. "Zoology of condensed matter: framids, ordinary stuff, extra-ordinary stuff." *Journal of High Energy Physics*, Jun 2015. **2015(6)**: 155. doi:10.1007/JHEP06(2015)155.

[17] A. Nicolis, R. Penco, F. Piazza, and R. A. Rosen. "More on gapped goldstones at finite density: More gapped goldstones." *Journal of High Energy Physics*, Nov 2013. **2013(11)**: 55. doi:10.1007/JHEP11(2013)055.

[18] E. A. Ivanov and V. I. Ogievetskii. "Inverse Higgs effect in nonlinear realizations." *Theoretical and Mathematical Physics*, Nov 1975. **25(2)**: 1050–1059. doi:10.1007/BF01028947.

[19] A. Nicolis and F. Piazza. "Spontaneous symmetry probing." *Journal of High Energy Physics*, Jun 2012. **2012(6)**: 25. doi:10.1007/JHEP06(2012)025.

[20] A. Nicolis and F. Piazza. "Implications of Relativity on Nonrelativistic Goldstone Theorems: Gapped Excitations at Finite Charge Density." *Physical Review Letters*, Jan 2013. **110**: 011602. doi:10.1103/PhysRevLett.110.011602.

[21] S. Endlich, A. Nicolis, R. Rattazzi, and J. Wang. "The quantum mechanics of perfect fluids." *Journal of High Energy Physics*, 2011. **04**: 102. doi:10.1007/JHEP04(2011)102.

[22] L. P. Kadanoff. "Scaling Laws for Ising Models Near T_c." *Physics*, June 1966. **2(6)**: 263–272. doi:10.1103/PhysicsPhysiqueFizika.2.263.

[23] K. G. Wilson. "Renormalization Group and Critical Phenomena. I. Renormalization Group and the Kadanoff Scaling Picture." *Physical Review B*, Nov 1971. **4**: 3174–3183. doi:10.1103/PhysRevB.4.3174.

[24] K. G. Wilson. "Renormalization Group and Critical Phenomena. II. Phase-Space Cell Analysis of Critical Behavior." *Physical Review B*, Nov 1971. **4**: 3184–3205. doi:10.1103/PhysRevB.4.3184.

[25] K. G. Wilson and M. E. Fisher. "Critical Exponents in 3.99 Dimensions." *Physical Review Letters*, Jan 1972. **28**: 240–243. doi:10.1103/PhysRevLett.28.240.

[26] J. J. M. Carrasco, M. P. Hertzberg, and L. Senatore. "The effective field theory of cosmological large scale structures." *Journal of High Energy Physics*, Sep 2012. **2012(9)**: 82. doi:10.1007/JHEP09(2012)082.

[27] G. Gubitosi, F. Piazza, and F. Vernizzi. "The effective field theory of dark energy." *Journal of Cosmology and Astroparticle Physics*, Feb 2013. **2013(02)**: 032–032. doi:10.1088/1475-7516/2013/02/032.

[28] W. D. Goldberger and I. Z. Rothstein. "Effective field theory of gravity for extended objects." *Physical Review D*, May 2006. **73**: 104029. doi:10.1103/PhysRevD.73.104029.

[29] G. Gabadadze and R. A. Rosen. "Effective field theory for quantum liquid in dwarf stars." *Journal of Cosmology and Astroparticle Physics*, Apr 2010. **2010(04)**: 028–028. doi:10.1088/1475-7516/2010/04/028.

[30] I. Tews, J. Carlson, S. Gandolfi, and S. Reddy. "Constraining the Speed of Sound inside Neutron Stars with Chiral Effective Field Theory Interactions and Observations." *The Astrophysical Journal*, Jun 2018. **860(2)**: 149. doi:10.3847/1538-4357/aac267.

[31] S. C. Zhang, T. H. Hansson, and S. Kivelson. "Effective-Field-Theory Model for the Fractional Quantum Hall Effect." *Physics Review Letters*, Jan 1989. **62**: 82–85. doi:10.1103/PhysRevLett.62.82.

[32] M. Greiter, F. Wilczek, and E. Witten. "Hydrodynamic Relations in Superconductivity." *Modern Physics Letters B*, 1989. **03(12)**: 903–918. doi:10.1142/S0217984989001400.

[33] M. Crossley, P. Glorioso, and H. Liu. "Effective field theory of dissipative fluids." *Journal of High Energy Physics*, Sep 2017. **2017(9)**: 95. doi:10.1007/JHEP09(2017)095.

[34] S. Endlich. *The Effective Field Theory Approach to Fluid Dynamics*. Ph.D. thesis, Columbia University, 2013.

[35] C. Cheung, A. L. Fitzpatrick, J. Kaplan, L. Senatore, and P. Creminelli. "The effective field theory of inflation." *Journal of High Energy Physics*, Mar 2008. **2008(03)**: 014. doi:10.1088/1126-6708/2008/03/014.

[36] S. Weinberg. "Effective field theory for inflation." *Physical Review D*, Jun 2008. **77**: 123541. doi:10.1103/PhysRevD.77.123541.

[37] J. Bloomfield, É. É. Flanagan, M. Park, and S. Watson. "Dark energy or modified gravity? An effective field theory approach." *Journal of Cosmology and Astroparticle Physics*, Aug 2013. **2013(08)**: 010–010. doi:10.1088/1475-7516/2013/08/010.

[38] R. Kase and S. Tsujikawa. "Effective field theory approach to modified gravity including Horndeski theory and Hořava-Lifshitz gravity." *International Journal of Modern Physics D*, 2014. **23(13)**: 1443008. doi:10.1142/S0218271814430081.

[39] E. Braaten. "Effective field theory for plasmas at all temperatures and densities." *Canadian Journal Physics*, 1993. **71(05-06)**: 215–218. doi:10.1139/p93-034.

[40] L. S. Brown and L. G. Yaffe. "Effective field theory for highly ionized plasmas." *Physics Reports*, 2001. **340(1)**: 1 – 164. doi:10.1016/S0370-1573(00)00068-5.

[41] Z.-B. Kang, F. Ringer, and I. Vitev. "Effective field theory approach to open heavy flavor production in heavy-ion collisions." *Journal of High Energy Physics*, Mar 2017. **2017(3)**: 146. doi:10.1007/JHEP03(2017)146.

[42] I. Brivio and M. Trott. "The Standard Model as an effective field theory." *Physics Reports*, 2019. **793**: 1 – 98. doi:10.1016/j.physrep.2018.11.002.

[43] S. Weinberg. *The Quantum Theory of Fields. Vol. 2: Modern Applications*. Cambridge University Press, 2013. ISBN 9781139632478, 9780521670548, 9780521550024.

[44] S. Willenbrock and C. Zhang. "Effective Field Theory Beyond the Standard Model." *Annual Review of Nuclear and Particle Science*, 2014. **64(1)**: 83–100. doi:10.1146/annurev-nucl-102313-025623.

[45] A. Nicolis. "Low-energy effective field theory for finite-temperature relativistic superfluids." 2011. arXiv:hep-th/1108.2513.

[46] D. T. Son. "Low-energy quantum effective action for relativistic superfluids." 2002. arXiv:hep-ph/0204199.

[47] J. Polchinski. *String Theory. Vol. 1: An Introduction to the Bosonic String*. Cambridge Monographs on Mathematical Physics. Cambridge University Press, 2007. ISBN 9780511252273, 9780521672276, 9780521633031. doi:10.1017/CBO9780511816079.

[48] G. P. Lepage. "How to renormalize the Schrödinger equation." In "Nuclear Physics. Proceedings, 8th Jorge Andre Swieca Summer School, Sao Jose dos Campos, Campos do Jordao, Brazil, January 26-February 7, 1997," 1997 pages 135–180. arXiv:nucl-th/9706029.

[49] B. Horn, A. Nicolis, and R. Penco. "Effective string theory for vortex lines in fluids and superfluids." *Journal of High Energy Physics*, 2015. **10**: 153. doi:10.1007/JHEP10(2015)153.

[50] A. Nicolis, R. Penco, and R. A. Rosen. "Relativistic fluids, superfluids, solids, and supersolids from a coset construction." *Physical Review D*, Feb 2014. **89**: 045002. doi:10.1103/PhysRevD.89.045002.

[51] D. Vollhardt and P. Woelfle. "Superfluid Helium 3: Link Between Condensed Matter Physics and Particle Physics." *Acta Physica Polonica B*, December 2000. **31**: 11.

[52] D. T. Son. "Effective Lagrangian and Topological Interactions in Supersolids." *Physical Review Letters*, May 2005. **94**: 175301. doi:10.1103/PhysRevLett.94.175301.

[53] A. F. Andreev and I. M. Lifshitz. "Quantum Theory of Defects in Crystals." *Soviet Physics JETP*, 1969. **29(6)**: 1107–1113. http://www.jetp.ac.ru/cgi-bin/dn/e_029_06_1107.pdf.

[54] L. Landau. "Theory of the Superfluidity of Helium II." *Physical Review*, Aug 1941. **60**: 356–358. doi:10.1103/PhysRev.60.356.

[55] S. Sunakawa, S. Yamasaki, and T. Kebukawa. "Energy Spectrum of the Excitations in Liquid Helium II." *Progress of Theoretical Physics*, Apr 1969. **41(4)**: 919–940. doi:10.1143/PTP.41.919.

[56] S. A. Hartnoll. "Lectures on holographic methods for condensed matter physics." *Class. Quant. Grav.*, 2009. **26**: 224002. doi:10.1088/0264-9381/26/22/224002. arXiv:hep-th/0903.3246.

[57] A. Esposito. *Low energy physics for the high energy physicist - Effective theories, holographic duality and all that*. Ph.D. thesis, Columbia University, 2013.

[58] S. Garcia-Saenz, E. Mitsou, and A. Nicolis. "A multipole-expanded effective field theory for vortex ring-sound interactions." *Journal of High Energy Physics*, Feb 2018. **2018(2)**: 22. doi:10.1007/JHEP02(2018)022.

[59] S. Golkar, M. M. Roberts, and D. T. Son. "The Euler current and relativistic parity odd transport." *Journal of High Energy Physics*, Apr 2015. **2015(4)**: 110. doi:10.1007/JHEP04(2015)110.

[60] L. V. Delacrétaz, A. Nicolis, R. Penco, and R. A. Rosen. "Wess-Zumino Terms for Relativistic Fluids, Superfluids, Solids, and Supersolids." *Physical Review Letters*, Mar 2015. **114**: 091601. doi:10.1103/PhysRevLett.114.091601.

[61] E. Cremmer and J. Scherk. "Spontaneous dynamical breaking of gauge symmetry in dual models." *Nuclear Physics B*, 1974. **72(1)**: 117 – 124. doi:10.1016/0550-3213(74)90224-7.

[62] I. L. Buchbinder, S. D. Odintsov, and I. L. Shapiro. *Effective Action in Quantum Gravity*. 1992.

[63] S. Endlich and A. Nicolis. "The incompressible fluid revisited: vortex-sound interactions." 2013. arXiv:hep-th/1303.3289.

[64] P. C. Hohenberg and B. I. Halperin. "Theory of dynamic critical phenomena." *Reviews of Modern Physics*, Jul 1977. **49**: 435–479. doi:10.1103/RevModPhys.49.435.

[65] J. Ortiz de Zárate and J. Sengers. *Hydrodynamic Fluctuations in Fluids and Fluid Mixtures*. Oxford: Elsevier Science, 1987.

[66] A. H. Taub. "General Relativistic Variational Principle for Perfect Fluids." *Physical Review*, Jun 1954. **94**: 1468–1470. doi:10.1103/PhysRev.94.1468.

[67] N. Andersson and G. L. Comer. "Relativistic fluid dynamics: Physics for many different scales." *Living Reviews in Relativity*, Jan 2007. **10(1)**: 1. doi:10.12942/lrr-2007-1.

[68] R. Jackiw, V. P. Nair, S.-Y. Pi, and A. P. Polychronakos. "Perfect fluid theory and its extensions." *Journal of Physics A: Mathematical and General*, Oct 2004. **37(42)**: R327–R432. doi:10.1088/0305-4470/37/42/r01.

[69] F. M. Haehl, R. Loganayagam, and M. Rangamani. "The fluid manifesto: Emergent symmetries, hydrodynamics, and black holes." *Journal of High Energy Physics*, Jan 2016. **2016(1)**: 184. doi:10.1007/JHEP01(2016)184.

[70] S. Dubovsky, T. Grégoire, A. Nicolis, and R. Rattazzi. "Null energy condition and superluminal propagation." *Journal of High Energy Physics*, Mar 2006. **2006(03)**: 025–025. doi:10.1088/1126-6708/2006/03/025.

[71] S. Grozdanov and J. Polonyi. "Viscosity and dissipative hydrodynamics from effective field theory." *Physical Review D*, May 2015. **91**: 105031. doi:10.1103/PhysRevD.91.105031.

[72] G. Torrieri. "Viscosity of an ideal relativistic quantum fluid: A perturbative study." *Physical Review D*, Mar 2012. **85**: 065006. doi:10.1103/PhysRevD.85.065006.

[73] S. Endlich, A. Nicolis, R. A. Porto, and J. Wang. "Dissipation in the effective field theory for hydrodynamics: First-order effects." *Physical Review D*, Nov 2013. **88**: 105001. doi:10.1103/PhysRevD.88.105001.

[74] S. Endlich, A. Nicolis, and J. Wang. "Solid inflation." *Journal of Cosmology and Astroparticle Physics*, Oct 2013. **2013(10)**: 011–011. doi:10.1088/1475-7516/2013/10/011.

[75] L. D. Landau and E. M. Lifshitz. *Theory of Elasticity*, volume 7 of *Course of Theoretical Physics*. New York: Elsevier Butterworth-Heinemann, 1986. ISBN 9780750626330.

[76] I. A. Todoshchenko, H. Alles, H. J. Junes, A. Y. Parshin, and V. Tsepelin. "Absence of low-temperature anomaly on the melting curve of ^{4}He." *Journal of Experimental and Theoretical Physics Letters*, Jul 2007. **85(9)**: 454–457. doi:10.1134/S0021364007090093.

[77] F. Böttcher, J.-N. Schmidt, M. Wenzel, J. Hertkorn, M. Guo, T. Langen, and T. Pfau. "Transient Supersolid Properties in an Array of Dipolar Quantum Droplets." *Physical Review X*, Mar 2019. **9**: 011051. doi:10.1103/PhysRevX.9.011051.

[78] L. Tanzi, E. Lucioni, F. Famà, J. Catani, A. Fioretti, C. Gabbanini, R. N. Bisset, L. Santos, and G. Modugno. "Observation of a Dipolar Quantum Gas with Metastable Supersolid Properties." *Physical Review Letters*, Apr 2019. **122**: 130405. doi:10.1103/PhysRevLett.122.130405.

[79] L. Chomaz, D. Petter, P. Ilzhöfer, G. Natale, A. Trautmann, C. Politi, G. Durastante, R. M. W. van Bijnen, A. Patscheider, M. Sohmen,

M. J. Mark, and F. Ferlaino. "Long-Lived and Transient Supersolid Behaviors in Dipolar Quantum Gases." *Physical Review X*, Apr 2019. **9**: 021012. doi:10.1103/PhysRevX.9.021012.

[80] M. Celoria, D. Comelli, and L. Pilo. "Fluids, Superfluids and Supersolids: Dynamics and Cosmology of Self Gravitating Media." *Journal of Cosmology and Astroparticle Physics*, 2017. **1709(09)**: 036. doi:10.1088/1475-7516/2017/09/036.

[81] R. J. Donnelly. "Quantized Vortices and Turbulence in Helium II." *Annual Review of Fluid Mechanics*, 1993. **25(1)**: 325–371. doi:10.1146/annurev.fl.25.010193.001545.

[82] G. P. Bewley, D. P. Lathrop, and K. R. Sreenivasan. "Visualization of quantized vortices." *Nature*, September 2006. **441(7093)**: 588. doi:10.1038/441588a.

[83] C. J. Pethick and H. Smith. *Bose–Einstein Condensation in Dilute Gases*. Cambridge University Press, 2nd edition, 2008. 10.1017/CBO9780511802850.

[84] R. Feynman. "Chapter II Application of Quantum Mechanics to Liquid Helium." volume 1 of *Progress in Low Temperature Physics*, pages 17 – 53. Elsevier, 1955. doi:10.1016/S0079-6417(08)60077-3.

[85] W. Thomson (Lord Kelvin). "XXIV. Vibrations of a columnar vortex." *The London, Edinburgh, and Dublin Philosophical Magazine and Journal of Science*, 1880. **10(61)**: 155–168. doi:10.1080/14786448008626912.

[86] L. D. Landau and E. M. Lifshitz. *Fluid Mechanics*. Toronto: Pergamon Press, 2nd edition, 1987.

[87] H. M. Nilsen, G. Baym, and C. J. Pethick. "Velocity of vortices in inhomogeneous Bose–Einstein condensates." *Proceedings of the National Academy of Sciences*, May 2006. **103(21)**: 7978–7981. doi:10.1073/pnas.0602541103.

[88] S. F. Hassan and R. A. Rosen. "Bimetric gravity from ghost-free massive gravity." *Journal of High Energy Physics*, Feb 2012. **2012(2)**: 126. doi:10.1007/JHEP02(2012)126.

[89] D. S. Rokhsar. "Vortex Stability and Persistent Currents in Trapped Bose Gases." *Physical Review Letters*, Sep 1997. **79**: 2164–2167. doi:10.1103/PhysRevLett.79.2164.

[90] E. P. Gross. "Structure of a quantized vortex in boson systems." *Il Nuovo Cimento (1955-1965)*, May 1961. **20(3)**: 454–477. doi:10.1007/BF02731494.

[91] E. P. Gross. "Hydrodynamics of a Superfluid Condensate." *Journal of Mathematical Physics*, 1963. **4(2)**: 195–207. doi:10.1063/1.1703944.

[92] L. P. Pitaevskii. "Vortex Lines in an Imperfect Bose Gas." *Soviet Physics JETP*, Aug 1961. **13(2)**: 451–454. http://jetp.ac.ru/cgi-bin/dn/e_013_02_0451.pdf.

[93] A. L. Fetter and J.-k. Kim. "Vortex Precession in a Rotating Nonaxisymmetric Trapped Bose-Einstein Condensate." *Journal of Low Temperature Physics*, Dec 2001. **125**: 239–248. doi:10.1023/A:1012919924475.

[94] B. Jackson, J. F. McCann, and C. S. Adams. "Vortex line and ring dynamics in trapped Bose-Einstein condensates." *Physical Review A*, Dec 1999. **61**: 013604. doi:10.1103/PhysRevA.61.013604.

[95] A. A. Svidzinsky and A. L. Fetter. "Stability of a Vortex in a Trapped Bose-Einstein Condensate." *Physical Review Letters*, Jun 2000. **84**: 5919–5923. doi:10.1103/PhysRevLett.84.5919.

[96] E. Lundh and P. Ao. "Hydrodynamic approach to vortex lifetimes in trapped Bose condensates." *Physical Review A*, May 2000. **61**: 063612. doi:10.1103/PhysRevA.61.063612.

[97] S. A. McGee and M. J. Holland. "Rotational dynamics of vortices in confined Bose-Einstein condensates." *Physical Review A*, Mar 2001. **63**: 043608. doi:10.1103/PhysRevA.63.043608.

[98] M. R. Matthews, B. P. Anderson, P. C. Haljan, D. S. Hall, C. E. Wieman, and E. A. Cornell. "Vortices in a Bose-Einstein Condensate." *Physical Review Letters*, Sep 1999. **83**: 2498–2501. doi:10.1103/PhysRevLett.83.2498.

[99] B. P. Anderson, P. C. Haljan, C. E. Wieman, and E. A. Cornell. "Vortex Precession in Bose-Einstein Condensates: Observations with Filled and Empty Cores." *Physical Review Letters*, Oct 2000. **85**: 2857–2860. doi:10.1103/PhysRevLett.85.2857.

[100] M. J. H. Ku, W. Ji, B. Mukherjee, E. Guardado-Sanchez, L. W. Cheuk, T. Yefsah, and M. W. Zwierlein. "Motion of a Solitonic Vortex in the BEC-BCS Crossover." *Physical Review Letters*, Aug 2014. **113**: 065301. doi:10.1103/PhysRevLett.113.065301.

[101] T. Yefsah, A. T. Sommer, M. J. H. Ku, L. W. Cheuk, W. Ji, W. S. Bakr, and M. W. Zwierlein. "Heavy solitons in a fermionic superfluid." *Nature*, Jul 2013. **499**: 426 EP –. doi:10.1038/nature12338.

[102] M. H. Anderson, J. R. Ensher, M. R. Matthew, C. E. Wieman, and E. A. Cornell. "Observation of Bose–Einstein Condensation in a Dilute Atomic Vapor." *Science*, Jul 1995. **269(5221)**: 198–201. doi:10.1126/science.269.5221.198.

[103] W. Ketterle. "Nobel lecture: When atoms behave as waves: Bose-Einstein condensation and the atom laser." *Reviews of Modern Physics*, Nov 2002. **74**: 1131–1151. doi:10.1103/RevModPhys.74.1131.

[104] S. Will. Private communication, 2017.

[105] P. G. Kevrekidis, W. Wang, R. Carretero-González, D. J. Frantzeskakis, and S. Xie. "Vortex precession dynamics in general radially symmetric potential traps in two-dimensional atomic Bose-Einstein condensates." *Physical Review A*, Oct 2017. **96**: 043612. doi:10.1103/PhysRevA.96.043612.

[106] T. P. Simula, T. Mizushima, and K. Machida. "Kelvin Waves of Quantized Vortex Lines in Trapped Bose-Einstein Condensates." *Physical Review Letters*, Jul 2008. **101**: 020402. doi:10.1103/PhysRevLett.101.020402.

[107] L. Koens and A. M. Martin. "Perturbative behavior of a vortex in a trapped Bose-Einstein condensate." *Physical Review A*, Jul 2012. **86**: 013605. doi:10.1103/PhysRevA.86.013605.

[108] L. Koens, T. P. Simula, and A. M. Martin. "Vibrations of a columnar vortex in a trapped Bose-Einstein condensate." *Physical Review A*, Jun 2013. **87**: 063614. doi:10.1103/PhysRevA.87.063614.

[109] P. G. Saffman. *Vortex Dynamics*. Cambridge Monographs on Mechanics. Cambridge University Press, 1993. doi:10.1017/CBO9780511624063.

[110] K. W. Schwarz. "Three-dimensional vortex dynamics in superfluid ^{4}He: Line-line and line-boundary interactions." *Physical Review B*, May 1985. **31**: 5782–5804. doi:10.1103/PhysRevB.31.5782.

[111] A. L. Gaunt, T. F. Schmidutz, I. Gotlibovych, R. P. Smith, and Z. Hadzibabic. "Bose-Einstein Condensation of Atoms in a Uniform Potential." *Physical Review Letters*, May 2013. **110**: 200406. doi:10.1103/PhysRevLett.110.200406.

[112] L. Chomaz, L. Corman, T. Bienaimé, R. Desbuquois, C. Weitenberg, S. Nascimbène, J. Beugnon, and J. Dalibard. "Emergence of coherence via transverse condensation in a uniform quasi-two-dimensional Bose gas." *Nature Communications*, Jan 2015. **6**: 6162 EP –. doi:10.1038/ncomms7162.

[113] B. Mukherjee, Z. Yan, P. B. Patel, Z. Hadzibabic, T. Yefsah, J. Struck, and M. W. Zwierlein. "Homogeneous Atomic Fermi Gases." *Physical Review Letters*, Mar 2017. **118**: 123401. doi:10.1103/PhysRevLett.118.123401.

[114] A. Aftalion and T. Riviere. "Vortex energy and vortex bending for a rotating Bose-Einstein condensate." *Physical Review A*, Sep 2001. **64**: 043611. doi:10.1103/PhysRevA.64.043611.

[115] J. J. García-Ripoll and V. M. Pérez-García. "Vortex bending and tightly packed vortex lattices in Bose-Einstein condensates." *Physical Review A*, Oct 2001. **64**: 053611. doi:10.1103/PhysRevA.64.053611.

[116] L. M. Aycock, H. M. Hurst, D. K. Efimkin, D. Genkina, H.-I. Lu, V. M. Galitski, and I. B. Spielman. "Brownian motion of solitons in a Bose–Einstein condensate." *Proceedings of the National Academy of Sciences*, 2017. **114(10)**: 2503–2508. doi:10.1073/pnas.1615004114.

[117] D. K. Efimkin and V. Galitski. "Moving solitons in a one-dimensional fermionic superfluid." *Physical Review A*, Feb 2015. **91**: 023616. doi:10.1103/PhysRevA.91.023616.

[118] R. Liao and J. Brand. "Traveling dark solitons in superfluid Fermi gases." *Physical Review A*, Apr 2011. **83**: 041604. doi:10.1103/PhysRevA.83.041604.

[119] S. Moroz, C. Hoyos, C. Benzoni, and D. T. Son. "Effective field theory of a vortex lattice in a bosonic superfluid." *SciPost Physics*, 2018. **5**: 39. doi:10.21468/SciPostPhys.5.4.039.

[120] G. Baym, C. Pethick, and D. Pines. "Superfluidity in Neutron Stars." *Nature*, 1969. **224(5220)**: 673–674. doi:10.1038/224673a0.

[121] G. Baym and D. Pines. "Neutron starquakes and pulsar speedup." *Annals of Physics*, 1971. **66(2)**: 816 – 835. doi:10.1016/0003-4916(71)90084-4.

[122] P. W. Anderson and N. Itoh. "Pulsar glitches and restlessness as a hard superfluidity phenomenon." *Nature*, 1975. **256(5512)**: 25–27. doi:10.1038/256025a0.

[123] R. I. Epstein and G. Baym. "Vortex pinning in neutron stars." *Astrophysical Journal*, May 1988. **328**: 680–690. doi:10.1086/166325.

[124] Ø. Elgarøy and F. V. De Blasio. "Superfluid vortices in neutron stars." *A&A*, 2001. **370(3)**: 939–950. doi:10.1051/0004-6361:20010160.

[125] P. Haensel, A. Potekhin, and D. Yakovlev. *Neutron Stars 1: Equation of State and Structure*. New York: Springer Science + Business Media LLC, 2007.

[126] V. Graber, N. Andersson, and M. Hogg. "Neutron stars in the laboratory." *International Journal of Modern Physics D*, 2017. **26(08)**: 1730015. doi:10.1142/S0218271817300154.

[127] A. Sedrakian and J. M. Cordes. "Vortex-interface interactions and generation of glitches in pulsars." *Monthly Notices of the Royal Astronomical Society*, Aug 1999. **307(2)**: 365–375. doi:10.1046/j.1365-8711.1999.02638.x.

[128] V. Khomenko and B. Haskell. "Modelling pulsar glitches: the hydrodynamics of superfluid vortex avalanches in neutron stars." *Publications of the Astronomical Society of Australia*, 2018. **35**: 20. doi:10.1017/pasa.2018.12.

[129] M. Ruderman. "Pulsar Wobble and Neutron Starquakes." *Nature*, 1970. **225(5235)**: 838–839. doi:10.1038/225838a0.

[130] H. Young, R. Freedman, M. Zemansky, F. Sears, and L. Ford. *Sears and Zemansky's University Physics: with Modern Physics*. San Francisco: Pearson Education, Inc., 13th edition, 2012.

[131] A. Nicolis and R. Penco. "Mutual interactions of phonons, rotons, and gravity." *Physical Review B*, Apr 2018. **97**: 134516. doi:10.1103/PhysRevB.97.134516.

[132] L. Brillouin. "Sur les tensions de radiation." *Annales de Physique*, 1925. **10(4)**: 528–586. doi:10.1051/anphys/192510040528.

[133] L. D. Landau. "T3 - On the Theory of Superfluidity of Helium II [J. Phys. (U.S.S.R.) 11, 91, 1947]." In Z. M. Galasiewicz (editor), "Helium 4," pages 243 – 246. Pergamon. ISBN 978-0-08-015816-7, 1971. doi:10.1016/B978-0-08-015816-7.50019-5.

[134] A. M. Schakel. *Boulevard of Broken Symmetries: Effective Field Theories of Condensed Matter*. 2008.

[135] R. Lindsay. *Mechanical Radiation*. New York: McGraw-Hill Book Company, Inc., 1960.

[136] M. P. Marder. *Condensed Matter Physics*. Hoboken: John Wiley & Sons, Inc., 2nd edition, 2010.

[137] A. D. Waite. *Sonar for Practicing Engineers*. Chichester: John Wiley & Sons, Ltd., 2002.

[138] N. N. Bogolyubov. "On the Theory of Superfluidity." *Journal of Physics (USSR)*, 1947. **11(1)**: 23–32. doi:10.1103/PhysRevLett.79.553. [Izv. Akad. Nauk Ser. Fiz.11,77(1947)], `https://www.ufn.ru/pdf/jphysussr/1947/11_1/3jphysussr19471101.pdf`.

[139] M. R. Andrews, D. M. Kurn, H.-J. Miesner, D. S. Durfee, C. G. Townsend, S. Inouye, and W. Ketterle. "Propagation of Sound in a Bose-Einstein Condensate." *Physical Review Letters*, Jul 1997. **79**: 553–556. doi:10.1103/PhysRevLett.79.553.

[140] T. Weber, J. Herbig, M. Mark, H.-C. Nägerl, and R. Grimm. "Bose-Einstein Condensation of Cesium." *Science*, 2003. **299(5604)**: 232–235. doi:10.1126/science.1079699.

[141] K. Aki and P. Richards. *Quantitative Seismology: Theory and Methods*. Sausalito: University Science Books, 2nd edition, 2002.

[142] C. W. Chou, D. B. Hume, T. Rosenband, and D. J. Wineland. "Optical Clocks and Relativity." *Science*, 2010. **329(5999)**: 1630–1633. doi:10.1126/science.1192720.

[143] C. Freier, M. Hauth, V. Schkolnik, B. Leykauf, M. Schilling, H. Wziontek, H.-G. Scherneck, J. Müller, and A. Peters. "Mobile quantum gravity sensor with unprecedented stability." *Journal of Physics: Conference Series*, Jun 2016. **723**: 012050. doi:10.1088/1742-6596/723/1/012050.

[144] S. L. Campbell, R. B. Hutson, G. E. Marti, A. Goban, N. Darkwah Oppong, R. L. McNally, L. Sonderhouse, J. M. Robinson, W. Zhang, B. J. Bloom, and J. Ye. "A Fermi-degenerate three-dimensional optical lattice clock." *Science*, 2017. **358(6359)**: 90–94. doi:10.1126/science.aam5538.

[145] A. B. Migdal. "Superfluidity and the Moments of Inertia of Nuclei." *Soviet Physics JETP*. **37(1)**.

[146] V. L. Ginzburg and D. A. Kirzhnits. "On the Superconductivity of Electrons at the Surface Levels." *Soviet Physics JETP*, 1964. **46**: 397–398. http://www.jetp.ac.ru/cgi-bin/dn/e_019_01_0269.pdf.

[147] H. Song, S. A. Bass, U. Heinz, T. Hirano, and C. Shen. "200 A GeV Au + Au Collisions Serve a Nearly Perfect Quark-Gluon Liquid." *Physical Review Letters*, May 2011. **106**: 192301. doi:10.1103/PhysRevLett.106.192301.

[148] Y. B. Zeldovich. "The Equation of State at Ultrahigh Densities and its Relativistic Limitations." *Soviet Physics JETP*, 1962. **41(5)**: 1609–1615. http://www.jetp.ac.ru/cgi-bin/dn/e_014_05_1143.pdf.

[149] S. Endlich, A. Nicolis, and R. Penco. "Ultraviolet completion without symmetry restoration." *Physical Review D*, Mar 2014. **89**: 065006. doi:10.1103/PhysRevD.89.065006.

[150] A. Esposito, S. Garcia-Saenz, A. Nicolis, and R. Penco. "Conformal solids and holography." *Journal of High Energy Physics*, Dec 2017. **2017(12)**: 113. doi:10.1007/JHEP12(2017)113.

[151] L. Alberte, M. Baggioli, A. Khmelnitsky, and O. Pujolàs. "Solid holography and massive gravity." *Journal of High Energy Physics*, Feb 2016. **2016(2)**: 114. doi:10.1007/JHEP02(2016)114.

[152] L. Alberte, M. Baggioli, and O. Pujolàs. "Viscosity bound violation in holographic solids and the viscoelastic response." *Journal of High Energy Physics*, Jul 2016. **2016(7)**: 74. doi:10.1007/JHEP07(2016)074.

[153] E. Kiritsis and J. Ren. "On Holographic Insulators and Supersolids." *Journal of High Energy Physics*, 2015. **09**: 168. doi:10.1007/JHEP09(2015)168.

[154] A. Nicolis. Private communication, 2018.

[155] E. Inönü and E. P. Wigner. "On the contraction of groups and their representations." *Proceedings of the National Academy of Sciences*, 1953. **39**: 510–524. doi:10.1073/pnas.39.6.510.

[156] H. Kleinert and V. Schulte-Frohlinde. *Critical Properties of ϕ^4-Theories*. Singapore: World Scientific Pub. Co. Inc., 2001.